

Author final response

We are grateful to both referees for their comments and suggestions. We have submitted our point-by-point responses and revised our manuscript according to the referee's suggestions. Below are our responses to referees and revised manuscript with a supplement.

Response to referee #1

Anonymous Referee #1

Received and published: 6 November 2017

Summary: This paper presents in situ observations of PAN and ozone from Nam Co, a remote site in the Tibetan Plateau. Given relatively sparse PAN data, publication of this data is of interest. The most important conclusions of the paper are also likely sound. 1) The evolution of the boundary layer is an important driver of the diurnal cycles that are observed at this location. The discussion around this point could be substantially shortened though. 2) The site occasionally experiences air that is influenced by the upper troposphere. 3) This remote location is influenced from long-range transport of air pollutants from North India. However, I recommend substantial revisions before the paper is published in ACP. Major improvements are needed in the description of the methods. Several sections have significant grammar issues that cloud communication. I did not correct all the grammar issues, because there were too many to make that reasonable. The paper will need to be edited prior to publication in ACP. Finally, several of the figures need to be improved.

Response: Thank you for your comments and suggestions. We have addressed the issues raised by both referees and revised the manuscript.

Major Comments: Section 2.2: The experimental details are insufficient and should be greatly expanded to include further details on the calibration technique and frequency. The detection limits and uncertainty should also be included. For PAN, please include additional information on the sampling. For example, how long was PAN was in the instrument, what was the inlet length, etc? It also appears that the instrument was calibrated with a relatively high NO reference gas. When was this NO reference gas calibrated? Also, if I understand the set-up, then that means that the calibration was done at a PAN mixing ratio substantially higher than the ambient measurements. Finally, Did the authors moisturize their carrier gas (presumably helium)? This is particularly important at the humidity levels that were experienced at this site. Without a humidified carrier gas, I would expect varying sensitivity to PAN that would not necessarily be accounted for by their indirect calibration with respect to CCl₄.

Response: We have added more details about the instruments and measurements, including the calibration technique and frequency, humidification of carrier gas, reference NO gas, inlet, detection limit and uncertainty, etc. The inlet tubing was 2-3 m and ambient air was sucked at 6 l/min by a pump. The NO reference gas was verified prior to campaigns using an NO standard (Air Liquide America Specialty Gases LLC, USA) traceable to the National Institute of Standards and Technology (NIST) reference material. High concentration of PAN was dynamically diluted to sub-ppb levels before

being used for calibrations. Our carrier gas (purified N₂) was humidified using CuSO₄•5H₂O. The varying sensitivity we observed was caused by other factors. Section 2.2 has been revised as follows:

"Ambient PAN was observed using a PAN analyzer (Meteorologie Consult GmbH, Germany), which consists of an automated gas chromatograph (GC) equipped with an electron capture detector (ECD) and a calibration unit. The equipment is the same one as used in previous observations in Beijing (Zhang et al., 2014) and elsewhere (e.g., Zellweger et al., 2000; Zhang et al., 2009a), with identical setup details depicted in Zhang et al. (2014). The GC with a pre-column and a main column was optimized by the factory for the separation of PAN and CCl₄ at 15°C within 10 min. Purified nitrogen (>99.999%, Chengweixin Gases, Beijing, China) was used as carrier gas. A cartridge with CuSO₄ 5H₂O was used to humidify the carrier gas before entering the GC columns. This can reduce the effects of varying humidity on the measurements (Flocke et al., 2005). Back-flushing was applied to the pre-column to prevent contamination and shorten analysis time. An NO reference gas (4.5 ppm, Huayuan Gases, Beijing, China) in nitrogen was introduced into the calibration unit and reacts with excess acetone vapor under the UV irradiation to yield concentrated PAN. Prior to each campaign the NO reference gas was verified using an NO standard (Air Liquide America Specialty Gases LLC, USA) traceable to the National Institute of Standards and Technology (NIST) reference material. Under similar conditions, the PAN yield was found to be 92% ±3% (Volz-Thomas et al., 2002). A continuous, stable flow of known PAN concentration was produced by subsequent dynamic dilution with purified ambient air and supplied to the PAN-GC for calibration. The lower detection limit was 50 ppt. Zellweger et al. (2000) achieved an overall uncertainty of ±3% under their conditions.

Surface O₃ was simultaneously observed using an O₃ analyzer (TE 49C, Thermo Environmental Instruments, Inc., USA). The O₃ analyzer has a lower detection limit 1.0 ppb and precision of ±1.0 ppb. Before and after each campaign the analyzer was calibrated using an O₃ calibrator (TE 49C PS) traceable to the Standard Reference Photometer (SRP) maintained by WMO World Calibration Centre in EMPA, Switzerland (Zellweger et al., 2009). All instruments were housed in a simply constructed one-storey building, located 0.15 km southeast of the station's main building. Ambient air was introduced through Teflon tubing (O.D. 1/4" and 2-3 m) to the PAN and O₃ analyzer at the flowrate of 2 l/min and 6 l/min, respectively. Meteorological data were collected using automatic meteorological station systems installed at different levels on a tower near the observation building.

Although measurements of PAN have been made previously at some high altitude sites in other areas using methods similar to ours (Ford et al., 2002; Fischer et al., 2010; Xue et al., 2011; Pandey Deolal et al., 2013), this is the first report of using the GC-ECD instrument for PAN measurement under the conditions of a high altitude site over 4700 m a.s.l. To track the performance of the PAN analyzer, frequent calibrations were made during the campaigns (e.g., on 9 and 10 July, 7, 9,

12, 14, 17, and 23 August 2011, and on 15, 16, 28 May, 6, 13, 20, 22, 27 June, 4, 12, and 13 July 2012) except the period from 16 July to 5 August 2011, where no carrier gas was available for the PAN observation due to a leakage. During the observation period in 2011, the instrument performance was somewhat instable, probably affected by the extreme ambient conditions at the site. The variation of environment temperature is suspected to have made it hard to keep the ECD inner temperature constant. This resulted in abrupt fluctuations in the 10-min chromatographic PAN signals sometimes during the measurement period in 2011. The instable performance of ECD caused varying detection sensitivity. Normally, we convert PAN signals of air samples to concentration data based on ratios of signals to theoretical PAN concentration of the standard gas produced during the calibrations. However, the jumping sensitivity made it improper to obtain PAN concentrations using the normal method. Thus, we applied an indirect calibration method. Our GC-ECD instrument was optimized for the separation and detection of both PAN and CCl₄. Therefore, it was possible to indirectly calculate the PAN concentrations, i.e., by using the ratios of the PAN to CCl₄ signal. Details about the indirect calibration are given in the supplement.

Although the indirect calibration is a viable way to obtain PAN concentrations, the uncertainty of final data could be larger than the direct calibration primarily due to the two assumptions mentioned in the supplement and some technical problems with the observation system. We are more confident of the data from 17 to 24 August 2011. During this period, the instruments performed well and the two calibrations in this period gave similar sensitivities. In view of this, we report and analyze in this paper mainly data from 17 to 24 August 2011, together with those obtained from 15 May to 13 July 2012, where our instruments performed well."

Section 3.4: There are worse grammar issues in this section compared to the other sections. The section should also provide the rationale for using the 500 hPa water vapor cut off for the analysis.

Response: We have tried to correct the grammar errors in this and other sections. The "500 hPa" in the figure caption of Fig. 6 should be "500 Pa". We did not set any cut off for water vapor but we think O₃ values greater than 70 ppb were more or less impacted by middle/upper tropospheric air. In Fig. 6(c) the 70 ppb cut-off for O₃ corresponds to about 500 Pa for water vapor. We state now in revised section 3.4: "The data points within the red rectangle in Fig. 6(c) are measurements associated with higher O₃ levels and lower WVP. We consider these as measurements with significant features of middle/upper tropospheric air since they are above the highest average hourly O₃ level (69.7 ppb) shown in Fig. 4(b) and associated with WVP < 500 Pa."

Page 13, Line 11: I do not understand this sentence.

Response: The sentence in lines 11-12 has been changed to "Figure 6 does not allow for an estimate of PAN abundance in upper levels".

Page 13: Line 16: What is omega? How should it be interpreted in this context.

Response: In this paper, omega represents vertical velocity of air parcel. The mean omega values for different grids are available in the reanalysis meteorological dataset. By analyzing the omega fields one can get an idea about air movement in vertical direction. Positive and negative omega values indicate descending and ascending, respectively. We have changed this sentence to **"Figure 7 displays the vertical velocity (omega) field and horizontal wind vectors at different times and air pressure levels, with the two cases being labeled with black rectangles (termed as Case 1 and Case 2). Positive and negative omega values indicate descending and ascending, respectively"**.

Page 14, Lines 22-32: If this section remains in the paper, I suggest that the authors reach out to someone from the MIPAS PAN community to do a proper comparison. There are many issues here. I do not believe that the sources and magnitude of uncertainty associated with the MIPAS PAN measurements are adequately or correctly summarized. It seems as though the paper is trying to compare an instantaneous in situ measurement with a monthly average, which is not the right approach. The authors also appear to assume that there is no PAN enhancement in the atmosphere between the UT observed by MIPAS and their ground site, which seems like a big leap. The interannual variability in PAN can be quite large in the free troposphere (e.g. Zhu et al., 2015 GRL), and so comparing different years may not be a good approach.

Zhu, L., E. V. Fischer, V. H. Payne, J. R. Worden, and Z. Jiang (2015), TES observations of the interannual variability of PAN over Northern Eurasia and the relationship to springtime fires, *Geophys. Res. Lett.*, DOI:10.1002/2015GL065328.

Response: We agree that it is not a right approach to compare our in-situ measurements with the satellite observations. Indeed there are issues, like changes of PAN during the transport, interannual variability in PAN, etc., that make such simple comparison meaningless. A proper comparison with MIPAS observations is not possible because MIPAS observations cover the period from March 2002 to April 2012 and most of our in-situ measurements were made during 15 May -13 July 2012. For these reasons we have removed the last two paragraphs from section 3.4. However, we think a collection of available PAN data for the Tibetan Plateau can be of interest for the readers. Therefore, we have revised Table 1 by adding more data and also considering referee's suggestions regarding this table (see below). And we have added a new section (section 3.6) to present and discuss our collection of available PAN data for the TP region.

"3.6 PAN levels at different heights over the TP"

In addition to this study, in-situ PAN measurements from the TP were only reported by Xue et al. (2011). As PAN is a key source of NO_x in remote regions, its concentration and distribution are important for understanding the photochemistry over regions like the TP. Here we provide a collection of PAN data for the TP region.

Table 1 summarizes the PAN data available for the TP from in-situ observations, satellite and space shuttle observations, and model simulations. Based on our in-situ observations at NMC (4.7 km), we obtained an averaged PAN level of 0.36 ppb for

17-24 August 2011 and 0.44 ppb for 15 May - 13 July 2012. In-situ observations at WLG (3.8 km) found an average PAN level of 0.44 for the period from 22 July to 16 August 2006 (Xue et al., 2011). The limited in-situ observations in the surface layer do not show substantial spatial and temporal differences in the average level of PAN. However, the PAN level did show significant increases in some cases with obvious transport impacts from the UTLS (e.g., 22 August 2011) and from South Asia (e.g., 1-6 June 2012).

Developments in remote sensing have made it possible to detect global PAN in the UTLS from the space. During 9-13 August 1997, observations using the Cryogenic Infrared Spectrometers and Telescopes for the Atmosphere (CRISTA) aboard the Space Shuttle showed PAN levels in the range of 0.1-0.2 ppb for 18 km over the TP (Ungermann et al., 2016). Based on the retrievals of satellite observations using the Michelson Interferometer for Passive Atmospheric Sounding (MIPAS), the average PAN levels in March 2003 were in the ranges of 0.15-0.23 ppb for 234 hPa and 0.35-0.45 ppb for 333 hPa over the TP, and those in August 2003 in the ranges of 0.15-0.23 ppb for 185 hPa and 0.35-0.50 ppb for 278 hPa (Moore and Remedios, 2010). The PAN level at 12 km over TP was about 0.10-0.15 ppb in October 2007 (Wiegele et al., 2012), which is very close to the range (0.1-0.2 ppb) on 21 October 2003 (Glatthor et al., 2007). Results from the model simulations by Fischer et al. (2014) showed that the PAN level during June-August 2008 varied in the range of 0.3-0.5 ppb in the 2-6 km layer and 0.2-0.4 ppb in the 6-10 km layer over the TP. Another model simulation study (Fadnavis et al., 2014) obtained a PAN range of 0.15-0.2 ppb for the 6-10 km layer and for June-September 1995-2004.

The satellite measurements and simulation results listed in Table 1 indicate a general decrease of PAN level from the upper troposphere to the lower stratosphere, consistent with the vertical distribution of PAN in the UTLS (Pope et al., 2016). These data represent PAN levels averaged over larger scales for certain periods. In-situ measurements on the ground showed average PAN levels very close to 333 hPa (about 10 km) values. So far, there has been no observation of the vertical distribution of PAN in the middle and lower troposphere over the TP. Based the results from the case studies in sections 3.4 and 3.5, we believe the PAN level in middle and lower tropospheric air over the TP may be more variable and sometimes elevated by transport of plumes from anthropogenic and biomass burning emissions. The significance of the transport impact deserves systematic studies, which is out the scope of this work."

The revised Table 1 has been moved to this new section.

Table 1 Measured and modeled PAN at different heights over the TP.

PAN (ppb)	Period	Height ^a	Method	Reference
0.35(0.11-0.76) ^b	17-24 August 2011	4.7 km	Ground measurements	this work
0.44(0.21-0.99) ^b	15 May - 13 July 2012	4.7 km	Ground measurements	
0.52(0.31-0.72) ^b	22 August 2011	4.7 km	Ground measurements	

0.40(0.24-0.52) ^b	25 May 2012	4.7 km	with impact from the UT Ground measurements with impact from the UT Ground measurements	
0.62(0.27-0.99) ^b	1-6 June 2012	4.7 km	with impact from South Asia	
0.44(0.14) ^c	22 July - 16 August 2006	3.8 km	Ground measurements	Xue et al.(2011)
0.35-0.45 ^d	March 2003	333 hPa	MIPAS	Moore and Remedios (2010)
0.15-0.23 ^d		234 hPa	MIPAS	
0.35-0.5 ^d	August 2003	278 hPa	MIPAS	
0.15-0.23 ^d		185 hPa	MIPAS	
0.1-0.15 ^d	October 2007	12 km	MIPAS	Wiegele et al.(2012)
0.1-0.2 ^d	21 October 2003	12 km	MIPAS	Glatthor et al.(2007)
0.1-0.2 ^d	9-13 August 1997	18 km	Space Shuttle experiment CRISTA-2	Ungermann et al.(2016)
0.3-0.5 ^d	June-August 2008	2-6 km	GEOS-Chem modeling	Fischer et al.(2014)
0.2-0.4 ^d		6-10km	GEOS-Chem simulation	
0.15-0.2 ^d	June-September 1995-2004	6-10km	ECHAM5-HAM MOZ model simulation	Fadnavis et al. (2014)

^a Either elevation above the sea level or air pressure layer.

^b Overall average with the range of hourly mean.

^c Overall average with standard deviation.

^d Reading based on the color scale given in the reference.

Section 3.5: This section again has major grammar issues and some logic issues. 1) PAN is only short-lived if it is warm. 2) Page 15, Lines 24-28 are too general to be of use, and may contain logic that does not apply to the conditions sampled at the site. 3) Page 17, Line 14: Are all the trajectories valid? Did the authors remove trajectories that had an altitude of zero agl? These trajectories are invalid. 4) The discussion of the TEMIS data seems distracting (page 16, lines 22-32). I recommend removing this.

Response: Indeed, PAN is quite stable in colder temperatures. The real temperature is important for thermal decomposition and should be considered.

We have revised the first paragraph of section 3.5 as follows:

"In warm environment, PAN is short-lived. Below 7 km, thermal decomposition is

the main loss process of PAN (Talukdar, 1995). Thus, although polluted air masses from south of the Himalayas can be transported to the TP along the monsoon stream, PAN in the air masses may experience significant loss during the travelling. Cox and Roffey (1977) estimated the lifetime of PAN at 25 °C to be about 2.7 h and 0.7 h for urban and rural daytime conditions, respectively, and that at 15 °C a factor of four longer. During our observations in summer 2012, surface air temperature at NMC varied from -0.5 °C to 19.4 °C, with an average of 8.4 °C. Thermal decomposition should be much slower under such temperature condition and only important during warmer daytime periods. However, thermal decomposition might still have removed a significant fraction of PAN during the long-range transport, particular over the warm low-elevation areas. The level of PAN observed at our site was the remaining PAN in the air masses, which should be significantly lower than that in the formation area. Nevertheless, PAN episodes were observed under certain meteorological conditions. One of such episodes occurred in early June 2012. As can be seen in Fig. 5, the PAN level humped during 1-6 June 2012. The maximum PAN level reached 1.0 ppb, and the diurnal minima on these days were even higher than the diurnal maxima on many of other observation days. The origin of the high PAN levels deserves an investigation."

All the trajectories were used in Fig. 12. We did not remove trajectories that had an altitude of zero agl. However, including the trajectories with zero agl does not cause misinterpretation. To prove this, we calculated forward air trajectories starting from matrices of locations in the domains west and south of the NMC site. The trajectories were calculated for 0600 UTC on each day during 1-12 June 2012. Figure R1 shows matrices of forward trajectories starting at 0600 UTC 3 June 2012 and 08 UTC 8 June 2012. The trajectories clearly indicate that the NMC site was impacted by air masses from different areas before and after 6 June. Around 4-5 June 2012, NMC was mainly impacted by air masses from the SW-W sector (North India, North Pakistan, and Nepal). Around 9-10 June, however, NMC was mainly impacted by air masses from the S-SW sector (Bangladesh, Bhutan, etc.). These results are consistent with those from the backward trajectories in Fig. 12.

To address your concern, we have re-drawn Fig. 12. The trajectories that had zero agl have been partly removed, i.e., only the last tracks of non-zero agl are plotted. In addition, we have included Figure R1 in the supplement as Figure S6 and revised the text (page 17, lines 12-14) as follows:

"Forward trajectories were also calculated for air masses originated from matrices of locations in the domains west and south of the NMC site. Examples of forward trajectories matrices are shown in Figure S6 for trajectories starting at 0600 UTC 3 June 2012 and 08 UTC 8 June 2012. The trajectories clearly indicate that the NMC site was impacted by air masses from different areas before and after 6 June. Around 4-5 June 2012, NMC was mainly impacted by air masses from the SW-W sector (North India, North Pakistan, and Nepal). Around 9-10 June, however, NMC was mainly impacted by air masses from the S-SW sector

(Bangladesh, Bhutan, etc.). These results are consistent with those from the backward trajectories in Fig. 12. The above analysis can explain the sudden decrease of the PAN level after 6 June 2012 on one hand, and on the other hand support the idea that the PAN episode observed during 1-6 June 2012 was mainly caused by plumes from North India, North Pakistan, and Nepal."

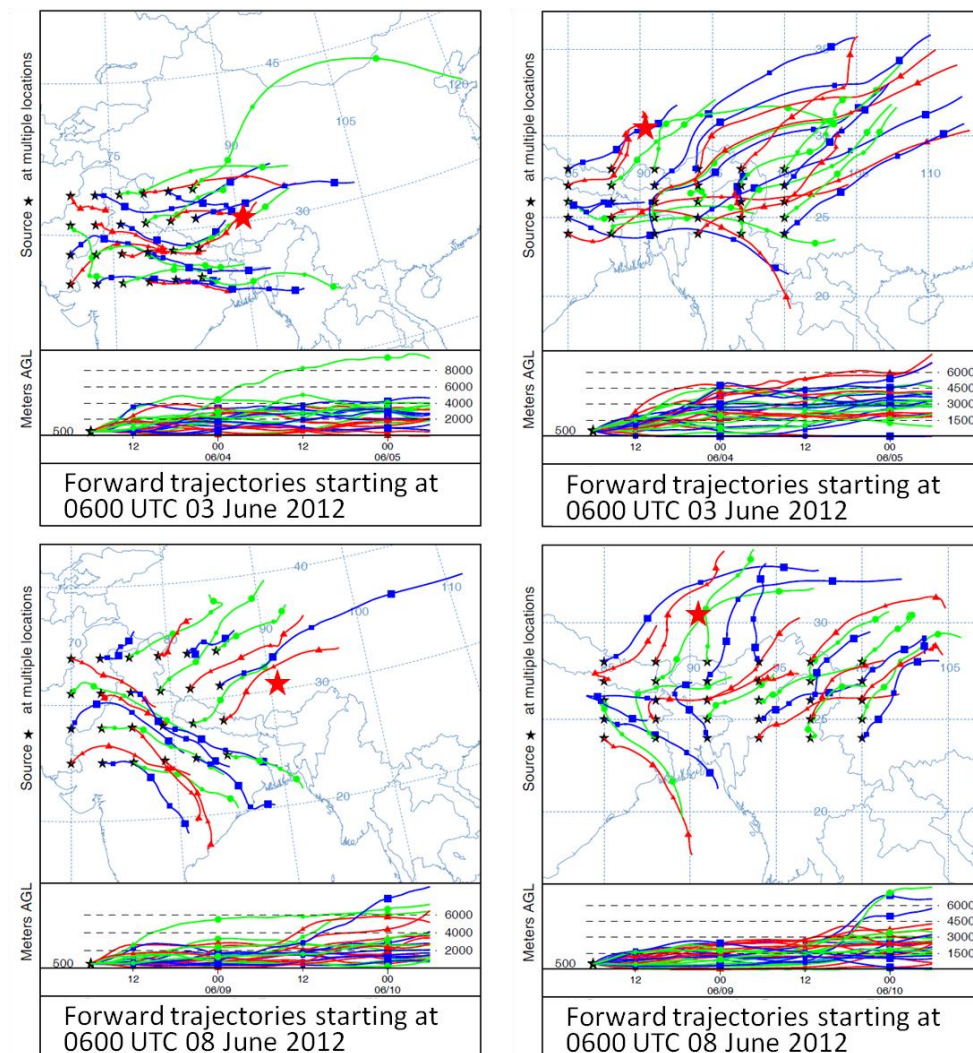


Figure R1 Matrices of 48-h air mass forward trajectories starting at 0600 UTC 3 June 2012 (upper panel) and 0600 UTC 8 June 2012 (bottom panel) from the domains west and south of the NMC site (red star). The online HYSPLIT model (https://ready.arl.noaa.gov/HYSPLIT_traj.php; Stein et al., 2015; Rolph et al., 2017) were used to produce the trajectory matrices. The starting height of the trajectories is 500 m above ground level.

We think the satellite measurements in Fig. S5 and the discussion here (page 16, lines 22-32) do provide relevant information. Referee #2 suggests including some discussions on biomass burning impact and using daily satellite data. We have followed these suggestions. We understand your concern. Therefore, we have moved the technical details to the supplement. This part of text has been revised as follows:

"Northern India suffers photochemical pollution, as indicated by observations of

high level of surface O₃ (Ghude et al., 2008) and tropospheric O₃ (Fishman et al., 2003). Emission inventories (Ohara et al., 2007; Zhang et al., 2009b) indicate that North India is one of the Asian emission centers for pollutants including NO_x and VOCs. In addition to anthropogenic sources, biomass burning is also an important source for PAN, and some of biomass burning plumes can penetrate the boundary layer and cause PAN formation over a large scale (Tereszchuk et al., 2013; Fischer et al., 2014; Zhu et al., 2015). Figure S5 shows tropospheric NO₂ and HCHO columns, together with maps of fire spots for 1-3 and 4-6 June 2012. As can be seen in this figure, NO₂ and HCHO in the troposphere over North India and North Pakistan were highly abundant during both periods. However, the NO₂ and HCHO levels were obviously higher during 1-3 June than during 4-6 June. The differences in NO₂ and HCHO levels might have been caused by open biomass burning since much more fire spots were observed during 1-3 June than during 4-6 June (see Figs. S5(e) and S5(f)). The high tropospheric NO₂ and HCHO columns suggest the presence of high concentrations of NO_x and VOCs, which may lead to rapid formation of O₃ and PAN under the summer conditions over the South Asian region. Since this region borders on the TP, it is likely that the PAN episode observed at our site during 1-6 June 2012 was mainly caused by long-range transport of plumes with high PAN and its precursors from South Asia."

Table 1: Please make it clear (perhaps with different sections) which are satellite or model output. Also, the observations presented in this work were not made at 350 hPa, and so it is odd to put this in the table. A better approach would be to present the mean of all the data collected, and then call out a subset of interest.

Response: Thank you for your suggestions. We have revised this table following your suggestions. A column called “Method” has been added to indicate ground measurements, satellite observations, model simulations, etc. Overall averages and ranges of PAN concentration for our campaigns have been included in the table. Data from our cases are given and indicated as ground measurements with impact from the UT or ground measurements with impact from South Asia. We have also included more data from literature. The table has been moved to the new section (section 3.6) and discussed there. Details are given above.

Figure 1: It is hard to read the green text on the Figure. Please use black or white. Please also add lat/lon to the map.

Response: All changes have been made following your suggestions.

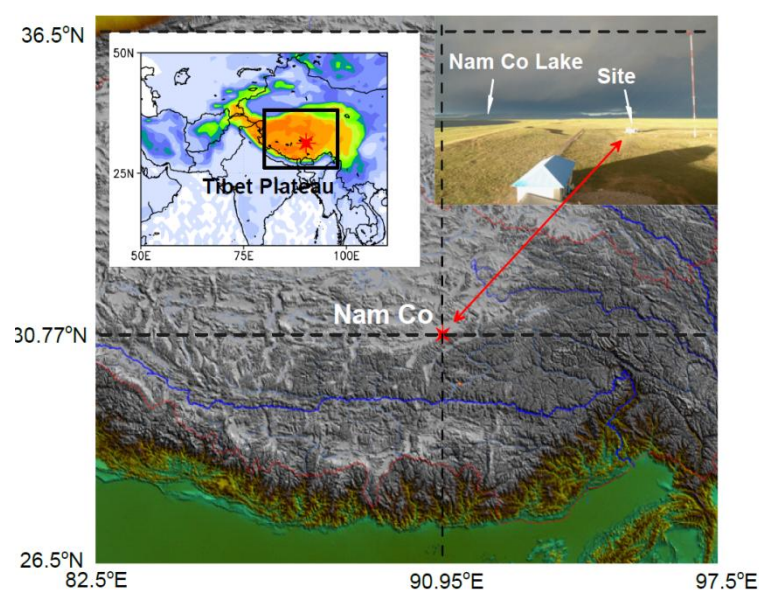


Fig.1 Map showing location of the observation site and local environment.

Figure 4: It is unclear why U and V wind speed need to be shown in addition to Wind speed.

Response: By including U and V wind speed we can show that in the low ΔO_3 case, stronger southerly wind prevailed, meaning a stronger monsoonal impact.

Figure 6: Use “O3 versus PAN” rather than “O3-PAN” in the caption description of the panels. There is a typo on the caption. It should be Pa, rather than hPa, correct?

Response: Thank you. It is Pa not hPa. We have corrected this error. The caption has been revised as follows:

"Fig. 6 Scatter plots of hourly O₃ versus PAN, Vapor Pressure versus O₃, Vapor Pressure versus PAN of group 1 (a,c,e) and group 2 (b,d,f), following Fig. 4. The correlation shown in Figs. 6(a) and 6(b) are significant at $\alpha=0.01$. The data points within the red rectangle in Fig. 6(c) represent O₃ levels higher than 70 ppb and WVP lower than 500 Pa."

Figure 9 & 10: It is really hard to see the trajectories. Overlaying black on dark blue is not a good choice here. It is also hard to see the underlying map. Please change the color scale of the PV fields.

Response: We have decided to interchange Figure 9 & 10 with Figure S2 & S3. All these figures have been modified. The color for trajectories has been changed to white. The color scale has been changed. The font sizes have been enlarged.

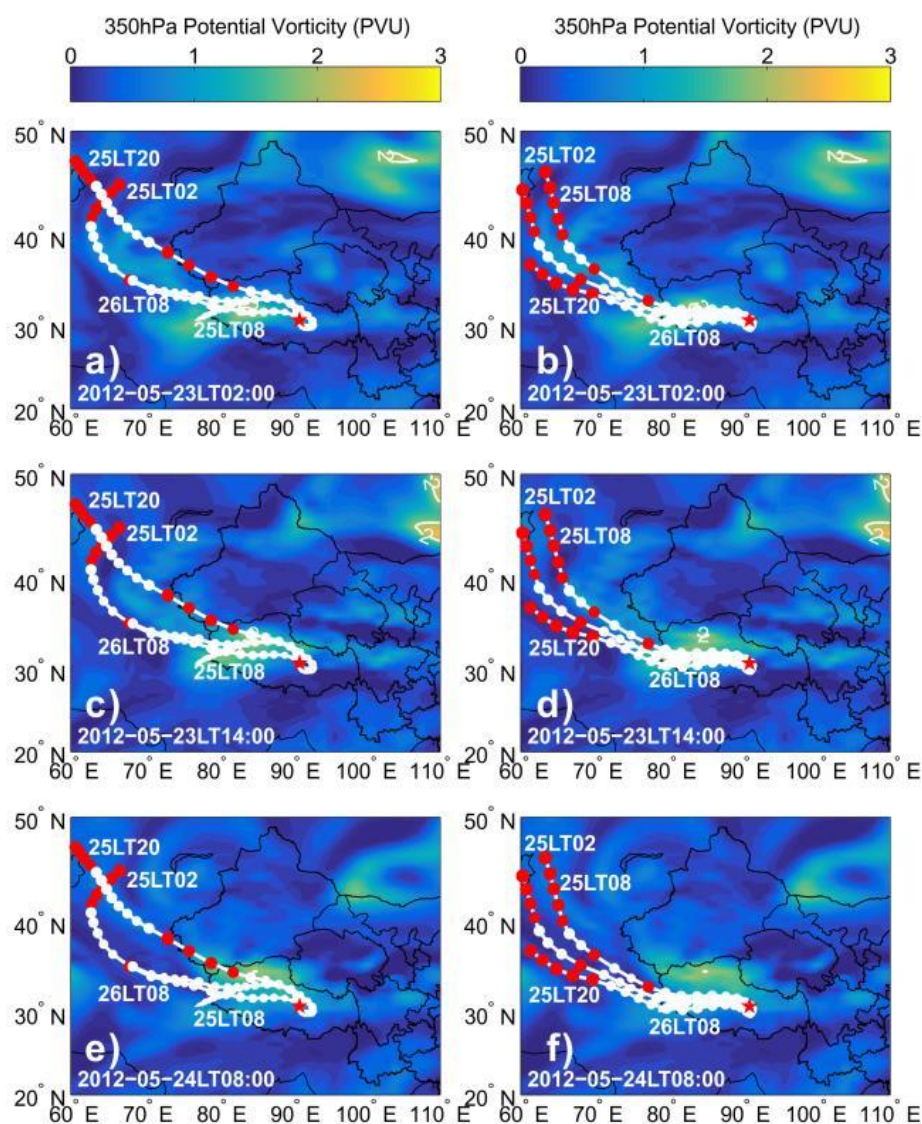


Figure 9 Plots showing 350 hPa potential vorticity fields at three time-points during 23-24 May 2012 and back trajectories of air masses arriving at 500 m (a,c,e) and 1500 m (b,d,f) above the ground of NMC (red star) during 25-26 May 2012.

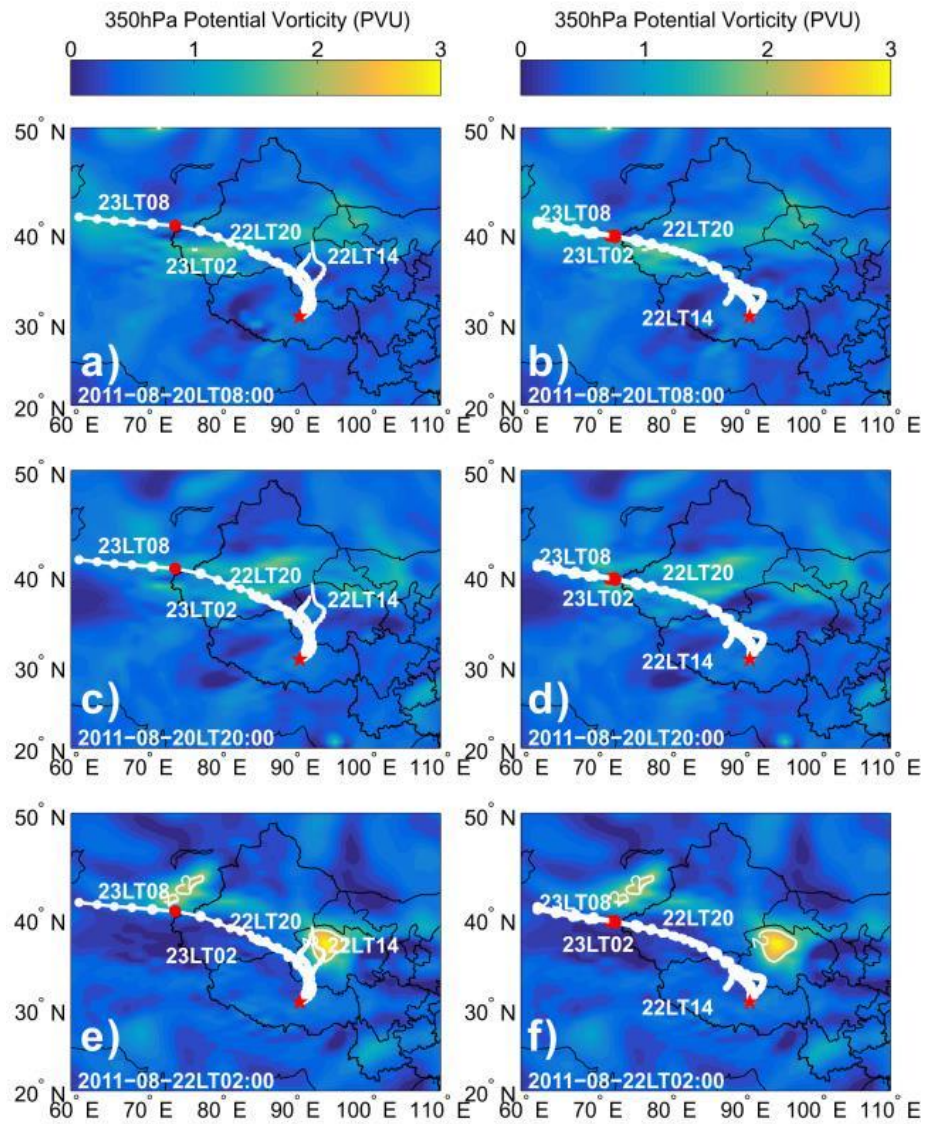


Figure 10 Same as Figure 9, but for 22-23 August 2011.

Figure 11: The font is too light and too small on the legend.

Response: All font sizes have been enlarged.

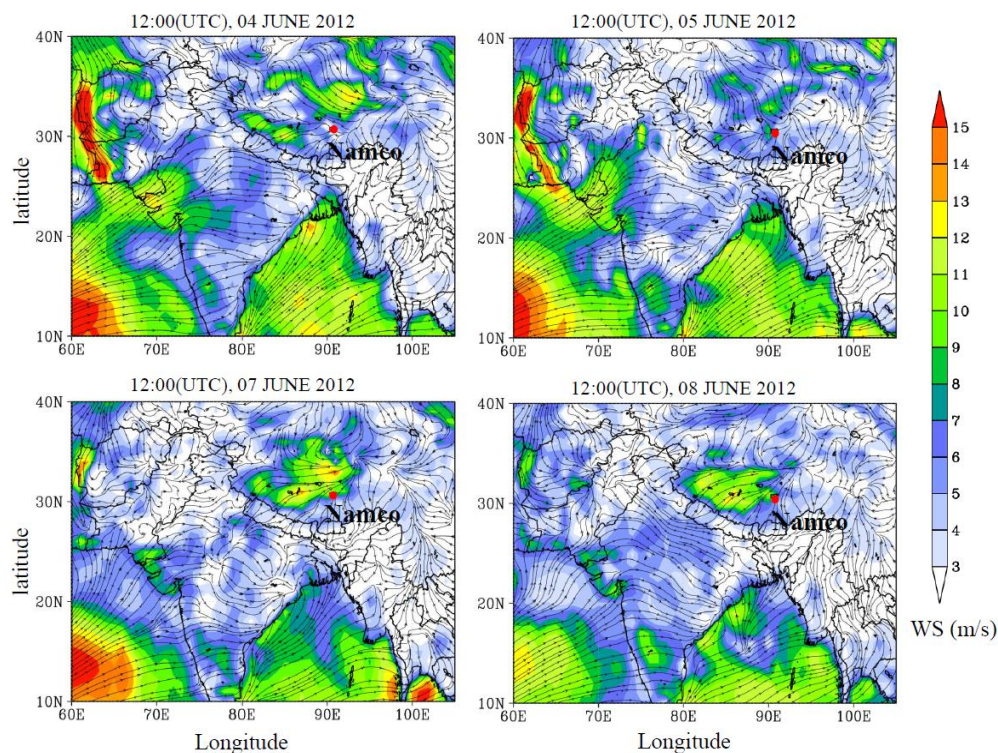


Fig. 11 Average fields of wind at $\sigma=0.995$ for 12:00 (UTC) of 4, 5, 7 and 8 June 2012.

Reference

- Cox, R.A. and Roffey, M.J.: Thermal decomposition of peroxyacetylnitrate in the presence of nitric oxide. *Environ. Sci. & Technol.*, 11(9), 900–906, 1977.
- Fadnavis, S., Schultz, M.G., Semeniuk, K., Mahajan, A.S., Pozzoli, L., Sonbawne, S., Ghude, S.D., Kiefer, M., and Eckert, E.: Trends in peroxyacetyl nitrate (PAN) in the upper troposphere and lower stratosphere over southern Asia during the summer monsoon season: regional impacts, *Atmos. Chem. Phys.*, 14, 12725–12743, 2014.
- Fischer, E. V., Jacob, D. J., Yantosca, R. M., Sulprizio, M. P., Millet, D. B., Mao, J., Paulot, F., Singh, H. B., Roiger, A. E., Ries, L., Talbot, R. W., Dzepina, K., and Pandey Deolal, S.: Atmospheric peroxyacetyl nitrate (PAN): a global budget and source attribution, *Atmos. Chem. Phys.*, 14, 2679–2698, 2014.
- Fishman, J., Wozniak, A.E., and Creilson, J.K.: Global distribution of tropospheric ozone from satellite measurements using the empirically corrected tropospheric ozone residual technique: Identification of the regional aspects of air pollution, *Atmos. Chem. Phys.*, 3, 893–907, 2003.
- Flocke, F.M., Weinheimer, A.J., Swanson, A.L., Roberts, J.M., Schmitt, R., and Shertz, S.: On the measurement of PANs by gas chromatography and electron capture detection, *J. Atmos. Chem.*, 52, 19–43, 2005.
- Ghude, S.D., Jain, S.L., Arya, B.C., Beig, G., Ahammed, Y.N., Kumar, A., Tyagi, B.: Ozone in ambient air at a tropical megacity, Delhi: characteristics, trends and cumulative ozone exposure indices, *J. Atmos. Chem.*, 60, 237–252, 2008.
- Glatthor, N., von Clarmann, T., Fischer, H., Funke, B., Grabowski, U., Hopfner, M., Kellmann, S., Kiefer, M., Linden, A., Milz, M., Steck, T., and Stiller, G. P.: Global peroxyacetyl nitrate (PAN) retrieval in the upper troposphere from limb emission spectra of the Michelson Interferometer for Passive

Atmospheric Sounding (MIPAS), *Atmos. Chem. Phys.*, 7, 2775–2787, doi:10.5194/acp-7-2775-2007, 2007.

Moore, D.P. and Remedios, J.J.: Seasonality of Peroxyacetyl nitrate (PAN) in the upper troposphere and lower stratosphere using the MIPAS-E instrument, *Atmos. Chem. Phys.*, 10, 6117–6128, 10.5194/acp-10-6117-2010, 2010.

Ohara, T., Akimoto, H., Kurokawa, J., Horii, N., Yamaji, K., Yan, X., and Hayasaka, T.: An Asian emission inventory of anthropogenic emission sources for the period 1980–2020, *Atmos. Chem. Phys.*, 7, 4419–4444, 2007.

Pope, R. J., Richards, N. A. D., Chipperfield, M. P., Moore, D. P., Monks, S. A., Arnold, S. R., Glatthor, N., Kiefer, M., Breider, T. J., Harrison, J. J., Remedios, J. J., Warneke, C., Roberts, J. M., Diskin, G. S., Huey, L. G., Wisthaler, A., Apel, E. C., Bernath, P. F., and Feng, W.: Intercomparison and evaluation of satellite peroxyacetyl nitrate observations in the upper troposphere–lower stratosphere, *Atmos. Chem. Phys.*, 16, 13541–13559, <https://doi.org/10.5194/acp-16-13541-2016>, 2016.

Rolph, G., Stein, A., and Stunder, B.: Real-time Environmental Applications and Display system: READY. *Environmental Modelling & Software*, 95, 210–228, 2017.

Stein, A.F., Draxler, R.R., Rolph, G.D., Stunder, B.J.B., Cohen, M.D., and Ngan, F.: NOAA's HYSPLIT atmospheric transport and dispersion modeling system, *Bull. Amer. Meteor. Soc.*, 96, 2059–2077, 2015.

Talukdar, R. K., Burkholder, J. B., Schmoltner, A.-M., Roberts, J. M., Wilson, R. R., and Ravishankara, A. R.: Investigation of the loss processes for peroxyacetyl nitrate in the atmosphere: UV photolysis and reaction with OH, *J. Geophys. Res.*, 100, 14163–14173, 10.1029/95JD00545, 1995.

Tereszczuk, K.A., Moore, D.P., Harrison, J.J., Boone, C.D., Park, M., Remedios, J.J., Randel, W.J., and Bernath, P.F.: Observations of peroxyacetyl nitrate (PAN) in the upper troposphere by the Atmospheric Chemistry Experiment-Fourier Transform Spectrometer (ACE-FTS), *Atmos. Chem. Phys.*, 13, 5601–5613, 10.5194/acp-13-5601-2013, 2013.

Ungermann, J., Ern, M., Kaufmann, M., Müller, R., Spang, R., Ploeger, F., Vogel, B., and Riese, M.: Observations of PAN and its confinement in the Asian summer monsoon anticyclone in high spatial resolution, *Atmos. Chem. Phys.*, 16, 8389–8403, 2016.

Volz-Thomas, A., Xueref, I., and Schmitt, R.: An automatic gas chromatograph and calibration system for ambient measurement, *Environ. Sci. Pollut. Res.*, 9, 72–76, 2002.

Wiegele, A., Glatthor, N., Höpfner, M., Grabowski, U., Kellmann, S., Linden, A., Stiller, G., and von Clarmann, T.: Global distributions of C₂H₆, C₂H₂, HCN, and PAN retrieved from MIPAS reduced spectral resolution measurements, *Atmos. Meas. Tech.*, 5, 723–734, 10.5194/amt-5-723-2012, 2012.

Xue, L.K., Wang, T., Zhang, J.M., Zhang, X.C., Deliger, Poon, C.N., Ding, A.J., Zhou, X.H., Wu, W.S., Tang, J., Zhang, Q.Z., and Wang, W.X.: Source of surface ozone and reactive nitrogen speciation at Mount Waliguan in western China: New insights from the 2006 summer study, *J. Geophys. Res.*, 116, 10.1029/2010jd014735, 2011.

Zellweger, C., Ammann, M., Buchmann, B., Hofer, P., Lugauer, M., Rüttimann, R., Streit, N., Weingartner, E., and Baltensperger, U.: Summertime NO_y Speciation at the Jungfraujoch, 3580 m asl, Switzerland, *J. Geophys. Res.*, 105, 6655–6667, 2000.

Zellweger, C., Klausen, J., Buchmann, B., and Scheel, H.-E.: System and Performance Audit of Surface Ozone, Carbon Monoxide, Methane and Nitrous Oxide at the GAW Global Station Mt. Waliguan and the Chinese Academy of Meteorological Sciences (CAMS) China, June 2009, WCC-Empa Report 09/2Rep., 61 pp, Empa, Dübendorf, Switzerland, available at: https://www.wmo.int/pages/prog/arep/gaw/documents/WLG_2009.pdf, 2009.

Zhang, H., Xu, X., Lin, W., and Wang, Y.: Wintertime peroxyacetyl nitrate (PAN) in the megacity Beijing: Role of photochemical and meteorological processes, *J. Environ. Sci.*, 26, 83–96, 10.1016/S1001-0742(13)60384-8, 2014.

Zhang, Q., Streets, D.G., Carmichael, G.R., He, K.B., Huo, H., Kannari, A., Klimont, Z., Park, I.S., Reddy, S., Fu, J.S., Chen, D., Duan, L., Lei, Y., Wang, L.T., Yao, Z.L., Asian emissions in 2006 for the NASA INTEX-B mission, *Atmos. Chem. Phys.* 9, 5131-5153, 2009b

Zhu, L., Fischer, E.V., Payne, V.H., Worden, J.R., and Jiang, Z.: TES observations of the interannual variability of PAN over Northern Eurasia and the relationship to springtime fires, *Geophys. Res. Lett.*, 42, 7230-7237, doi:10.1002/2015GL065328, 2015.

Response to Referee #2

Anonymous Referee #2

Xu et al. presented simultaneous measurements of two important atmospheric gases, peroxyacetyl nitrate (PAN) and ozone, at Nam Co in central Tibetan Plateau. Distinct diurnal cycles of PAN and ozone were found. Possible causes from evolutions of planetary boundary layer and long-range transport were explored. I think this is an important measurement and study, given the relatively few remote observational sites for PAN globally, which will be a valuable addition to our literature and an important reference for global model validation. The topic is well within the subject of ACP and the conclusions are generally supported by the data, with sound measurement method. However, the paper can not be accepted at the present form, which needs to be substantially improved by solving my following comments, both scientifically and technically.

Response: Thank you for your comments and suggestions. We have addressed the issues raised by both referees and revised the manuscript.

Major comments:

1. Fischer et al. (2014) reported that biomass burnings were also important sources for PAN, which could transport to remote regions through the penetration of planetary boundary layer height, thus efficiently arriving at higher altitude, such as Nam Co. Therefore, biomass burnings from forest fires and agriculture residues over South and southeastern Asia could be sources for PAN at Nam Co. The authors in this paper have not touched the discussions of this possible source. I recommend that this should be explored in the discussion part. For instance, the authors could use OMI product to examine the fire frequency occurring over South and southeastern Asia, such as in Bangladesh, during June 1-6, 2012. With this examination, probably we could have better ideas what kinds of plumes affecting the spikes of PAN at Nam Co.

Fischer, E. V., Jacob, D. J., Yantosca, R. M., Sulprizio, M. P., Millet, D. B., Mao, J., Paulot, F., Singh, H. B., Roiger, A., Ries, L., Talbot, R. W., Dzepina, K., and Pandey Deolal, S.: Atmospheric peroxyacetyl nitrate (PAN): a global budget and source attribution, *Atmos. Chem. Phys.*, 14, 2679-2698, doi:10.5194/acp-14-2679-2014, 2014.

Response: Thank for your suggestions. Indeed biomass burning is an important source of air pollutants over South and Southeast Asia and may exert a significant impact on the formation of PAN over and downwind of the region. We have tried to obtain fire data. Using NASA's Web Fire Mapper we produced maps with fire spots for the periods 1-6 and 7-12 June 2012 (Figure R2). We can see on the maps many fire spots along the Himalaya Mountains in North India, North Pakistan and West Nepal. Some scattered fire spots can also be seen in other areas of India and Pakistan. During both periods no fire spot was observed in Bangladesh. Therefore, it is likely that biomass burning emissions in North India, North Pakistan and West Nepal might have contributed to the high PAN levels we observed at NMC during 1-6 June 2012.

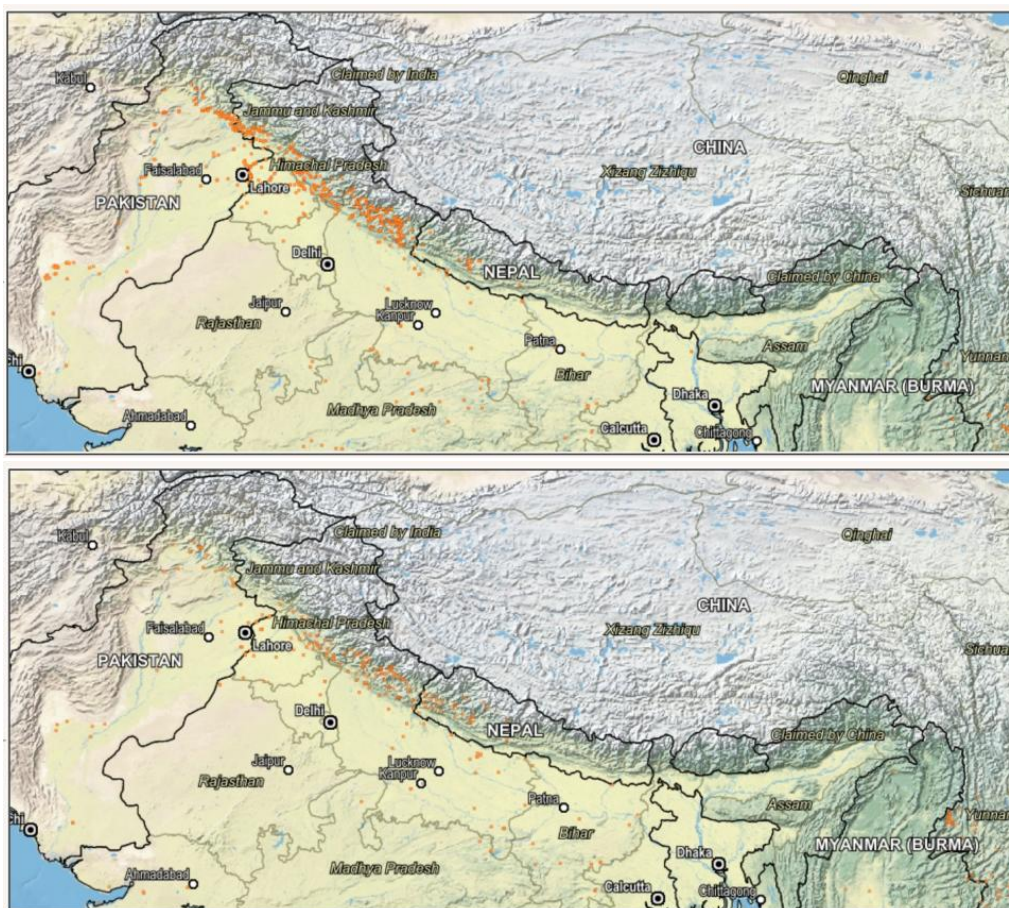


Figure R2 Maps with fire spots for the periods 1-6 (upper) and 7-12 (bottom) June 2012. Fire spots maps present the fire locations (orange dots) observed by MODIS and are produced by NASA's Web Fire Mapper (<https://firms.modaps.eosdis.nasa.gov/firemap/>).

Since pollutants from biomass burning were mixed with those from other sources and the NMC site is very distant from the biomass burning areas, we have not made quantitative comparison of observed PAN concentration with fire data. Following your suggestions we have included in the revised Figure S5 maps with fire spots for the periods 1-3 and 4-6 June 2012. We have revised the last 13 lines of the second paragraph in section 3.5 as follows:

"Northern India suffers photochemical pollution, as indicated by observations of high level of surface O_3 (Ghude et al., 2008) and tropospheric O_3 (Fishman et al., 2003). Emission inventories (Ohara et al., 2007; Zhang et al., 2009b) suggest that North India is one of the Asian emission centers for pollutants including NO_x and VOCs. In addition to anthropogenic sources, biomass burning is also an important source for PAN, and some of biomass burning plumes can penetrate the boundary layer and cause PAN formation over a large scale (Tereszchuk et al., 2013; Fischer et al., 2014; Zhu et al., 2015). Figure S5 shows tropospheric NO_2 and HCHO columns, together with maps of fire spots for 1-3 and 4-6 June 2012. As can be seen in this figure, NO_2 and HCHO in the troposphere over North India and North Pakistan were highly abundant during both periods. However, the NO_2

and HCHO levels were obviously higher during 1-3 June than during 4-6 June. The differences in NO₂ and HCHO levels might be caused open biomass burning since much more fire spots were observed during 1-3 June than during 4-6 June (see Figs. S5(e) and S5(f)). The high tropospheric NO₂ and HCHO columns suggest the presence of high concentrations of NO_x and VOCs, which may lead to rapid formation of O₃ and PAN under the summer conditions over that South Asian region. Since the region borders on the TP, it is likely that the PAN episode observed at our site during 1-6 June 2012 was mainly caused by long-range transport of plumes with high PAN and its precursors from South Asia."

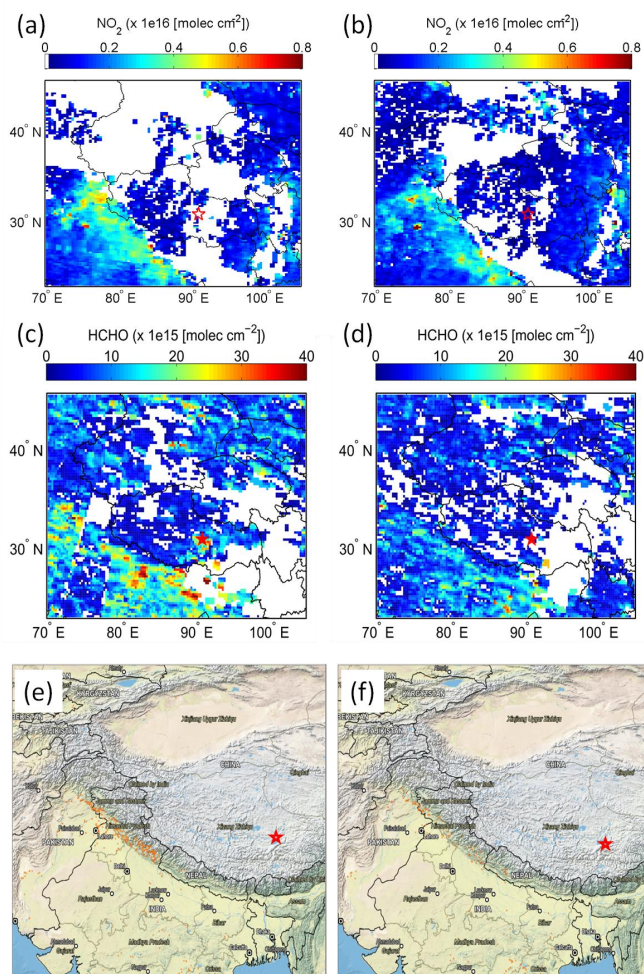


Figure S5 Average column densities of tropospheric NO₂ (a,b) and HCHO (c,d), and maps with fire spots (e,f) for the periods 1-3 (a,c,e) and 4-6 June 2012 (b,d,f). Daily tropospheric NO₂ data are from the OMI observations and made available by NASA (<https://daac.gsfc.nasa.gov/datasets>). Daily tropospheric HCHO are from GOME-2 observations and provided by the Tropospheric Emission Monitoring Internet Service (TEMIS) at The Royal Netherlands Meteorological Institute (KNMI), The Netherlands (<http://www.temis.nl/index.php>). Fire spots maps present the fire locations (orange dots) observed by MODIS and are produced by NASA's Web Fire Mapper (<https://firms.modaps.eosdis.nasa.gov/firemap/>).

2. The authors employed KNMI monthly mean tropospheric NO₂ column density

product to infer the abundance of NO_x sources over northern India. I recommend that the authors use the daily NO₂ product to show the day-to-day variability of tropospheric NO₂ column densities from June 1-12, 2012. NASA recently released its tropospheric NO₂ standard product version 3 with global gridded daily product at the resolution of 0.25° latitude x 0.25° longitude degree resolution (<https://daac.gsfc.nasa.gov/datasets>).

Response: Following your suggestion we obtained daily NO₂ data from NASA. However, the spatial coverage of the daily data is poor so that it is hardly possible to obtain reliable day-to-day variation of tropospheric NO₂ over the TP and surroundings. Therefore, we have made plots of 3-day averages of tropospheric NO₂ and HCHO, which have been included in the revised Figure S5 (see above).

3. Other possible in-situ sources for NO_x and PAN are the photolysis of nitrate in the snowpack, with deposited nitrogen sources coming from long-range transport. Since the sea level of Nam Co is over 4 km, which is similar to Summit, Greenland in the Arctic (Huang et al., 2017), I am wondering whether there is snow deposited during wintertime, and slightly melt during summer? If yes, this should be discussed as well. Huang, Y., S. Wu, L. J. Kramer, D. Helmig, and R. E. Honrath, Tropospheric ozone and its precursors at Summit, Greenland: comparison between model and observations, *Atmos. Chem. Phys. Discuss.*, doi:10.5194/acp-2017-463, 2017.

Response: Yes, snowpack at Summit, Greenland was found to emit PAN (Ford et al., 2002) and may account for the difference between observed and modeled PAN (Huang et al., 2017). Summit, Greenland is permanently covered with snow. Even though, ambient PAN over there is dominated by transport instead of snowpack emission (Ford et al., 2002). The NMC site (4.7 km a.s.l.) is about 20 km distant from the Nyainqentanglha Mountains. The yearly mean snow line altitude of the mountains was about 5.8 km a.s.l. in 2013 (Zhang et al., 2016). In summer, the snow line is even higher though snow may exist on the glaciers extending down to 5.5 km a.s.l (Qu et al., 2014). At this time, we cannot exclude the possibility that PAN may be released by the snowpack on the high mountains. However, the influence of this source on our PAN measurements might be very limited because of the large distance between NMC and the snow areas.

To discuss the snowpack influence, we have added a paragraph in section 3.1:

"It is noteworthy that the NMC site is about 20 km distant from the Nyainqentanglha Mountains. Permanent snow cover exists on the mountains. Experiments by Ford et al. (2002) indicated that snowpack at Summit, Greenland emitted PAN. Snowpack may also emit NO_x, HONO, etc., and indirectly influence the O₃ formation over Summit (Huang et al., 2017). However, the snowpack influence may only play a minor role in the budget of PAN and O₃. For example, ambient PAN over the Summit site was dominated by transport instead of snowpack emission though the site is permanently covered with snow (Ford et al., 2002). The annual mean snow line altitude of the Nyainqentanglha Mountains was about 5.8 km a.s.l. in 2013 (Zhang et al., 2016). In summer, the snow line is even

higher though snow may exist on the glaciers extending to lower elevations (Qu et al., 2014). At this time, we cannot exclude the possibility of snowpack influence on our measurements. However, this influence might be very limited because of the large distance between NMC and the snow areas. Therefore, we focus on other factors that may influence the variations of PAN and O₃ at NMC."

Technical comments:

Page 1 Line 19: PAN is an oxidant precursor. Only the peroxyacyl radical out of PAN decomposition can be as oxidant.

Response: You mean page 2 line 19. We have changed "oxidants" to "species".

Page 1 Line 21: the number and unit of tropospheric ozone radiative forcing are incorrect. Please double check.

Response: We have checked again in the cited reference (chapter 8 in IPCC AR5) and confirmed that both the numbers and unit are correct. Table 8.6 of AR5 shows that tropospheric ozone has a global mean radiative forcing of +0.40 (0.20 to 0.60) W m⁻² for the 1750-2011 period. We have been using (± 0.20) instead of (0.20 to 0.60).

Page 1 Lines 25-26: change NO_x as "nitrogen oxides (NO_x)" because it appears for the first time in the text. Same thing for NO₂ and other chemical species.

Response: Changed.

Page 1 Lines 29-32: Kramer et al. (2015) have presented 2-year in-situ measurements of PAN at Summit, Greenland whose sea level height is over 3km. I suggest the authors including this reference here, demonstrating the long lifetime of PAN and the consequences of long-range transport.

Kramer, L. J., Helmig, D., Burkhardt, J. F., Stohl, A., Oltmans, S., and Honrath, R. E.: Seasonal variability of atmospheric nitrogen oxides and non-methane hydrocarbons at the GEOSummit station, Greenland, Atmos. Chem. Phys., 15, 6827-6849, doi:10.5194/acp-15-6827-2015, 2015.

Response: Yes, this paper is cited.

Page 9 Line 21: change "calculated of" to "calculated for".

Response: Changed.

Page 12: consider changing the title of Section 3.4 as "O₃/PAN abundance from UT/LS"

Response: As pointed out by referee #1, we cannot attribute the O₃ and PAN levels observed on the ground to those in the UTLS. We have changed the title of section 3.4 to "**O₃ and PAN abundance under the impact from UTLS**", which may avoid misunderstanding. To keep consistency, we have been using UTLS instead of UT/LS.

Page 12 Line 7: delete "respectively" here.

Response: Yes, deleted.

Page 12 Lines 27-30: The transport of ozone from Stratosphere-Troposphere Exchange (STE) always accompanies with high ozone and low water vapor events, which have been illustrated in Helmig et al. (2007) and Huang et al. (2017). The authors should discuss these two previous studies, although in different locations, but in similar altitude and mechanism.

Helmig, D., Oltmans, S. J., Morse, T. O., and Dibb, J. E.: What is causing high ozone at Summit, Greenland?, Atmos. Environ., 41, 5031-5043, doi:10.1016/j.atmosenv.2006.05.084, 2007.

Huang, Y., S. Wu, L. J. Kramer, D. Helmig, and R. E. Honrath, Tropospheric ozone and its precursors at Summit, Greenland: comparison between model and observations, Atmos. Chem. Phys. Discuss., doi:10.5194/acp-2017-463, 2017.

Response: Yes, we have added here "**Observations at Summit (3212 m a.s.l), Greenland showed that air masses from the UTLS always accompanied with high ozone and low water vapor events (Helmig et al., 2007; Huang et al., 2017).**"

Page 13 Line 16: what is omega mentioned here? Please explain clearly.

Response: In this paper, omega represents vertical velocity of air parcel. The mean omega values for different grids are available in the reanalysis meteorological dataset. By analyzing the omega fields one can get an idea about air movement in vertical direction. Positive and negative omega values indicate descending and ascending, respectively. We have changed this sentence to "**Figure 7 displays the vertical velocity (omega) field and horizontal wind vectors at different times and air pressure levels, with the two cases being labeled by black rectangles (termed as Case 1 and Case 2). Positive and negative omega values indicate descending and ascending, respectively**".

Page 15 Line 6: change "Fadnavis et al., (2014" to "Fadnavis et al., 2014".

Response: Changed.

Page 16 Lines 11-14: there is some grammar issue here. Re-organize this sentence.

Response: This part has been rewritten as "**These wind fields give a clue to the origin of high level of PAN observed during 1-6 June 2012. As indicated by the wind fields in Figs. 11 and S4, after 30 May the NMC site was influenced by westerly and southwesterly winds, which could transport air masses from South Asia to the NMC site.**"

Page 16 Line 15: change "wind" to "winds".

Response: We have changed "**wind field**" to "**wind fields**".

Page 16 Line 22: what does "photochemical pollution" mean here? Please be specific.

Response: Here photochemical pollution means high levels of O₃. We have modified this sentence to "**Northern India suffers photochemical pollution, as indicated by observations of high level of surface O₃ (Ghude et al., 2008) and tropospheric O₃**"

(Fishman et al., 2003)."

Page 17 Lines 15-16: there is grammar error in this sentence.

Response: This sentence has been changed to **"Although the TP is one of the cleanest regions of the world, transport of anthropogenic pollutants to this region deserves attention."**

Page 35: there is a typo for Y-axis title in Fig. (g). Changed "wiind" to "wind". Also, I suggest to use the consistent local time, not BJT.

Response: Thank you. Changed.

Page 36: what Group 1 and Group 2 represent in the figure? This need to be clearly clarified.

Response: The selection of groups 1 and 2 is described in the first paragraph in section 3.3. We have added in the figure caption **"Groups 1 and 2 represent two groups of days with different ΔO_3 enhancement (ΔO_3) during 5:00-10:00LT, with Group 1 including 15 days with the greatest ΔO_3 (denoted as High ΔO_3 in Fig. 4) and Group 2 including 15 days with the smallest ΔO_3 (denoted as Low ΔO_3 in Fig. 4)."**

Page 38: what is the color bar unit? I suggest the authors making the colors of specific humidity bolder, which is so light and can not be seen clearly here. Perhaps change the two boxes for case 1 and case 2 in black color.

Response: The color bar unit is hPa/s. We have re-drawn this figure following your suggestions.

Figure 7 consists of two panels, (a) and (b), showing meteorological data over time and height. The y-axis for both panels is 'Level (hPa)' ranging from 100 to 500. The x-axis is 'Date'. Panel (a) covers the period from 20 May 2012 to 28 May 2012, with a specific date '30' marked. Panel (b) covers the period from 18 August 2011 to 25 August 2011, with a specific date '20' marked. Both panels display Omega (shaded regions), specific humidity (red lines), and horizontal wind field (black arrows). A color bar at the bottom indicates the unit for Omega, ranging from 0.05 to 0.4 hPa/s. Two specific events are highlighted with black boxes: 'Case 1' in panel (a) and 'Case 2' in panel (b).

Fig. 7 Omega (shaded), specific humidity (red line) and horizontal wind field in dependence of time and height in two time frames. (a) From 20 to 28 May 2012; (b) From 18 to 25 August 2011. Case 1 and Case 2 correspond to two significant downdraft events.

Page 39: in Fig. 8b, change the Y-axis label for ozone as "O3 (ppbv)" to be consistent across the whole manuscript.

Response: Changed.

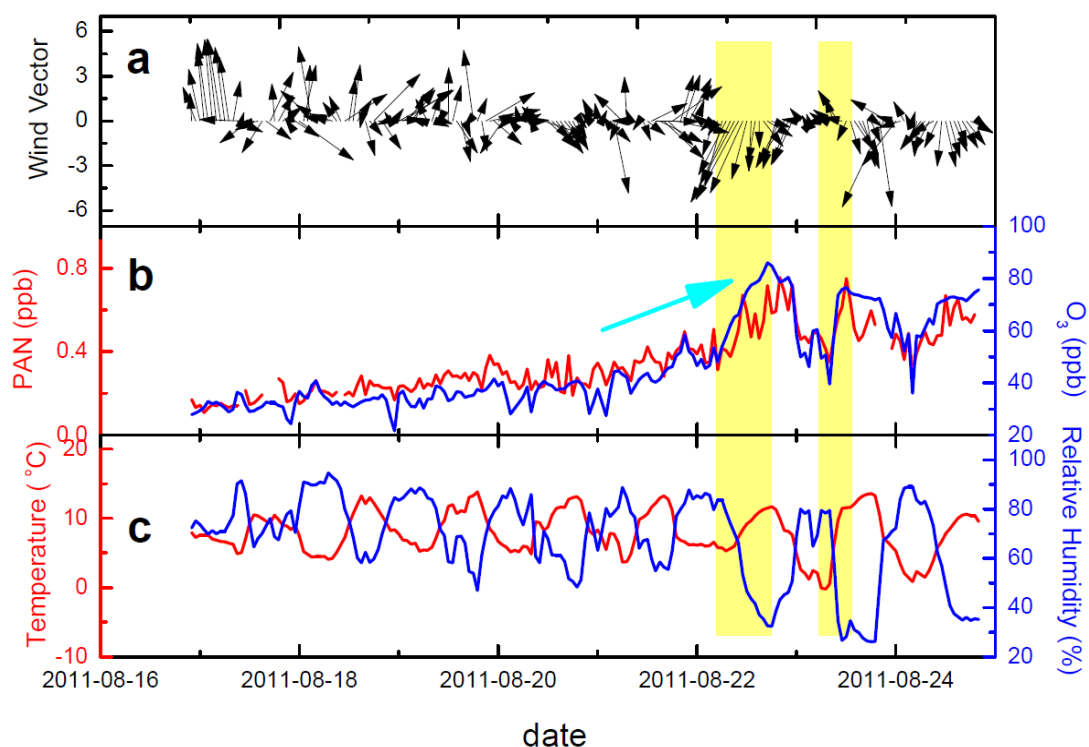


Fig. 8 Time series of (a) surface wind vectors, (b) PAN and O₃, and (c) temperature and relative humidity during 17-24 August 2011. Yellow shadows represent the short periods controlled by downward motion. The blue arrow indicates the increasing trend of PAN and O₃.

Pages 40-41: Figures 9 and 10 need to be substantially improved in quality: (1) all the fonts are so light; (2) change the BJT as LT; (3) change the caption of Figure 10 as "Same as Figure 9, but for August 22-23, 2011."

Response: We have decided to interchange Figure 9 & 10 with Figure S2 & S3. All these figures have been modified. The color for trajectories has been changed to white. The color scale has been changed. The font sizes have been enlarged.

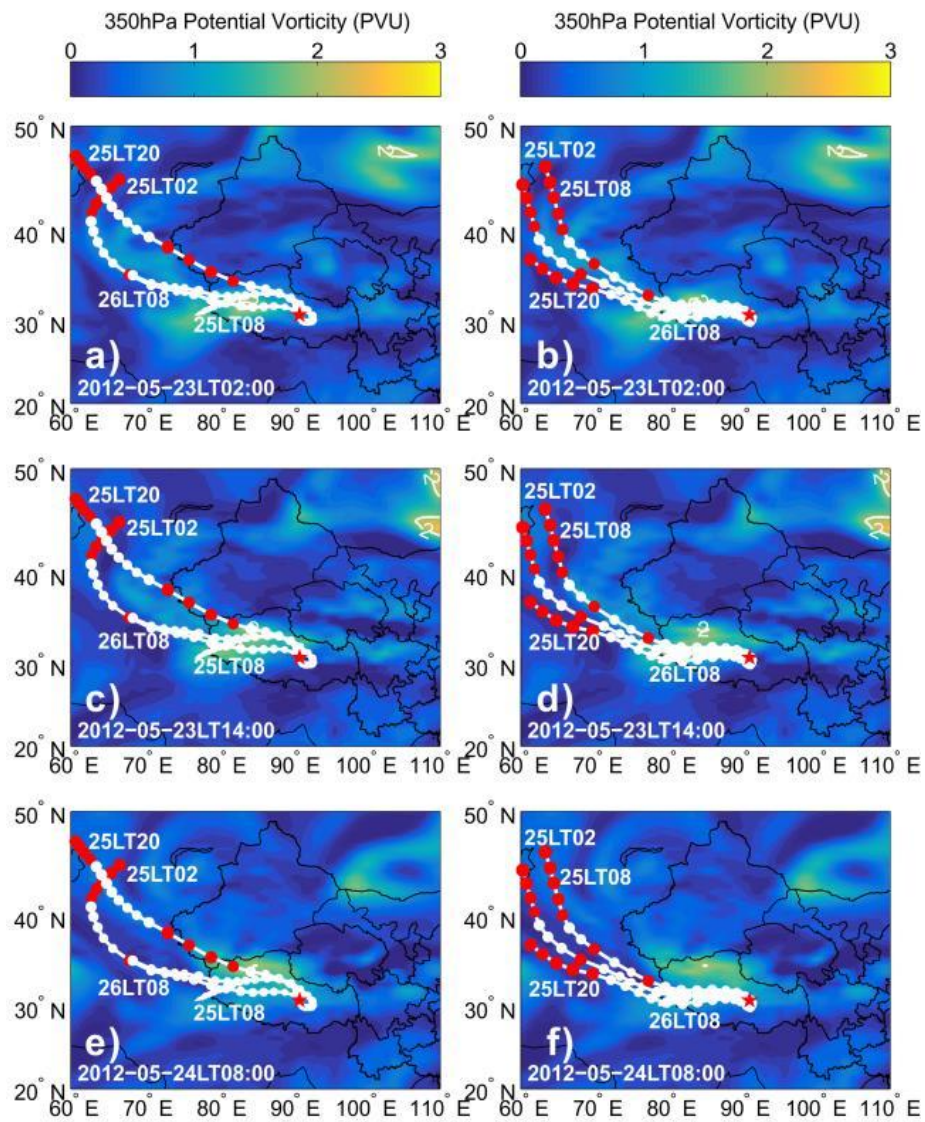


Fig. 9 Plots showing 350 hPa potential vorticity fields at three time-points during 23-24 May 2012 and back trajectories of air masses arriving at 500 m (a,c,e) and 1500 m (b,d,f) above the ground of NMC (red star) during 25-26 May 2012.

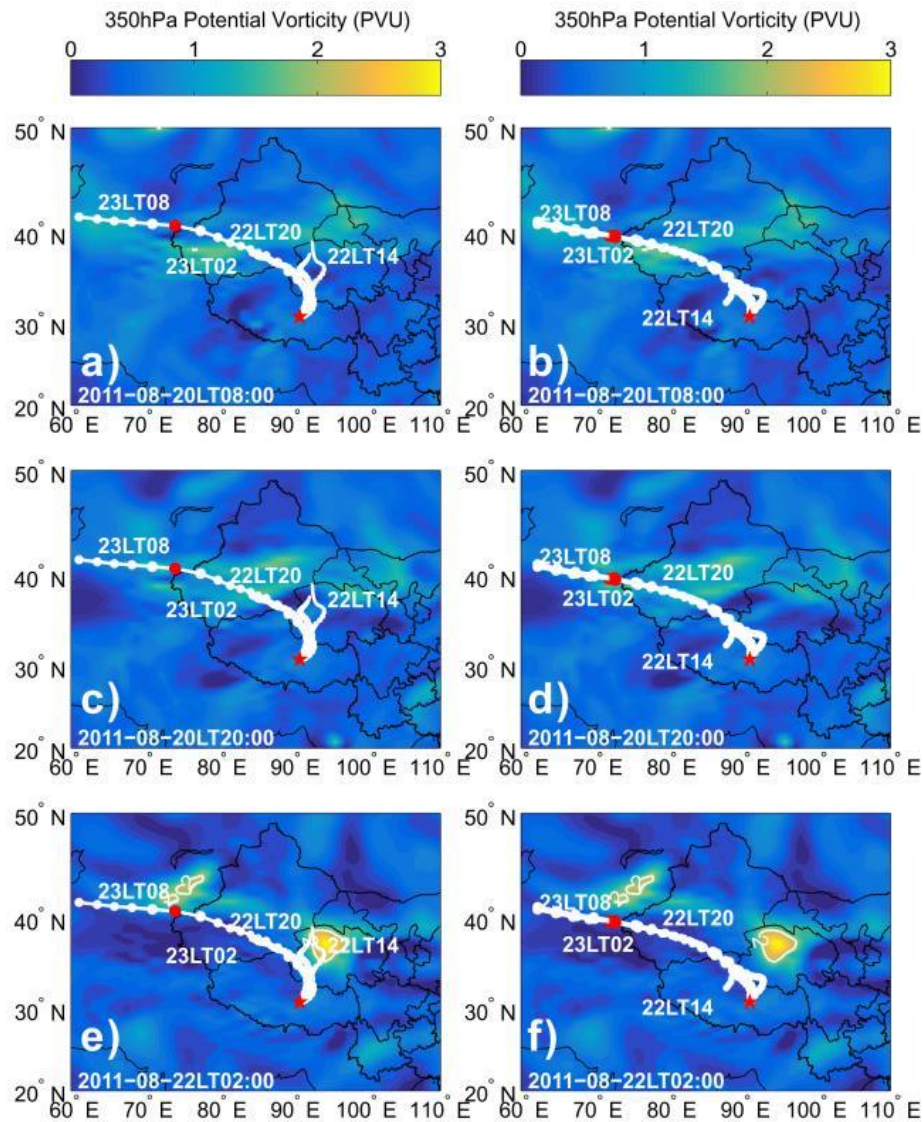


Figure 10 Same as Figure 9, but for 22-23 August 2011.

Page 43: for Figure 12, what is the color bar unit? Also, I suggest to plot the country border because it helps us to identify the origins of air masses from HYSPLIT backward trajectory.

Response: The color bar unit was meter above ground level (magl). The plots have been re-drawn to show the borders and include the color bar unit, which has been changed to km.

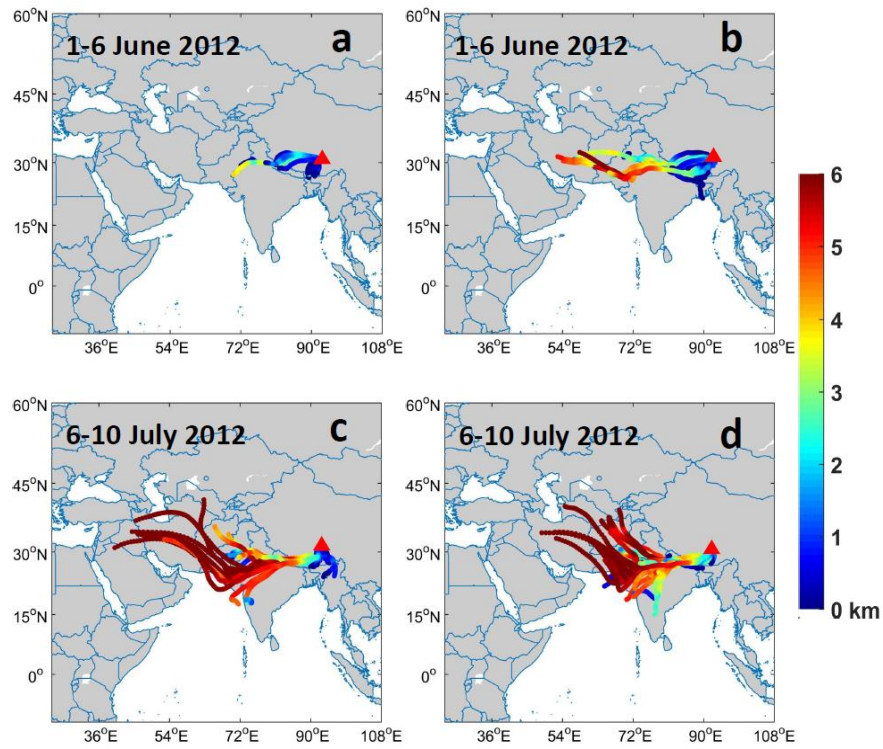


Fig. 12 Backward air trajectories arriving at NMC with endpoint heights of 500 meters (a,c) 1500 meters (b,d) for the periods 1-6 June 2012 (a,b) and 7-10 June 2012 (c,d). The color scale shows trajectory heights in km above ground level.

First simultaneous measurements of peroxyacetyl nitrate (PAN) and ozone at Nam Co in the central Tibetan Plateau: impacts from the PBL evolution and transport processes

Xiaobin Xu¹, Hualong Zhang^{1,*}, Weili Lin^{1,2,**}, Ying Wang¹, Wanyun Xu¹, and Shihui Jia^{1,***}

[1]{State Key Laboratory of Severe Weather & Key Laboratory for Atmospheric Chemistry of China Meteorological Administration, Chinese Academy of Meteorological Sciences, Beijing, China}

[2]{Meteorological Observation Center, China Meteorological Administration, Beijing, China}

[*]{now at : Guangdong Meteorological Observatory, Guangzhou, Guangdong, China}

[**]{now at: College of Life and Environmental Sciences, Minzu University of China, Beijing, China}

[***]{now at: School of Environment and Energy, South China University of Technology, Guangzhou, Guangdong, China}

Correspondence to: Xiaobin Xu (~~xuxb@camse~~xiaobin_xu@189.cn)

Abstract

Both peroxyacetyl nitrate (PAN) and ozone (O₃) are key photochemical products in the atmosphere. Most of the previous in-situ observations of both gases have been made in polluted regions and at low altitude sites. Here we present first simultaneous measurements of PAN and O₃ at Nam Co (NMC, 90°57'E, 30°46'N, 4745 m a.s.l.), a remote site in the central Tibetan Plateau (TP). The observations were made during summer periods in 2011 and 2012. The PAN ~~concentrations~~levels averaged 0.36 ppb (range: 0.11-0.76 ppb) and 0.44 ppb (range: 0.21-0.99 ppb) during ~~1617-25-24~~ August 2011 and 15 May to 13 July 2012, respectively. The O₃ ~~concentration~~level varied from 27.9 ppb to 96.4 ppb, with an average of 60.0 ppb. Profound diurnal cycles of PAN and O₃ were observed, with minimum values around 5:00 LT,

steep rises in the early morning, and broader platforms of high values during 9:00-20:00 LT. The evolution of planetary boundary layer (PBL) played a key role in shaping the diurnal patterns of both gases, particularly the rapid increases of PAN and O₃ in the early morning. Air entrainment from the free troposphere into the PBL seemed to cause the early morning increase and be a key factor of sustaining the daytime high concentrations of both gases. The days with higher daytime PBL (about 3 km) showed stronger diurnal variations of both gases and were mainly distributed in the drier pre-monsoon period, while those with shallower daytime PBL (about 2 km) showed minor diurnal variations ~~of both gases~~ and were mainly distributed in the humid monsoon period. Episodes of higher PAN levels were occasionally observed ~~occasionally~~ at NMC. These PAN episodes were caused either by rapid downward transport of air masses from the middle/upper troposphere or by long-range transport of PAN plumes from North India, etc. The maximum PAN level in the downward transport cases ranged from 0.5 ppb to 0.7 ppb ~~and may indicate the PAN abundance in the middle/upper troposphere~~. In the long-range transport case, the PAN level varied in the range of 0.63-1.0 ppb, with an average of 0.6 ppb. This long-range transport process influenced most of the western and central TP region for about a week in early June 2012. Our results suggest that polluted air masses from South Asia can significantly enhance the PAN level over the TP. As PAN act as a reservoir of NO_x, the impacts of pollution transport from South Asia on tropospheric photochemistry over the TP region deserve further studies.

1 Introduction

Peroxyacetyl nitrate (PAN) and ozone (O₃) are important oxidants-species in the troposphere. They are toxic for human and vegetation. Tropospheric O₃ contributes significantly to global warming with a radiative forcing of +40 (± 0.20) W/m² (Myhre et al., 2013). Tropospheric O₃ originates mainly from ~~the~~ photochemical reactions within the troposphere and to a lesser extent from the stratosphere (Lelieveld and Dentener, 2000), while PAN in the troposphere is nearly exclusively formed in oxidation of volatile organic compounds (VOCs) in the presence of nitrogen oxides (NO_x) (Fischer et al., 2014). PAN is produced in the association reaction between peroxyacetyl radical (CH₃C(O)O₂· (PA) and nitrogen dioxide (NO₂). As one of the key radicals, PA is produced by oxidation of a number of VOCs (Roberts, 2007; LaFranchi et al., 2009; Fischer et al., 2014). Since both VOCs and NO_x are largely emitted by anthropogenic sources, PAN is primarily produced in and downwind of industrial and

populated areas. In additional to anthropogenic sources, PAN is also formed in biomass burning plumes (Tereszczuk et al., 2013; Fischer et al., 2014; Zhu et al., 2015). With different lifetimes at different temperatures (Cox and Roffey, 1977), PAN is instable under warm conditions, but stays longer in colder environment, ~~thus~~. Due to this characteristis PAN is revealed-ubiquitous in the middle to upper troposphere (Singh, 1987; Talbot et al., 1999; Russo et al., 2003; Kramer et al., 2015); ~~ultimately resulting~~and can be transported in higher altitude in a global scale ~~transport~~. PAN can decompose and release NO₂ when it reaches warm environment, becoming one of the key sources of NO_x in remote areas. This makes PAN an important reservoir of NO₂. Inter-comparisons among models and between model and observation showed very large PAN differences in many regions of the atmosphere (Thakur et al., 1999; Sudo et al., 2002; von Kuhlmann et al., 2003; Singh et al., 2007), but confirmed the important role ~~for-of~~ PAN in sustaining O₃ production over remote regions (Hudman et al., 2004; Zhang et al., 2008). Since tropospheric O₃ and OH are principally controlled by the abundance of NO_x, decomposition of PAN would have great implications for the budget of these key atmospheric oxidants. It has been indicated that regional increase of O₃ can be attributed to an intercontinental and even global transport of PAN (Hudman et al., 2004; Fischer et al., 2011) and most of the conveying paths are in the free troposphere, driving PAN plumes travelling to remote areas (Roiger et al., 2011; ~~—~~; Pandey Deolal et al., 2013). Thus, a considerable amount of PAN has been detected in remote areas with sparse anthropogenic emission (Zanis, 2007).

Up to now the main methods to directly obtain the PAN concentration are ground-based and aircraft observations. Although PAN has been measured in a great deal of campaigns during past decades, the observational data of PAN ~~are~~have been very inhomogeneously distributed over the world, with most of them being from North America, West Europe, and Pacific region (Fischer et al., 2014). PAN measurements are extremely lacking in many areas over the Eurasian continent, northeastern African, Oceanic regions, the Indian Ocean, and the Tibetan Plateau (TP) region.

The TP region covers an area of about 2,500,000 km², with an average elevation of about 4000 m above sea level. The world's highest plateau acts as a heat ~~core~~source in summer, heating the air above and prompting its ascending motion (Yeh et al., 1957). In addition to the thermal effect, the South Asian monsoon also exerts a convergence effect driving the ascending motion (Chen et al., 2012). Accompanied by the ascending motion, water vapor

1 and air pollutants emitted or formed in the boundary layer can be rapidly transported to the
2 upper troposphere and lower stratosphere (UTLS) (Dessler and Sherwood, 2004; Gettelman
3 and Kinnison, 2004, Fu et al., 2006; Lelieveld et al., 2007; Law et al., 2010). Convective
4 transport over the TP and surrounding areas can be clearly tracked by satellite observations of
5 some longer-lived species, such as CO (Park et al., 2007, 2009), PAN (Ungermann et al.,
6 2016), CH₄ (Xiong et al., 2009) and HCN (Randel et al., 2010). Elevated concentrations of
7 some relatively short-lived anthropogenic pollutants in the UTLS region are also reported
8 (Park et al., 2008, Tian et al., 2008; Gu et al., 2016). Such rapid, upward transport of
9 pollutants and water vapor may have great implications on atmospheric composition and
10 climate of regional and global scales. Efforts have been made to understand the impacts of
11 upward transport of air masses over the TP, among which is the potential relationship with the
12 ozone valley over the TP reported by Zhou et al. (1995).

13 The TP region is very sparsely populated with nearly no industrial emissions of pollutants.
14 Although the TP has been nearly unpolluted, the high altitude and the correspondingly
15 intensified UV radiation make it an interesting region for studies of photochemical products,
16 such as O₃ and PAN. However, there have been only sparse reports of measurements of O₃
17 and related species from the TP mainly due to the poor accessibility and logistic difficulties of
18 this vast region. So far, most of the published measurements of O₃ and its precursors over the
19 TP have been from sites at the edges of the TP (Ma et al., 2002a, 2002b; Ding and Wang,
20 2006; Wang et al., 2006; Zhu et al., 2006; Cristofanelli et al., 2010; Xue et al., 2011; Zheng et
21 al., 2011; Ma et al., 2014; Wang et al., 2015b; Xu et al., 2016, [2017](#)[2018](#)). Only three
22 publications present measurements of O₃ and related species from sites in the central TP, with
23 one reporting data from urban observations (Ran et al., 2014) and two showing results from
24 remote sites (Lin et al., 2015; Yin et al., 2017).

25 Observational data of PAN from the TP are extremely lacking. The only field observation of
26 ambient PAN in the TP was made by Xue et al. (2011), who measured PAN and other
27 reactive species at Mt. Waliguan, a global atmosphere watch (GAW) station located at the
28 northeast edge of the TP. The average level of PAN was 0.44 (± 0.14) ppb for a two-week
29 period in summer 2006. This observation offers a preliminary detection of ambient PAN over
30 the northeast TP. So far, there has been no published in-situ measurement of PAN from the
31 central TP. In addition to the traditional observation methods, remote sensing techniques can
32 also be applied to acquire the global PAN distribution from satellites (Remedios et al., 2007;

Moore and Remedios, 2010; Wiegele et al., 2012; Tereszchuk et al., 2013; Fadnavis et al., 2014). However, the PAN data retrieved from satellite observations need further validations and do not cover the lower and middle troposphere.

Here we present the first simultaneous measurements of PAN and O₃ at a site in the central TP. We study the diurnal variations of observed concentrations and the links to the evolution of planetary boundary layer (PBL). We also investigate the vertical and horizontal transport and discuss the implications of our measurements.

2 Observations

2.1 Site

The observations of PAN and other species were made from 11 July to 31 August 2011 and from 15 May to 13 July 2012 at the Nam Co Comprehensive Observation and Research Station, Chinese Academy of Sciences (CAS) (NMC, 90°57'E, 30°46'N, 4730 m a.s.l.). West and north of the NMC site is the Nam Co Lake, with the nearest distance to the lake being about 1.5 km. The Nyainqentanglha mountains (about 5000-6800 m a.s.l.) stand south and east of the site, with the mountain ridge being more than 20 km distant from the site. The TP region has a population density of less than 2 person/km² (<http://sedac.ciesin.columbia.edu/gpw/>). The largest city of Tibet, Lhasa, is about 120 km south ~~from~~of the NMC site, far beyond the continuous ridges of the Nyainqentanglha Mountains. The nearest population center, Dangxiong township is located about 35 km southeast of the NMC site. The direct transport of air pollutants from Lhasa and Dangxiong is ~~hardly possible~~limited due to the blocking of the high mountain ridges. There is a road about 1.3 km southeast of the NMC site, connecting the tourism site of the Nam Co Lake to Dangxiong and the No. 109 National Road. More details about NMC and its surrounding can be found in literature (Ma et al., 2011; Lin et al., 2015; Yin et al. 2017).

2.2 Instruments and data correction

Ambient PAN was observed using a PAN analyzer (Meteorologie Consult GmbH, Germany), which consists of an automated gas chromatograph (GC) equipped with an electron capture detector (ECD) and a calibration unit. The equipment is the same one as used in previous observations in Beijing (Zhang et al., 2014) and elsewhere (e.g., Zellweger et al., 2000; Zhang et al., 2009a), with identical setup details depicted in ~~the paper~~Zhang et al. (2014). The GC

with a pre-column and a main column was optimized by the factory for the separation of PAN and CCl₄ at 15°C within 10 min. Purified nitrogen (>99.999%, Chengweixin Gases, Beijing, China) was used as carrier gas. A cartridge with CuSO₄·5H₂O was used to humidify the carrier gas before entering the GC columns. This can reduce the effects of varying humidity on the measurements (Flocke et al., 2005). Back-flushing was applied to the pre-column to prevent contamination and shorten analysis time. ~~In respect of the calibration system, a~~ An NO reference gas (4.5 ppm, Huayuan Gases, Beijing, China) in nitrogen was introduced into the calibration unit and reacts with excess acetone vapor under the UV irradiation to yield concentrated PAN. Prior to each campaign the NO reference gas was verified using an NO standard (Air Liquide America Specialty Gases LLC, USA) traceable to the National Institute of Standards and Technology (NIST) reference material. ~~Under the same~~ similar conditions, the PAN ~~standard is produced with the efficiency of~~ yield was found to be 93.92% ± 7.3% (Volz-Thomas et al., 2002). A continuous, stable flow of known PAN concentration was produced by subsequent dynamic dilution with purified ambient air and supplied to the PAN-GC for calibration. The lower detection limit was 50 ppt. Zellweger et al. (2000) achieved an overall uncertainty of ±3% under their conditions.

Surface O₃ was simultaneously observed using an O₃ analyzer (TE 49C, Thermo Environmental Instruments, Inc., USA), ~~which~~. The O₃ analyzer has a lower detection limit 1.0 ppb and precision of ±1.0 ppb. Before and after each campaign the analyzer was regularly calibrated using an O₃ calibrator (TE 49C PS) traceable to the Standard Reference Photometer (SRP) maintained by WMO World Calibration Centre in EMPA, Switzerland (Zellweger et al., 2009). All instruments were housed in a simply constructed one-storey building, located 0.15 km southeast of the station's main building. Ambient air was introduced through Teflon tubing (O.D. 1/4" and 2-3 m) to the PAN and O₃ analyzer at the flowrate of 2 l/min and 6 l/min, respectively. Meteorological data were collected using automatic meteorological station systems installed at different levels on a tower near the observation building.

Although measurements of PAN have been made previously at some ~~high-high~~ altitude sites in other areas using methods similar to ours (Ford et al., 2002; Fischer et al., 2010; Xue et al., 2011; Pandey Deolal et al., 2013), this is the first report of using the GC-ECD instrument for PAN measurement under the conditions of a high-altitude site over 4700 m a.s.l. To track the performance of the PAN analyzer, frequent calibrations were made during the campaigns (e.g., on 9 and 10 July, 7, 9, 12, 14, 17, and 23 August 2011, and on 15, 16, 28 May, 6, 13, 20, 22,

27 June, 4, 12, and 13 July 2012) except the period from 16 July to 5 August 2011, where no carrier gas was available for the PAN observation due to a leakage. During the observation period in 2011, the instrument performance was somewhat instable, probably affected by the extreme ambient conditions at the site. The variation of environment temperature is suspected to have made it hard to keep the ECD inner temperature constant. This resulted in abrupt fluctuations in the 10-min chromatographic PAN signals sometimes during the measurement period in 2011. The instable performance of ECD caused varying detection sensitivity. Normally, we convert PAN signals of air samples to concentration data based on ratios of signals to theoretical PAN concentration of the standard gas produced during the calibrations. However, the jumping sensitivity ~~makes-made~~ it improper to obtain PAN concentrations using the normal method. Thus, we applied another indirect calibration method, ~~which we call the indirect calibration~~. Our GC-ECD instrument ~~i~~was optimized for the separation and detection of both PAN and CCl₄. Therefore, it ~~is~~-was possible to indirectly calculate the PAN concentrations, i.e., by using the ratios of the PAN to CCl₄ signal. Details about the indirect calibration are given in the supplement.

Although the indirect calibration is a viable way to obtain PAN concentrations, the uncertainty of final data could be larger than the direct calibration primarily due to the two assumptions mentioned in the supplement and some technical problems with the observation system. We are more confident of the data from ~~16-17~~ to ~~25-24~~ August 2011. During this period, the instruments performed well and the two calibrations ~~before and after~~in this period gave ~~almost identical~~similar ~~sensitivity~~sensitivities. In view of this, we report and analyze in this paper mainly data from ~~16-17~~ to ~~25-24~~ August 2011, together with those obtained from 15 May to ~~10-13~~ July 2012, where our instruments ~~worked stably~~performed well.

2.3 Meteorological data and analysis

Local meteorological variables, including temperature, relative humidity, 3-dimensional winds, etc., were observed by corresponding sensors installed at 2 m, 10 m, and 20 m of the meteorological tower at the NMC station. The National Centers for Environmental Prediction (NCEP) reanalysis data, together with the local meteorological data, are used in this paper to facilitate the interpretation of our PAN and O₃ measurements. Global Data Assimilation System (GDAS, 3 hourly, 1° × 1° in longitude and latitude, and 26 pressure levels, <http://ready.arl.noaa.gov/gdas1.php>) ~~data was-were~~ obtained from National Oceanic and

Atmospheric Administration (NOAA) Air Resources Laboratory (ARL). The GDAS data were used as input to the Hybrid Single-Particle Lagrangian Integrated Trajectory (HYSPLIT) model (V4.9) for simulating backward air trajectories ending at 500 m and 1500 m above the NMC site. The HYSPLIT model is developed by NOAA/ARL (Draxler and Hess, 1997). In addition, NCEP FNL(final) Operational Global Analysis data (6 hourly, $1^{\circ} \times 1^{\circ}$ in longitude and latitude, and 26 pressure levels, <http://rda.ucar.edu/datasets/ds083.2/#!description>) were acquired from National Center for Atmospheric Research (NCAR). These data were used to obtain meteorological fields for analyzing weather patterns and air circulations over the TP.

3 Results and discussion

3.1 Surface concentrations of PAN and O₃

The PAN ~~concentration~~level averaged 0.36 ppb in the period of 16-25 August 2011, ranging from 0.11 ppb to 0.76 ppb. A clear increasing trend is found in the time series of PAN data in this period. The origin of increasing PAN in such period will be discussed in section 3.24. In 2012, the effective observation covered nearly two months (from 15 May to 13 July), long enough to obtain the PAN levels under different atmospheric conditions during the South Asian Monsoon period. The observed PAN ~~concentration~~ in this period varied from 0.16 ppb to 0.99 ppb, with an average of 0.44 ppb. This result is close to the PAN levels observed in summer 2006 at Waliguan (WLG), a remote site at the northeastern edge of the TP (Xue et al., 2011). The O₃ concentration varied from 27.9 ppb to 96.4 ppb, with an average of 60.0 ppb, nearly identical to the average O₃ level at WLG. There were little day-to-day and diurnal variations when the PAN and O₃ measurements from WLG were not impacted by relatively polluted airmasses from the eastern sector (Xue et al., 2011). In contrast, our PAN and O₃ measurements from NMC show profound variations. The reasons of the variations, particularly the diurnal variations, should be investigated.

It is noteworthy that the NMC site is about 20 km distant from the Nyainqentanglha Mountains. Permanent snow cover exists on the mountains. Experiments by Ford et al. (2002) indicated that snowpack at Summit, Greenland emitted PAN. Snowpack may also emit NO_x, HONO, etc., and indirectly influence the O₃ formation over Summit (Huang et al., 2017). However, the snowpack influence may only play a minor role in the budget of PAN and O₃. For example, ambient PAN over the Summit site was dominated by transport instead of snowpack emission though the site is permanently covered with snow (Ford et al., 2002). The

annual mean snow line altitude of the Nyainqentanglha Mountains was about 5.8 km a.s.l. in 2013 (Zhang et al., 2016). In summer, the snow line is even higher though snow may exist on the glaciers extending to lower elevations (Qu et al., 2014). At this time, we cannot exclude the possibility of snowpack influence on our measurements. However, this influence might be very limited because of the large distance between NMC and the snow areas. Therefore, we focus on other factors that may influence the variations of PAN and O₃ at NMC.

3.2 Diurnal cycles of PAN and O₃ and potential impacts from the PBL evolution

The 10-min PAN and O₃ concentrations observed in 2012 were used to obtain the averaged diurnal patterns (Fig. 2). As can be seen in Fig. 2, during night time both PAN and O₃ show a decreasing trend and reach the valley around 5:00 Local Time (LT, here LT=Beijing Time – 2h), demonstrating their steady loss during night. From 5:00 LT to 10:00 LT, both gases can be characterized by rapid increase, with the average levels of PAN and O₃ being lifted over 0.10 ppb and 15.0 ppb, respectively. Subsequently, O₃ increases at a much lower rate before reaching its peak around 16:00 LT and then starts to decline. Unlike O₃, PAN behaves more fluctuating after its peak time (around 12:00 LT), with a larger deviation from the trace of O₃.

It is noteworthy to see the sharp early-morning increase of PAN and O₃ as shown in Fig. 2. If the observed increase of both gases had been caused by photochemical productions, considerable amount of their precursors would be required to fuel the photochemical reactions. However, according to the EDGAR 3.2FT2000 database, anthropogenic emission in TP is extremely low, with emissions of NO_x and CO being respectively no more than 0.1×10^{-12} kg/m²/s and 1×10^{-12} kg/m²/s in the surrounding areas (http://themasites.pbl.nl/tridion/en/themasites/edgar—/emission_data/edgar_32ft2000/index-2.html). Surface NO_x at NMC was below the lower detection limit of the commercial NO_x analyzers like TE42CTL and Eco Physics CLD88p that we deployed there. In addition, the key condition for the photochemistry, i.e., the UV radiation, ~~is was~~ not ~~expected to be~~ strong enough to drive ~~the photochemistry~~ cal reactions in the very early morning (say around 5:00 LT), as the sunrise in that TP area occurs around 6:00 LT in summer. Therefore, it is hypothesized that the main factor driving the rapid PAN and O₃ ascending-increase in the early morning ~~is was~~ not photochemistry but the mixing process during the PBL evolution. To prove this hypothesis, we display scatter plots in Fig. 3, showing the correlations between the

increment of O_3 concentration (ΔO_3) and that of PAN concentration (ΔPAN) for two time periods of the day, and the correlation between the increments of O_3 and temperature (ΔT). Figure 3(a) represents data from the 5:00-9:00 LT period, when the solar radiation becomes gradually intensive. Figures 3(b) and 3 (c) show data from the 2:00-4:00 LT period, when no solar radiation is available for the local photochemical reactions.

Significant linear correlation between ΔO_3 and ΔPAN is found for both the early morning period (Fig. 3(a)) and the dark period (Fig. 3(b)), with correlation coefficients of 0.745 and 0.711, respectively. Although photochemical reactions, in which both O_3 and PAN are produced, can lead to ~~the a~~ ΔO_3 - ΔPAN correlation, they cannot occur during the dark period. Therefore, the significant correlation in Fig. 3(b) should be attributed to some meteorological processes instead of photochemical process. Moreover, the ΔO_3 - ΔT correlation shown in Fig. 3(c) further indicates that the concentrations of surface O_3 and PAN at the site may be ~~changed-influenced~~ purely ~~due to~~by some meteorological processes that change air temperature as well. The net change of O_3 could be positive before dawn, and occurred on those days with simultaneously rising PAN and temperature. The rising temperature could be related to the dry adiabatic heating process during air masses ~~sinking~~descending. Such a process happens when the PBL is extended, not necessarily driven by solar radiation. Downward transport of PAN and O_3 may accompany such process. Therefore, the PBL evolution might have significantly impacted the diurnal variations of PAN and O_3 at NMC.

3.3 Insight into the PBL evolution

The evolution of PBL plays one of the key roles in the diurnal variations of surface meteorological parameters and air pollutants, and is influenced by the dominating synoptic situation. It has different diurnal patterns under different synoptic situations. Here we take the O_3 enhancement (ΔO_3) in the early morning as an indicator quantity to find out major differences in the evolution of the PBL and some related parameters under different synoptic situations. We selected 30 days from the observation period in 2012 and separated them into two groups, with ~~group~~Group one-1 including 15 days with the greatest ΔO_3 values (High ΔO_3) and ~~group~~Group two-2 including 15 days with the smallest ΔO_3 values (Low ΔO_3). For the two groups, average diurnal variations were calculated ~~offor~~ PAN, O_3 and some meteorological parameters, i.e., wind speed at 2 m above ground (W_s), U wind speed at 2 m above ground (U_s), V wind speed at 2 m (V_s), the ratio between the 2-m and 10-m wind

speeds (WSR), the temperature difference between 20 m and 10 m (TD), and water vapor pressure (WVP). The obtained diurnal variations are plotted in Fig. 4.

A stable nocturnal boundary layer (NBL) forms gradually in the night (Stull, 1988). A temperature inversion can occurs in the NBL, with the air temperature increasing with height. A nocturnal jet may form over the NBL so that a larger gradient of wind speed may exists in the NBL. Such stratification prevents the air from being vertical mixed in the night and is broken in the early morning. As a result, the concentrations of O₃ and PAN at the ground-level decrease largely in the nighttime because of chemical and physical losses and increase rapidly in the early morning because of the downward mixing of upper-level air containing more O₃ and PAN. This evolution of PBL, however, can be strongly impacted by some systematic processes so that the day-night differences of PBL are weakened or even disappear. We believe that the two groups of data presented in Fig. 4 represent approximately two circumstances of the PBL evolution, with the High-ΔO₃ group being less or not impacted and the Low-ΔO₃ group being strongly impacted by the systematic processes.

As can be seen in Fig. 4, the Low-ΔO₃ group showed much smaller diurnal variations of PAN, O₃, Ws, WVP, and WSR, suggesting a weak day-night cycle of the PBL. Compared with the values in the Low-ΔO₃ group, the nighttime values of PAN, O₃, Ws, and WSR in the High-ΔO₃ group were much lower, and that of TD much higher. Lower WSR and higher TD in the night indicate a more stable NBL, which explains the lower PAN and O₃ levels as discussed above. After dawn the values of PAN, O₃, Ws, WSR, and TD in the High-ΔO₃ group changed rapidly back to their daytime levels, indicating the break of the stable NBL. It is noteworthy that there were virtually no or only minor differences in the daytime values of PAN, Ws, WSR, and TD between the two groups. The daytime O₃ in the High-ΔO₃ group reached significantly higher levels than that in the Low-ΔO₃ group. Moreover, the WVP value in the High-ΔO₃ group was lower than that in the Low-ΔO₃ group during the entire day. These phenomena imply that the High-ΔO₃ group is related to drier days and PBL conditions favoring the increase of surface O₃ during daytime (e.g., through downward mixing) and destruction during nighttime, while the Low-ΔO₃ group is related to more humid days and PBL conditions that inhibit the variation of surface O₃.

The PBL evolution was investigated in previous field experiments in the TP. Li et al. (2011) found that there were some differences in the diurnal evolution of the PBL structure between dry and rainy seasons. In the dry season, namely the pre-monsoon period, a shallow but strong

inversion layer could be clearly observed at night. The occurrence of the inversion layer is high in the pre-monsoon period, simply because the PBL structure is primarily driven by sensible heat (Ma et al., 2005). The outflow of sensible heat at night is massive according to thermal analysis. In the rainy season, a shallower but more persistent wet convection evolves, forcing efficient exchange of quantities and also comparably smaller gradients of meteorological elements. The daytime PBL height can reach 4-5 km above the ground in the dry pre-monsoon period, while it is usually about 1-2 km above the ground in the wet monsoon period (Li et al., 2011; Chen et al., 2013). In our case, prevailing monsoonal features are perceivable in meteorological measurements associated with the Low- ΔO_3 group, such as ~~the weaker westerly wind~~ (U wind, Fig. 4(g)), stronger southerly wind (V wind, Fig. 4(h)) and higher WVP (Fig. 4(d)). Unlike the dry season, the convection intensity in the wet season ~~has had~~ a much smaller diurnal variation, as suggested by the smaller day-night differences of WSR and TD. Thus, in the wet season, downward transport of PAN and O_3 during nighttime ~~may might have been~~ much more effective than that in the dry season. This can explain the observed nighttime differences in the PAN and O_3 concentrations between the Low- ΔO_3 and High- ΔO_3 groups (Figs. 4(a) and 4(b)).

To know more details about the two groups of days discussed above, the distribution of the ~~two groups of~~ Group 1 and Group 2 days, together with parameters including the PBL height, precipitable water of entire atmosphere (PWAT), WVP, and the PAN and O_3 concentrations are shown in Fig. 5. The PBL height and PWAT values are obtained from the NCEP FNL reanalysis data. It can be seen that the surface measured WVP is in good accordance with the PWAT in trend. The whole observation period in 2012 can be divided into dry period and wet period. The transition between the wet and dry periods can be easily identified based on the changes of the PBL height, and the PWAT and WVP values. It can also be seen in the variation of the daily rainfall at NMC (Fig. S1). We can see a sudden seasonal change in the middle of June, when the depth of PBL was suppressed after 16 June 2012 (marked with green bar in Fig. 5) and the water amount became more abundant, suggesting the onset of the South Asian monsoon. The distributions of the two groups of days are labeled on Fig. 5(a). Although there are some irregular cases, the High- ΔO_3 days (~~group~~ Group 1) are mostly distributed in the dry period and the Low- ΔO_3 days (~~group~~ Group 2) in the wet period. This supports our analysis in previous paragraph. The time series of the PBL height indicates that the daily maximum PBL heights in the dry period were much higher than those in the wet

period, with only a few exceptions. Such phenomenon agrees with the observational results from Naqu, about 230 km northeast of NMC (Li et al., 2011). The nocturnal PBL height in the dry period could be extremely low (frequently lower than 200 m). This explains the lower nighttime PAN and O₃ values in the High-ΔO₃ group (Fig. 4).

In the pre-monsoon there may be episodes with monsoon features. An example of this is the period of a few days around early June 2012, where the PBL height was considerably suppressed, and the PWAT, WVP as well as the concentrations of PAN and O₃ were significantly enhanced (Fig. 5). In this relatively humid episode, the nighttime concentrations of PAN and O₃ were largely elevated, which may be attributable to the PBL structure and airmasses transported from the polluted region (see section 3.5).

In conclusion, the South Asian monsoon brings not only more water vapor over the central Tibet area but also effectively drives the PBL evolution, which plays an important role in shaping the diurnal patterns of PAN and O₃ at the NMC site.

3.4 PAN abundance in upper levels O₃ and PAN abundance under the impact from UTLS

It is noticeable in Fig. 4 that the levels of daytime O₃ were considerably different between the two groups, while those of daytime PAN were close to each other. In the average diurnal curves of O₃ and PAN shown in (Fig. 4), The-the highest hourly O₃ levels concentrations for the two gGroups 1 and 2 were 69.7±2.4 ppb and 59.0±2.5 ppb, respectively, and the highest hourly PAN concentrations levels were 0.48±0.02 ppb and 0.49±0.05 ppb, respectively. Observations at WLGXue et al. (2011) pointed-outshowed that air masses from higher altitudes (i.e., upper troposphere/lower stratosphere, UT/LS) could have significant impact on surface contained higher O₃ and lower PAN in the plateau (Xue et al., 2011). As shown in Fig. 5, the daytime PBL heights in group-Group 1 could extend to reach much higher altitudes than those-that in group-Group 2, indicating a higher probability of downward mixing of O₃-richer air from the middle and upper troposphere on the days in group-Group 1. Therefore, the higher daytime O₃ value for gGroup 1 is qualitatively consistent with the observational results from WLG (Xue et al., 2011). Only negligible distinction of daytime PAN was found between the two groups-1 and 2, implying that on average, The-air masses from higher altitudes seemed-did not to-cause additional-increase-in-the-lower or higher daytime level-of-surface PAN, as suggested by the negligible distinction of daytime PAN between groups 1 and 2.

To gain more insight in air masses from upper origins, we attempt to label the upper-differentiate air masses originated in the upper troposphere in the whole observation periods from other air masses. Following the categorizing way in section 3.3, scatter plots of PAN-O₃, WVP-O₃, and WVP-PAN are shown in Fig. 6 for the two groups. Since we have confirmed the meteorological features associated with both groups, some relationship characteristics could be well comprehended. Surface O₃-levels of air pollutants at any sites depend mainly on local chemistry, transport and dry-deposition. Since the TP is a pristine and high-altitude region with little emissions of O₃ and PAN precursors, local chemistry cannot cause large day-to-day variations in O₃ of these species, as shown in Ma et al. (2002b). Therefore, a large fluctuation in the daytime O₃-levels indicates usually a substantial change of transport contribution to O₃, particularly vertical transport. In general, the O₃ level increases from the ground to the UTLS. Suppose photochemistry did not vary considerably, the amount of O₃ could in some degree represent the impact of upper airmass. Using the Tropospheric Emission Spectrometer (TES) observations, Worden et al. (2009) elaborately depicted the 3-dimensional distribution of tropospheric O₃. This is also true over the TP and its surrounding areas, as shown by Worden et al. (2009), which shows a gradual increase of the O₃ concentration with height under tropopause and a steep increase from upper troposphere to lower stratosphere. In some cases, air masses in the UTLS with O₃ close to or higher than 100 ppb can be downward transported to near ground, causing high surface O₃ events. Such cases have been often observed at high altitude sites (Ding and Wang, 2006; Wang et al., 2006; Helmig et al., 2007; Cristofanelli et al., 2010; Lefohn et al., 2012; Ma et al., 2014; Huang et al., 2017; Xu et al., 2018) and occasionally also at some low altitude sites (e.g., Lefohn et al., 2012). Thus, surface O₃ concentration observed at sites in the TP region can sometimes be used as an indicator of air masses from the higher altitudes and also reflects the depth of developed PBL. Observations at Summit (3212 m a.s.l), Greenland showed that air masses from the UTLS always accompanied with high ozone and low water vapor events (Helmig et al., 2007; Huang et al., 2017). As the WVP profile over the TP shows a clear decrease with height (Chen et al., 2013), air masses from high altitudes over the TP can also be indicated by lower WVP.

To gain more insight in air masses from upper origins, we attempt to differentiate air masses originated in the upper troposphere from other air masses. Following the grouping of days in section 3.3, scatter plots of PAN-O₃, WVP-O₃, and WVP-PAN are shown in Fig. 6 for the two groups. The data points within the red rectangle in Fig. 6(c) are measurements associated

1 with higher O₃ levels and lower WVP. We consider these as measurements with significant
2 features of middle/upper tropospheric air since they are above the highest average hourly O₃
3 level (69.7 ppb) shown in Fig. 4(b) and associated with WVP < 500 Pa.

4 Fig. 6(b) displays a good positive PAN-O₃ correlation for ~~group~~ Group 2, which is consistent
5 with simultaneous photochemical production of both secondary ~~oxidants~~ pollutants. However,
6 the dataset from ~~group~~ Group 1 shows a much weaker PAN-O₃ correlation (Fig. 6(a)),
7 indicating a ~~more obscure~~ weaker relationship between PAN and O₃ altitude in ~~group~~ Group 1.
8 Nearly no correlation between PAN and WVP is found (Fig. 6(e)), ~~supporting the above~~
9 ~~viewpoint~~. At present, the actual causes of the poor PAN-O₃ and PAN-WVP correlations are
10 unknown. However, it is reasonable to believe that on the days in ~~group~~ Group 1, the
11 observed O₃ level was more influenced by air masses from ~~the upper troposphere/lower~~
12 ~~stratosphere~~ UT/LS, where the O₃ level is higher ~~(Worden et al., 2009) but and~~ the PAN level
13 ~~is lower than at the surface~~ (Worden et al., 2009; Moore and Remedios, 2010). In addition, it
14 is suspected that the horizontal variability of PAN ~~is~~ was larger than that of O₃ during our
15 observations.

16 Figure 6 does not allow for an ~~The ambiguity in the relationship between PAN and altitude~~
17 ~~makes it impossible to estimate~~ of the PAN abundance in upper levels ~~simply from the data~~
18 ~~shown in Fig. 6. Nevertheless~~ However, we can make use of some cases with deep convection
19 and apparent downward transport activities in the dry period. Here we try to deduce the
20 origins of air masses in two cases and roughly estimate the PAN concentrations associated
21 with air masses in ~~from~~ upper levels. The two cases chosen for analysis are 25 May 2012 and
22 24 August 2011. Figure 7 displays the vertical velocity (omega) fields and horizontal wind
23 vectors at different times and air pressure ~~height~~ levels, with the two cases being labeled ~~by~~
24 with red-black rectangles (termed as Case 1 and Case 2). Positive and negative omega values
25 indicate descending and ascending, respectively. Both cases ~~are~~ were ~~segments of the~~ from dry
26 periods, when the PBL could reach higher heights and favor the entrainment of upper air-
27 masses.

28 Figure 7(a) shows that positive omega dominated the PBL from early 25 May 2012 to early
29 26 May 2012 (Case 1), with the range of higher omega (>0.1 ~~mhPa/s~~) extending from surface
30 to 350 hPa, and a distinct valley of specific humidity line of 2g/kg, indicating a strong
31 downward ~~motion~~ core transport. In response to this downward transport, PAN and O₃ were
32 both elevated to higher levels and WVP ~~dropped~~ decreased to about 200 Pa (Fig. 5). A similar

~~downward motion core case~~ occurred ~~on~~ during 22-23 August 2011 (Case 2), as shown in Fig. 7(b). ~~The downdraft motion core~~ On 22 August, the height with descending air extended from the ground up to 300 hPa and lasted all day long, with very high intensity ($\omega > 0.4$ 3 mhPa/s) ~~after the noontime~~. For better understanding of Case 2, we display in Fig. 8 the time series of O_3 , PAN, and related meteorological parameters during 16-25 August 2011 ~~in Fig. 8~~. ~~There was a rapid rising trend of the~~ The O_3 and PAN levels increased rapidly on 22 August 2011, as indicated by the arrow in Fig. 8(b). In parallel with ~~this trend~~ the increases of O_3 and PAN levels, relative humidity and wind vector changed ~~sharp~~ rapidly, with the former dropping dramatically from 80% to about 30% and the later turning from southerly to northerly. Similar rapid variations were also observed partly during 23-24 August 2011, corresponding to the subsiding of dry air masses (Fig. 7(b)).

It is noticeable that the daytime levels of O_3 and PAN did not show much distinction among the days from 22 to ~~25-24~~ August 2011. This suggests that the air masses ~~measured arriving at our site~~ during the period might originate from ~~the~~ similar height and area. To prove this, we calculated backward trajectories with endpoints at 500 m and 1500 m above the ground of the NMC site. Some of the trajectories for the two selected cases, 25 May 2012 (Case 1) and 22 August 2011 (Case 2), are plotted in Figs. 9 and 10, respectively, overlaying on the ~~250-350~~ hPa potential vorticity (PV) fields at three time points during 23-24 May 2012 (for Case 1) and during 20-22 August 2011 (for Case 2), respectively. Similar plots with the same trajectories and ~~350-250~~ hPa PV fields are shown in Figs. S2 and S3 for Case 1 and Case 2, ~~respective~~ respectively. In both cases stratospheric intrusions occurred as indicated by the higher PV values (>2). In Case 1 (Figs. 9 and S2) higher PV covered the zone from 30°N to beyond 50°N. In Case 2 (Figs. 10 and S3), higher PV extended from about 40°N to beyond 50°N. In both cases air masses arrived ~~arriving~~ at the NMC site originated from or travelled through the zones between 350 hPa and 250 hPa that were obviously impacted by stratospheric intrusions. Therefore, the PAN and O_3 measurements in both cases were influenced by ~~upper level~~ air masses that contained stratospheric air from the UTLS. In addition to ~~this the~~ transport feature, the ~~rapidly increasing~~ elevated O_3 and ~~decreasing~~ decreased water vapour amount in surface air also indicate ~~that surface air masses originated impacts of from high level air masses~~. For Case 1 and Case 2, the PAN ~~concentration level~~ was elevated respectively up to 0.52 ppb and ~~0.6-0.72~~ ppb, which can be regarded as the estimated maximum PAN levels observed under the high altitudes (around 350 hPa) impact from UTLS.

Table 1 summarizes the PAN levels in the upper troposphere over the TP. A prominent progress in detection of global upper tropospheric PAN is based on the application of infrared spectrometers. There exists some detection error as retrieval band of PAN would inevitably be contaminated by irrelevant compounds, such as water vapor and CCl₄ and the variability of some atmospheric parameters would also bring interferences (Remedios et al., 2007). In summer, there exists more uncertainty using remote sensing method due to higher amount of water vapor over the TP region; hence a direct comparison with field measurement is required. According to the satellite results (Moore and Remedios, 2010), the retrieved PAN levels at 333 hPa and 234 hPa in March 2003 were in the ranges of 0.3–0.5 ppb and 0.15–0.2 ppb, respectively, implying a decreasing trend of the PAN concentration along height in the upper troposphere. In August 2003 the PAN levels at 278 hPa and 185 hPa did not show evident increment compared with March 2003. Model results from Fischer et al. (2014) show similar ranges of PAN levels. The trajectories shown in Figs. 9, 10, S2 and S3 indicate that air masses could originate from the upper troposphere (~350 hPa), thus could well match the other observation heights listed in Table 1. Our estimates of PAN level are close to or greater than the upper ranges of the PAN levels reported in the literature (Glatthor et al., 2007; Moore and Remedios, 2010; Wiegele et al., 2012; Fadnavis et al., (2014; Fischer et al., 2014). Taking into account the thermal decomposition and photolysis of PAN during the transport, the actual PAN levels in the upper troposphere could be higher than our estimates. Therefore, the retrieval from MIPAS-E measurements might have underestimated the PAN level in the upper troposphere.

Moreover, an enhancement of PAN was observed during 21–26 August 2011, with a range of 0.6–0.7 ppb, indicating that PAN was accumulated in an elevated level in later summer. Such PAN level was not acquired by Moore and Remedios (2010) who reported a maximum of PAN of 0.5 ppb in August, implying again the possibility of underestimation of PAN in satellite retrieval. It is noted that the satellite observations were made years before our measurements. Any potential long-term changes or interannual variations in PAN may also cause some differences. Fadnavis et al. (2014) reported a maximum increase rate of 4.5 ± 3.1 ppt yr⁻¹ for PAN in the UTLS over the Asian summer monsoon region in the summer monsoon season during 2002–2011. However, such small trend in PAN cannot explain the above discrepancy.

3.5 A PAN episode driven by South Asian monsoon

In warm environment, PAN is short-lived. Below 7 km, thermal decomposition is the main loss process of PAN (Talukdar, 1995). Thus, although polluted air masses from south of the Himalayas can be transported to the TP along the monsoon stream, PAN in the air masses may experience ~~great-significant~~ loss during the travelling. Cox and Roffey (1977) estimated the lifetime of PAN at 25 °C to be about 2.7 h and 0.7 h for urban and rural daytime conditions, respectively, and that at 15 °C a factor of four longer. During our observations in summer 2012, surface air temperature at NMC varied from -0.5 °C to 19.4 °C, with an average of 8.4 °C. Thermal decomposition should be much slower under such temperature condition and only important during warmer daytime periods. However, thermal decomposition might still have removed a significant fraction of PAN during the long-range transport, particular over the warm low-elevation areas. The level of PAN observed at our site was the remaining PAN in the air masses, which should be significantly lower than that in the formation area. Nevertheless, PAN episodes ~~can-be-were~~ observed under certain meteorological conditions. One of such episodes occurred in early June 2012. As can be seen in Fig. 5, the PAN level humped during 1-6 June 2012, ~~with some diurnal variations~~. The maximum PAN level reached 1.0 ppb, and the diurnal minima on these days were even higher than the diurnal maxima on many of other observation days. The origin of the high PAN ~~concentrations-levels~~ deserves an investigation.

Data in Fig. 5 indicate that the monsoon flow prevailed persistently after the middle of June 2012, and there were also some features of monsoon impact during 1-6 June 2012 when the PAN level was increased to near 1 ppb. After this abrupt rising, PAN dropped down to much lower level, suggesting a substantial change in air mass. To understand this phenomenon, we calculated average fields of wind, relative humidity, and omega at sigma=0.995 for the periods 30-31 May using the FNL reanalysis data. During 30-31 May 2012, the major part of Indian subcontinent was controlled by an anticyclone system and a large convergence zone formed over the central TP (see Fig. S4). The NMC site was within this convergence zone and obviously influenced by airflow from North India. Figure ~~40-11~~ shows the average wind fields for 12:00 (UTC) of 4, 5, 7 and 8 June 2012. These wind fields give a clue to the origin ~~can help us to understand the~~ of high level of PAN observed during 1-6 June 2012. As indicated by the wind fields can be seen in Figs. 11 and S4, ~~the week~~ after 30 May the NMC site was ~~under the control of a large convergence zone and~~ influenced by westerly and

southwesterly winds, which could transport air masses from ~~North India~~South Asia to the NMC site. After this period, the site was influenced by significantly different air masses. For example, the average wind fields shown in Figs. 11c and 11d indicate that after 7 June 2012, strong southerly and southeasterly winds developed over East India and Southeast Nepal, and southerly wind prevailed over the area surrounding NMC ~~was controlled by southerly wind,~~ which promoted the transport of air masses from the Bay of Bengal. Although most of the central and western TP was ~~still under the control of~~within the convergence zone, NMC and its surrounding were outside of its direct impact. Such change in air masses arriving NMC inevitably caused substantial differences in photochemistry. ~~As indicated by observations (Ghude et al., 2008; Fishman et al., 2003),~~ Northern India suffers photochemical pollution, As indicated by observations of high level of surface O₃ (Ghude et al., 2008); and tropospheric O₃ (Fishman et al., 2003). Emission inventories (Ohara et al., 2007; Zhang et al., 2009b) ~~suggest indicate~~ that North India is one of the Asian emission centers for pollutants including NO_x and VOCs. In additional to anthropogenic sources, biomass burning is also an important source for PAN, and some of biomass burning plumes can penetrate the boundary layer and cause PAN formation over a large scale (Tereszczuk et al., 2013; Fischer et al., 2014; Zhu et al., 2015). Tropospheric NO₂ and HCHO can be derived from satellite observations based on the DOAS technique (Boersma et al., 2011; De Smedt et al., 2008, 2012). Figure S5 shows tropospheric NO₂ and HCHO columns ~~during June, 2012, made available by the Tropospheric Emission Monitoring Internet Service (TEMIS) at The Royal Netherlands Meteorological Institute (KNMI), The Netherlands (http://www.temis.nl/index.php)~~together with maps of fire spots for 1-3 and 4-6 June 2012. As can be seen in this figure, ~~both~~NO₂ and HCHO in the troposphere over North India and North Pakistan were highly abundant ~~induring both periods June, 2012.~~ However, the NO₂ and HCHO levels were obviously higher during 1-3 June than during 4-6 June. The differences in NO₂ and HCHO levels might have been caused by open biomass burning since much more fire spots were observed during 1-3 June than during 4-6 June (see Figs. S5(e) and S5(f)). ~~The high NO₂ and HCHO concentrations e high tropospheric NO₂ and HCHO columns suggest the that presence the of high concentrations of NO_x and VOCs over the North India region were high., which NO_x and VOCs are species for photochemical reactions may leading to rapid formation of O₃, and PAN, etc under the summer conditions over the South Asian region. Since this region borders on the TP. Therefore,~~ it is likely that the PAN episode

observed at our site during 1-6 June 2012 was mainly caused by long-range transport of plumes with high PAN and its precursors from North India/South Asia.

To further support the above view, we made calculations of backward air trajectories. The results are presented in Fig. 12. The 5-day trajectories were calculated for endpoints at 500 m and 1000 m above ground for 1-6 June and 7-10 June 2012, respectively. Obviously, air trajectories arriving NMC during 1-6 June were quite different from those during 7-10 June, particularly those with endpoints at 500 m (Figs. 12a and 12c). About a half of the trajectories during 1-6 June originated from or moved through the PBL over North India (Fig. 12a), while nearly none of the trajectories during 7-10 June had an opportunity to pass through the PBL over North India (Fig. 12c). Most of the trajectories during 7-10 June originated either from the free troposphere over western Asia and Indian subcontinent or from the PBL south of NMC. Forward trajectories were also calculated for air masses originated from matrices of locations in the domains west and south of the NMC site. Examples of forward trajectories matrices are shown in Figure S6 for trajectories starting at 0600 UTC 3 June 2012 and 08 UTC 8 June 2012. The trajectories clearly indicate that the NMC site was impacted by air masses from different areas before and after 6 June. Around 4-5 June 2012, NMC was mainly impacted by air masses from the SW-W sector (North India, North Pakistan, and Nepal). Around 9-10 June, however, NMC was mainly impacted by air masses from the S-SW sector (Bangladesh, Bhutan, etc.). These results are consistent with those from the backward trajectories in Fig. 12. These-The above analysis can explain the sudden decrease of the PAN level after 6 June 2012 on one hand, and on the other hand support the idea that the PAN episode observed during 1-6 June 2012 was mainly caused by plumes from North India, North Pakistan, and Nepal.

Although the TP is one of the cleanest regions of the world, transport of anthropogenic pollutants to this region deserves attention. Some recent studies have showed that air pollutants can be transported to the Himalayas or to the TP region through passes like river valleys from the surroundings (Cong et al., 2007; Cong et al., 2009; Bonasoni et al., 2010; Kopacz et al., 2011; Lüthi et al., 2015; Shen et al., 2015; Zhang et al., 2015). The main source regions are South and East Asia. During the South Asian monsoon, the TP is predominately influenced by air masses from the Indian subcontinent. Impacts of transported pollutants on atmospheric environment over the Himalayas and TP, particularly the climate and hydrological effects of deposition of black carbon and other substances on Himalayan glaciers,

have caused concerns (Ramanathan et al., 2007; Ming et al., 2012; Zhao et al., 2013; Qu et al., 2014; Wang et al., 2015; Zhang et al., 2015).

So far, studies of pollutants transport ~~of pollutants~~ to the TP and its effect ~~have~~ are mainly ~~about~~ focused on aerosols (compositions and optical depth) and less attention has been paid to the transport of gaseous pollutants. There has been no previous report about impacts of long-range transport of pollutants on tropospheric photochemistry over the central TP region. Our results show, for the first time, that long-range transport of polluted air masses from North India and other South Asian areas can significantly enhance ambient level of PAN at NMC. Although we have no observational data of PAN from other sites in the TP, it is likely that the entire convergence zone in the central and western TP (Figs. ~~10-11~~ and S4) was more or less impacted by the pollutants from North India, South Asia. This implies that photochemistry over a large area in the TP was probably disturbed for at least ten days in the cases shown in Figs. 11 and S4. PAN transported to the TP region may be thermally and/or photolytically decomposed to release NO_x, acting as a chemical source of atmospheric NO_x over the TP, a region with very little anthropogenic emission of NO_x. The impacts of the transport of PAN and other related species on tropospheric photochemistry over the TP need to be studied in the future.

3.6 PAN levels at different heights over the TP

In addition to this study, in-situ PAN measurements from the TP are only reported by Xue et al. (2011). As PAN is a key source of NO_x in remote regions, its concentration and distribution are important for understanding the photochemistry over regions like the TP. Here we provide a collection of PAN data for the TP region.

Table 1 summarizes the PAN data available for the TP from in-situ observations, satellite and space shuttle observations, and model simulations. Based on our in-situ observations at NMC (4.7 km), we obtained an averaged PAN level of 0.36 ppb for 17-24 August 2011 and 0.44 ppb for 15 May - 13 July 2012. In-situ observations at WLG (3.8 km) found an average PAN level of 0.44 for the period from 22 July to 16 August 2006 (Xue et al., 2011). The limited in-situ observations in the surface layer do not show substantial spatial and temporal differences in average level of PAN. However, the PAN level did show significant increases in some cases with obvious transport impacts from the UTLS (e.g., 22 August 2011) and from South Asia (e.g., 1-6 June 2012).

Developments in remote sensing have made it possible to detect global PAN in the UTLS from the space. During 9-13 August 1997, observations using the Cryogenic Infrared Spectrometers and Telescopes for the Atmosphere (CRISTA) aboard the Space Shuttle showed PAN levels in the range of 0.1-0.2 ppb for 18 km over the TP (Ungermann et al., 2016). Based on the retrievals of satellite observations using the Michelson Interferometer for Passive Atmospheric Sounding (MIPAS), the average PAN levels in March 2003 were in the ranges of 0.15-0.23 ppb for 234 hPa and 0.35-0.45 ppb for 333 hPa over the TP, and those in August 2003 in the ranges of 0.15-0.23 ppb for 185 hPa and 0.35-0.50 ppb for 278 hPa (Moore and Remedios, 2010). The PAN level at 12 km over TP was about 0.10-0.15 ppb in October 2007 (Wiegele et al., 2012), which is very close to the range (0.1-0.2 ppb) on 21 October 2003 (Glatthor et al., 2007). Results from the model simulations by Fischer et al. (2014) showed that the PAN level during June-August 2008 varied in the range of 0.3-0.5 ppb in the 2-6 km layer and 0.2-0.4 ppb in the 6-10 km layer over the TP. Another model simulation study (Fadnavis et al., 2014) obtained a PAN range of 0.15-0.2 ppb for the 6-10 km layer and for June-September 1995-2004.

The satellite measurements and simulation results listed in Table 1 indicate a general decrease of PAN level from the upper troposphere to the lower stratosphere, consistent with the vertical distribution of PAN in the UTLS (Pope et al., 2016). These data represent PAN levels averaged over larger scales for certain periods. In-situ measurements on the ground showed average PAN levels very close to 333 hPa (about 10 km) values. So far, there has been no observation of the vertical distribution of PAN in the middle and lower troposphere over the TP. Based on the results from the case studies in sections 3.4 and 3.5, we believe the PAN level in middle and lower tropospheric air over the TP may be more variable and sometimes elevated by transport of plumes from anthropogenic and biomass burning emissions. The significance of the transport impact deserves systematic studies, which is out the scope of this work.

4 Conclusions

For the first time, we made simultaneous ground-based measurements of two photochemical products, PAN and O₃ at Nam Co, a remote site in the central Tibetan Plateau (TP) region. Our effective PAN data cover two summer periods, i.e., 16-25 August 2011 and 15 May to 13 July 2012. The average concentrations of PAN were 0.36 ppb (range: 0.11-0.76 ppb) and 0.44 ppb (range: 0.21-0.99 ppb) in the 2011 and 2012 periods, respectively. During

the observation in 2012, the O₃ ~~concentration~~ varied from 27.9 ppb to 96.4 ppb, with an average of 60.0 ppb, very close to the summertime O₃ level found at Waliguan, a global baseline station at the northeastern edge of the TP.

PAN and O₃ showed profound and similar diurnal cycles, with valleys around 5:00 LT, steep rises in the early morning, and broader platforms of high values during 9:00-20:00 LT. Such patterns of diurnal variations of both gases, particularly the sharp increases even before sunrise, cannot be attributed solely to local photochemistry. Our analysis suggests that the PBL evolution played a key role in shaping the diurnal patterns of both ~~oxidant~~gases. PAN and O₃ in the shallow nocturnal PBL were significantly removed by their sinks, such as chemical reactions and dry deposition. In the early morning, the elevation of the PBL height caused downward mixing of upper air containing higher PAN and O₃, leading to steep rises of the concentrations of these gases. The downward mixing and photochemistry sustained the higher levels of PAN and O₃ in the daytime. However, there were day-to-day differences in the PBL evolution, which could cause large differences in the diurnal variations of PAN and O₃. We identified two groups of days with different meteorological conditions and different diurnal patterns of trace gases and meteorological parameters. Days in ~~group~~Group 1 were mainly distributed in the pre-monsoon period, with higher daytime height of PBL (about 3 km), lower humidity, and larger day-night variations of PAN and O₃. Days in ~~group~~Group 2 were mainly distributed in the monsoon period, with shallower daytime PBL (about 2 km), higher humidity, and much smaller day-night variations of PAN and O₃.

There were some cases with obvious rapid transport of air masses during our observations. We identified two cases of rapid downward transport of air masses from the ~~middle and upper troposphere~~UTLS. The observed maximum PAN levels during these two cases ranged from 0.5 ppb to 0.7 ppb. ~~They may represent those in the middle and upper troposphere.~~ These PAN levels are higher than those retrieved from satellite measurements for the UTLS. Therefore, it is likely that the tropospheric PAN over the TP may be disturbed for short periods, which is not easily captured by satellite observation. In addition to vertical transport of PAN, we also identified a case of strong long-range transport of PAN plumes. During this case, relatively polluted air masses from the PBL over North India, North Pakistan, and Nepal were able to be transported over the western and central TP to NMC, causing a profound episode of PAN with maximum close to 1 ppb during 1-6 June 2012. In contrast, significantly lower PAN levels were observed when air masses originated from other areas. Although

1 transport of aerosols from South and Southeast Asia and its impacts on atmospheric
2 environment over Himalayas and the TP have been intensively studied in recent years,
3 [transport of](#) gaseous pollutants [and its impacts](#) have received less attention. Our results show,
4 for the first time, that polluted air masses from South Asia can significantly enhance the
5 ambient level of PAN at NMC. The space scale and frequency of this phenomenon and its
6 impacts on tropospheric photochemistry over the TP region remain to be studied in the future.

7 **Data availability.** The observational data analyzed in this paper can be made available for
8 scientific purposes by contacting the corresponding author
9 (xuxb Xiaobin_xu@camsema189.cn).

10 **Competing interests.** The authors declare that they have no conflict of interest.

11 **Acknowledgements.** The authors thank the staff of the Nam Co station and Xizang
12 Meteorological Bureau for logistical support. This work was supported by the China Special
13 Fund for Meteorological Research in the Public Interest (GYHY201106023), the Natural
14 Science Foundation of China (No.41330422) and Basic Research Fund of CAMS (2011Z003
15 and 2013Z005).

References

- Bonasoni, P., Laj, P., Marinoni, A., Sprenger, M., Angelini, F., Arduini, J., Bonafè U., Calzolari, F., Colombo, T., Decesari, S., Di Biagio, C., di Sarra, A. G., Evangelisti, F., Duchi, R., Facchini, M. C., Fuzzi, S., Gobbi, G. P., Maione, M., Panday, A., Roccato, F., Sellegri, K., Venzac, H., Verza, G. P., Villani, P., Vuillermoz, E., and Cristofanelli, P.: Atmospheric Brown Clouds in the Himalayas: first two years of continuous observations at the Nepal Climate Observatory-Pyramid (5079 m), *Atmos. Chem. Phys.*, 10, 7515-7531, 2010.
- Boersma, K.F., Eskes, H.J., Dirksen, R. J., van der A, R. J., Veefkind, J. P., Stammes, P., Huijnen, V., Kleipool, Q. L., Sneep, M., Claas, J., Leitao, J., Richter, A., Zhou, Y., and Brunner, D.: An improved retrieval of tropospheric NO₂ columns from the Ozone Monitoring Instrument, *Atmos. Meas. Tech.*, 4, 1905-1928, 2011
- Chen, B., Xu, X. D., Yang, S., and Zhao, T. L.: Climatological perspectives of air transport from atmospheric boundary layer to tropopause layer over Asian monsoon regions during boreal summer inferred from Lagrangian approach, *Atmos. Chem. Phys.*, 12, 5827-5839, 10.5194/acp-12-5827-2012, 2012.
- Chen, X., An, J. A., Su, Z., Torre, L., Kelder, H., Peet, J., Ma, Y., and Fu, R.: The Deep Atmospheric Boundary Layer and Its Significance to the Stratosphere and Troposphere Exchange over the Tibetan Plateau, *PloS One*, 8, e56909, 10.1371/journal.pone.005690, 2013.
- Cong, Z. Y., Kang, S. C., Liu, X. D., and Wang, G. F.: Elemental composition of aerosol in the Nam Co region, Tibetan Plateau, during summer monsoon season, *Atmos. Environ.*, 41, 1180–1187, 2007.
- Cong, Z. Y., Kang, S., Smirnov, A., and Holben, B.: Aerosol optical properties at Nam Co, a remote site in central Tibetan Plateau, *Atmos. Res.*, 92, 42–48, 2009.
- Cox, R.A. and Roffey, M.J.: Thermal decomposition of peroxyacetylnitrate in the presence of nitric oxide. *Environ. Sci. & Technol.*, 11(9), 900–906, 1977.
- Cristofanelli, P., Bracci, A., Sprenger, M., Marinoni, A., Bonafè U., Calzolari, F., Duchi, R., Laj, P., Pichon, J. M., Roccato, F., Venzac, H., Vuillermoz, E., and Bonasoni, P.: Tropospheric ozone variations at the Nepal Climate Observatory-Pyramid (Himalayas, 5079m a.s.l.) and influence of deep stratospheric intrusion events, *Atmos. Chem. Phys.*, 10, 6537–6549, 2010.

1 De Smedt, I., Van Roozendaal, M., Stavrakou, T., Müller, J.-F., Lerot, C., Theys, N., Valks,
2 P., Hao, N., and van der, N.A.: Improved retrieval of global tropospheric formaldehyde
3 columns from GOME-2/MetOp-A addressing noise reduction and instrumental degradation
4 issues. *Atmos. Meas. Tech.*, 5, 2933-2949, 2012.

5 De Smedt, I., Müller, J.-F., Stavrakou, T., van der, A., R. J., Eskes, H. J., and Van Roozendaal,
6 M.: Twelve years of global observations of formaldehyde in the troposphere using GOME
7 and SCIAMACHY sensors, *Atmos. Chem. Phys.*, 8(16), 4947-4963, 2008.

8 Dessler, A. E., and Sherwood, S. C.: Effect of convection on the summertime extratropical
9 lower stratosphere, *J. Geophys. Res.*, 109, D23301-D23310, 10.1029/2004jd005209, 2004.

10 Ding, A. and Wang, T.: Influence of stratosphere-to-troposphere exchange on the seasonal
11 cycle of surface ozone at Mount Waliguan in western China, *Geophys. Res. Lett.*, 33, L03803,
12 doi:10.1029/2005GL024760, 2006.

13 Draxler, R.R. and Hess, G.D.: Description of the HYSPLIT 4 modeling system. NOAA
14 Technical Memorandum. ERLARL-224, NOAA Air Resources Laboratory, Silver Spring,
15 MD. 24, 1997.

16 Fadnavis, S., Schultz, M.G., Semeniuk, K., Mahajan, A.S., Pozzoli, L., Sonbawne, S., Ghude,
17 S.D., Kiefer, M., and Eckert, E.: Trends in peroxyacetyl nitrate (PAN) in the upper
18 troposphere and lower stratosphere over southern Asia during the summer monsoon season:
19 regional impacts, *Atmos. Chem. Phys.*, 14, 12725–12743, 2014.

20 Fischer, E. V., Jaffe, D. A., Reidmiller, D. R., and Jaegle, L.: Meteorological controls on
21 observed peroxyacetyl nitrate at Mount Bachelor during the spring of 2008, *J. Geophys. Res.*,
22 115, D03302, doi:10.1029/2009jd012776, 2010.

23 Fischer, E. V., Jaffe, D. A., and Weatherhead, E. C.: Free tropospheric peroxyacetyl nitrate
24 (PAN) and ozone at Mount Bachelor: potential causes of variability and timescale for trend
25 detection, *Atmos. Chem. Phys.*, 11, 5641-5654, 10.5194/acp-11-5641-2011, 2011.

26 Fischer, E. V., Jacob, D. J., Yantosca, R. M., Sulprizio, M. P., Millet, D. B., Mao, J., Paulot,
27 F., Singh, H. B., Roiger, A. E., Ries, L., Talbot, R. W., Dzepina, K., and Pandey Deolal, S.:
28 Atmospheric peroxyacetyl nitrate (PAN): a global budget and source attribution, *Atmos.*
29 *Chem. Phys.*, 14, 2679-2698, 2014.

1 Fishman, J., Wozniak, A.E., and Creilson, J.K.: Global distribution of tropospheric ozone from
 2 satellite measurements using the empirically corrected tropospheric ozone residual technique:
 3 Identification of the regional aspects of air pollution, *Atmos. Chem. Phys.*, 3, 893–907, 2003.

4 [Flocke, F.M., Weinheimer, A.J., Swanson, A.L., Roberts, J.M., Schmitt, R., and Shertz, S.:
 5 On the measurement of PANs by gas chromatography and electron capture detection, *J.*
 6 *Atmos. Chem.*, 52, 19-43, 2005.](#)

7 Ford, K. M., Campbell, B. M., Shepson, P. B., Bertman, S. B., Honrath, R. E., Peterson, M.,
 8 and Dibb, J. E.: Studies of Peroxyacetyl nitrate (PAN) and its interaction with the snowpack
 9 at Summit, Greenland, *J. Geophys. Res.*, 107, 4102-4111, 2002.

10 Fu, R., Hu, Y., Wright, J. S., Jiang, J. H., Dickinson, R. E., Chen, M., Filipiak, M., Read, W.
 11 G., Waters, J. W., Wu, D. L., and Affiliations, A.: Short circuit of water vapor and polluted
 12 air to the global stratosphere by convective transport over the Tibetan Plateau, *PNAS*, 103,
 13 5664-5669, 10.1073/pnas.0601584103, 2006.

14 Gettelman, A., and Kinnison, D. E.: Impact of monsoon circulations on the upper troposphere
 15 and lower stratosphere, *J. Geophys. Res.*, 109, D22101-D22114, 10.1029/2004jd004878,
 16 2004.

17 Ghude, S.D., Jain, S.L., Arya, B.C., Beig, G., Ahammed, Y.N., Kumar, A., Tyagi, B.: Ozone
 18 in ambient air at a tropical megacity, Delhi: characteristics, trends and cumulative ozone
 19 exposure indices, *J. Atmos. Chem.*, 60, 237–252, 2008.

20 Glatthor, N., von Clarmann, T., Fischer, H., Funke, B., Grabowski, U., Hopfner, M.,
 21 Kellmann, S., Kiefer, M., Linden, A., Milz, M., Steck, T., and Stiller, G. P.: Global
 22 peroxyacetyl nitrate (PAN) retrieval in the upper troposphere from limb emission spectra of
 23 the Michelson Interferometer for Passive Atmospheric Sounding (MIPAS), *Atmos. Chem.*
 24 *Phys.*, 7, 2775–2787, doi:10.5194/acp-7-2775-2007, 2007.

25 Gu, Y., Liao, H., and Bian, J.: Summertime nitrate aerosol in the upper troposphere and lower
 26 stratosphere over the Tibetan Plateau and the South Asian summer monsoon region, *Atmos.*
 27 *Chem. Phys.*, 16, 6641-6663, doi:10.5194/acp-16-6641-2016, 2016.

28 [Helmig, D., Oltmans, S. J., Morse, T. O., and Dibb, J. E.: What is causing high ozone at
 29 Summit, Greenland?, *Atmos. Environ.*, 41, 5031-5043, doi:10.1016/j.atmosenv.2006.05.084,
 30 2007.](#)

- Huang, Y., Wu, S., Kramer, L. J., Helmig, D., and Honrath, R. E.: Surface ozone and its precursors at Summit, Greenland: comparison between observations and model simulations, *Atmos. Chem. Phys.*, 17, 14661-14674, <https://doi.org/10.5194/acp-17-14661-2017>, 2017.
- Hudman, R.C., Jacob, D.J., Cooper, O.R., Evans, M.J., Heald, C.L., Park, R.J., Fehsenfeld, F., Flocke, F., Holloway, J., Hübner, G., Kita, K., Koike, M., Kondo, Y., Neuman, A., Nowak, J., Oltmans, S., Parrish, D., Roberts, J.M., and Ryerson, T.: Ozone production in transpacific Asian pollution plumes and implications for ozone air quality in California, *J. Geophys. Res.*, 109, D23S10-D23S23, 10.1029/2004jd004974, 2004.
- Kopacz, M., Mauzerall, D. L., Wang, J., Leibensperger, E. M., Henze, D. K., and Singh, K.: Origin and radiative forcing of black carbon transported to the Himalayas and Tibetan Plateau, *Atmos. Chem. Phys.*, 11, 2837-2852, 10.5194/acp-11-2837-2011, 2011.
- Kramer, L. J., Helmig, D., Burkhart, J. F., Stohl, A., Oltmans, S., and Honrath, R. E.: Seasonal variability of atmospheric nitrogen oxides and non-methane hydrocarbons at the GEOSummit station, Greenland, *Atmos. Chem. Phys.*, 15, 6827-6849, doi:10.5194/acp-15-6827-2015, 2015.
- LaFranchi, B. W., Wolfe, G. M., Thornton, J. A., Harrold, S. A., Browne, E. C., Min, K. E., Wooldridge, P. J., Gilman, J. B., Kuster, W. C., Goldan, P. D., de Gouw, J. A., McKay, M., Goldstein, A. H., Ren, X., Mao, J., and Cohen, R. C.: Closing the peroxy acetyl nitrate budget: observations of acyl peroxy nitrates (PAN, PPN, and MPAN) during BEARPEX 2007, *Atmos. Chem. Phys.*, 9(19), 7623–7641, 2009.
- Law, K. S., Fierli, F., Cairo, F., Schlager, H., Borrmann, S., Streibel, M., Real, E., Kunkel, D., Schiller, C., Ravegnani, F., Ulanovsky, A., D'Amato, F., Viciani, S., Volk, C.M.: Air mass origins influencing TTL chemical composition over West Africa during 2006 summer monsoon, *Atmos. Chem. Phys.*, 10, 10753–10770, 2010.
- Lelieveld, J., Brühl, C., Jöckel, P., Steil, B., Crutzen, P. J., Fischer, H., Giorgetta, M. A., Hoor, P., Lawrence, M. G., Sausen, R., and Tost, H.: Stratospheric dryness: model simulations and satellite observations, *Atmos. Chem. Phys.*, 7, 1313-1332, 2007.
- Lelieveld, J. and Dentener, F. J.: What controls tropospheric ozone? *J. Geophys. Res.*, 105(D3), 3531–3551, 2000.

- 1 [Lefohn, A. S., Wernli, H., Shadwick, D., Oltmans, S. J., and Shapiro, M.: Quantifying the](#)
- 2 [importance of stratospheric-tropospheric transport on surface ozone concentrations at high-](#)
- 3 [and low-elevation monitoring sites in the United States, Atmos. Environ., 62, 646-656, 2012.](#)
- 4 Li, M., Y. Ma, W. Ma, H. Ishiakawa, F. Sun, S. Ogino, Structural difference of atmospheric
- 5 boundary layer between dry and rainy seasons over the central Tibetan Plateau (in
- 6 Chinese), Journal of Glaciology and Geocryology, 33, 72-79, 2011.
- 7 Lin, W., Xu, X., Zheng, X., Jaxi, D., Ciren, B., Two-year measurements of surface ozone at
- 8 Dangxiong, a remote highland site in the Tibetan Plateau, J. Environ. Sci., 31, 133-145, 2015.
- 9 Lüthi, Z.L., Škerlak, B., Kim, S.-W., Lauer, A., Mues, A., Rupakheti, M., and Kang, S.:
- 10 Atmospheric Brown Clouds reach the Tibetan Plateau by crossing the Himalayas, Atmos.
- 11 Chem. Phys., 15, 6007-6021, 2015.
- 12 Ma, J., Liu, H., and Hauglustaine, D.: Summertime tropospheric ozone over China simulated
- 13 with a regional chemical transport model 1. Model description and evaluation, J. Geophys.
- 14 Res., 107, ACH 27-21–ACH 27-13, doi:10.1029/2001JD001354, 2002a.
- 15 Ma, J., Tang, J., Zhou, X., and Zhang, X.: Estimates of the Chemical Budget for Ozone at
- 16 Waliguan Observatory, J. Atmos. Chem., 41, 21–48, doi:10.1023/A:1013892308983, 2002b.
- 17 Ma, J., Lin, W. L., Zheng, X.D., Xu, X.B., Li, Z., and Yang, L.L.: Influence of air mass
- 18 downward transport on the variability of surface ozone at Xianggelila Regional Atmosphere
- 19 Background Station, southwest China, Atmos. Chem. Phys., 14, 5311–5325, 2014.
- 20 Ma, Y., Fan, S., Ishikawa, H., Tsukamoto, O., Yao, T., Koike, T., Zuo, H., Hu, Z., and Su, Z.:
- 21 Diurnal and inter-monthly variation of land surface heat fluxes over the central Tibetan
- 22 Plateau area, Theoret. Appl. Climat., 80, 259-273, 2005.
- 23 Ma, W., Ma, Y., and Bob, S.: Feasibility of Retrieving Land Surface Heat Fluxes from
- 24 ASTER Data Using SEBS: a Case Study from the NamCo Area of the Tibetan Plateau, Arctic,
- 25 Antarctic, and Alpine Research, 43(2), 239-245, 2011.
- 26 Ming, J., Du, Z., Xiao, C., Xu, X., and Zhang, D.: Darkening of the mid-Himalaya glaciers
- 27 since 2000 and the potential causes, Environ. Res. Lett. 7, 014021, doi:10.1088/1748-
- 28 9326/7/1/014021, 2012.

1 Moore, D.P. and Remedios, J.J.: Seasonality of Peroxyacetyl nitrate (PAN) in the upper
2 troposphere and lower stratosphere using the MIPAS-E instrument, *Atmos. Chem. Phys.*, 10,
3 6117-6128, 10.5194/acp-10-6117-2010, 2010.

4 Myhre, G., Shindell, D., Brón, F.-M., Collins, W., Fuglestedt, J., Huang, J., Koch, D.,
5 Lamarque, J.-F., Lee, D., Mendoza, B., Nakajima, T., Robock, A., Stephens, G., Takemura, T.,
6 and Zhang, H.: Anthropogenic and Natural Radiative Forcing. In: *Climate Change 2013: The*
7 *Physical Science Basis. Contribution of Working Group I to the Fifth Assessment Report of*
8 *the Intergovernmental Panel on Climate Change* [Stocker, T.F., D. Qin, G.-K. Plattner, M.
9 Tignor, S.K. Allen, J. Boschung, A. Nauels, Y. Xia, V. Bex and P.M. Midgley (eds.)].
10 Cambridge University Press, Cambridge, United Kingdom and New York, NY, USA, 2013.

11 Ohara, T., Akimoto, H., Kurokawa, J., Horii, N., Yamaji, k., Yan, X., and Hayasaka, T.: An
12 Asian emission inventory of anthropogenic emission sources for the period 1980–2020,
13 *Atmos. Chem. Phys.*, 7, 4419–4444, 2007.

14 Pandey Deolal, S., Staehelin, J., Brunner, D., Cui, J., Steinbacher, M., Zellweger, C., Henne,
15 S., and Vollmer, M. K.: Transport of PAN and NO_y from different source regions to the
16 Swiss high alpine site Jungfraujoch, *Atmos. Environ.*, 64, 103–115,
17 doi:10.1016/j.atmosenv.2012.08.021, 2013.

18 Park, M., Randel, W. J., Gettelman, A., Massie, S. T., and Jiang, J. H.: Transport above the
19 Asian summer monsoon anticyclone inferred from Aura Microwave Limb Sounder tracers, *J.*
20 *Geophys. Res.*, 112, 10.1029/2006jd008294, 2007.

21 Park, M., Randel, W. J., Emmons, L. K., Bernath, P. F., Walker, K. A., and Boone, C. D.:
22 Chemical isolation in the Asian monsoon anticyclone observed in Atmospheric Chemistry
23 Experiment (ACE-FTS) data, *Atmos. Chem. Phys.*, 8, 757-764, 10.5194/acp-8-757-2008,
24 2008.

25 Park, M., Randel, W. J., Emmons, L. K., and Livesey, N. J.: Transport pathways of carbon
26 monoxide in the Asian summer monsoon diagnosed from Model of Ozone and Related
27 Tracers (MOZART), *J. Geophys. Res.*, 114, D08303-D08313, 10.1029/2008jd010621, 2009.

28 [Pope, R. J., Richards, N. A. D., Chipperfield, M. P., Moore, D. P., Monks, S. A., Arnold, S.](#)
29 [R., Glatthor, N., Kiefer, M., Breider, T. J., Harrison, J. J., Remedios, J. J., Warneke, C.,](#)
30 [Roberts, J. M., Diskin, G. S., Huey, L. G., Wisthaler, A., Apel, E. C., Bernath, P. F., and Feng,](#)
31 [W.: Intercomparison and evaluation of satellite peroxyacetyl nitrate observations in the upper](#)

[troposphere–lower stratosphere, Atmos. Chem. Phys., 16, 13541-13559,
https://doi.org/10.5194/acp-16-13541-2016, 2016.](https://doi.org/10.5194/acp-16-13541-2016)

Qu, B., Ming, J., Kang, S.-C., Zhang, G.-S., Li, Y.-W., Li, C.-D., Zhao, S.-Y., Ji, Z.-M., and Cao, J.-J.: The decreasing albedo of the Zhadang glacier on western Nyainqentanglha and the role of light-absorbing impurities, *Atmos. Chem. Phys.*, 14, 11117-11128, doi:10.5194/acp-14-11117-2014, 2014.

Ramanathan, V., Ramana, M. V., Roberts, G., Kim, D., Corrigan, C., Chung, C., Winker, D.: Warming trends in Asia amplified by brown clouds solar absorption, *Nature*, 448, 575–578, 2007.

Ran, L., Lin, W.L., Deji, Y.Z., La, B., Tsering, P.M., Xu, X.B., and Wang, W.: Surface gas pollutants in Lhasa, a highland city of Tibet: current levels and pollution implications, *Atmos. Chem. Phys.* 14, 10721–10730, 2014.

Randel, W. J., Park, M., Emmons, L., Kinnison, D., Bernath, P., Walker, K. A., Boone, C., and Pumphrey, H.: Asian Monsoon Transport of Pollution to the Stratosphere, *Science Magazine*, 328, 611-613, 10.1126/science.1182274, 2010.

Remedios, J. J., Allen, G., Waterfall, A. M., Oelhaf, H., Kleinert, A., and Moore1, D. P.: Detection of organic compound signatures in infra-red, limb emission spectra observed by the MIPAS-B2 balloon instrument, *Atmos. Chem. Phys.*, 7, 1599-1613, 10.5194/acp-7-1599-2007, 2007.

Roiger, A., Aufmhoff, H., Stock, P., Arnold, F., and Schlager, H.: An aircraft-borne chemical ionization - ion trap mass spectrometer (CI-ITMS) for fast PAN and PPN measurements, *Atmos. Meas. Tech.*, 4, 173-188, 10.5194/amt-4-173-2011, 2011.

Roberts, J. M.: PAN and Related Compounds, in: *Volatile Organic Compounds in the Atmosphere*, edited by: Koppmann,R., Blackwell Publishing, 500, Oxford, UK, 2007.

Russo, R. S., Talbot, R. W., Dibb, J. E., Scheuer, E., Seid, G., Jordan, C. E., Fuelberg, H. E., Sachse, G. W., Avery, M. A., Vay, S. A., Blake, D. R., Blake, N. J., Atlas, E., Fried, A., Sandholm, S. T., Tan, D., Singh, H. B., Snow, J., and Heikes, B. G.: Chemical composition of Asian continental outflow over the western Pacific: Results from Transport and Chemical Evolution over the Pacific (TRACE-P), *J. Geophys. Res.*, 108, 10.1029/2002jd003184, 2003.

1 Shen, R.-Q., Ding, X., He, Q.-F., Cong, Z.-Y., Yu, Q.-Q., and Wang, X.M.: Seasonal
2 variation of secondary organic aerosol tracers in Central Tibetan Plateau, *Atmos. Chem. Phys.*,
3 15, 8781-8793, 2015.

4 Singh, H.B.: Reactive nitrogen in the troposphere. *Environ. Sci. & Technol.*, 21(4), 320–327,
5 1987.

6 Singh, H.B., Salas, L., Herlth, D., Kolyer, R., Czech, E., Avery, M., Crawford, J.H., Pierce,
7 R.B., Sachse, G.W., Blake, D.R., Cohen, R. C., Bertram, T.H., Perring, A., Wooldridge, P.J.,
8 Dibb, J., Huey, G., Hudman, R.C., Turquety, S., Emmons, L.K., Flocke, F., Tang, Y.,
9 Carmichael, G.R., and Horowitz, L.W.: Reactive nitrogen distribution and partitioning in the
10 North American troposphere and lowermost stratosphere, *J. Geophys. Res.*, 112, D12S04,
11 doi:10.1029/2006JD007664, 2007.

12 Sudo, K., Takahashi, M., and Akimoto, H.: CHASER: A global chemical model of the
13 troposphere 2. Model results and evaluation, *J. Geophys. Res.*, 107, 4586,
14 doi:10.1029/2001jd001114, 2002.

15 Stull, R.B.: *An Introduction to Boundary Layer Meteorology*, Kluwer Academic, Dordrecht,
16 The Netherlands, 1988.

17 Talbot, R. W., Dibb, J. E., Scheuer, E. M., Kondo, Y., Koike, M., Singh, H. B., Salas, L. B.,
18 Fukui, Y., Ballenthin, J. O., Meads, R. F., Miller, T. M., Hunton, D. E., Viggiano, A. A.,
19 Blake, D. R., Blake, N. J., Atlas, E., Flocke, F., Jacob, D. J., and Jaegle, L.: Reactive nitrogen
20 budget during the NASA SONEX Mission, *Geophys. Res. Lett.*, 26, 3057-3060,
21 10.1029/1999GL900589, 1999.

22 Talukdar, R. K., Burkholder, J. B., Schmoltner, A.-M., Roberts, J. M., Wilson, R. R., and
23 Ravishankara, A. R.: Investigation of the loss processes for peroxyacetyl nitrate in the
24 atmosphere: UV photolysis and reaction with OH, *J. Geophys. Res.*, 100, 14163–14173,
25 10.1029/95JD00545, 1995.

26 Thakur, A.N., Singh, H.B., Mariani, P., Chen, Y., Wang, Y., Jacob, D.J., Brasseur, G., Müller,
27 J.F., and Lawrence, M.: Distribution of reactive nitrogen species in the remote free
28 troposphere: data and model comparisons, *Atmos. Environ.*, 33, 1403–1422,
29 doi:10.1016/s1352-2310(98)00281-7, 1999.

30 Tereszchuk, K.A., Moore, D.P., Harrison, J.J., Boone, C.D., Park, M., Remedios, J.J., Randel,
31 W.J., and Bernath, P.F.: Observations of peroxyacetyl nitrate (PAN) in the upper troposphere

1 by the Atmospheric Chemistry Experiment-Fourier Transform Spectrometer (ACE-FTS),
 2 Atmos. Chem. Phys., 13, 5601-5613, 10.5194/acp-13-5601-2013, 2013.

3 Tian, W., Chipperfield, M., and Huang, Q.: Effects of the Tibetan Plateau on total column
 4 ozone distribution, Tellus B, 60, 622-635, 10.1111/j.1600-0889.2008.00338.x, 2008.

5 Ungermann, J., Ern, M., Kaufmann, M., Müller, R., Spang, R., Ploeger, F., Vogel, B., and
 6 Riese, M.: Observations of PAN and its confinement in the Asian summer monsoon
 7 anticyclone in high spatial resolution, Atmos. Chem. Phys., 16, 8389–8403, 2016.

8 Volz-Thomas, A., Xueref, I., and Schmitt, R.: An automatic gas chromatograph and
 9 calibration system for ambient measureme, Environ. Sci. Pollut. Res., 9, 72-76, 2002.

10 von Kuhlmann, R., Lawrence, M.G., Crutzen, P.J., and Rasch, P.J.: A model for studies of
 11 tropospheric ozone and nonmethane hydrocarbons: Model evaluation of ozone-related species,
 12 J. Geophys. Res, 108, 4729, doi:10.1029/2002jd003348, 2003.

13 Wang, M., Xu, B., Cao, J., Tie, X., Wang, H., Zhang, R., Qian, Y., Rasch, P. J., Zhao, S., Wu,
 14 G., Zhao, H., Joswiak, D. R., Li, J., and Xie, Y.: Carbonaceous aerosols recorded in a
 15 southeastern Tibetan glacier: analysis of temporal variations and model estimates of sources
 16 and radiative forcing, Atmos. Chem. Phys., 15, 1191-1204, doi:10.5194/acp-15-1191-2015,
 17 2015.

18 Wang, T., Wong, H.L.A., Tang, J., Ding, A., Wu, W.S., and Zhang, X.C.: On the origin of
 19 surface ozone and reactive nitrogen observed at a remote mountain site in the northeastern
 20 Qinghai-Tibetan Plateau, western China, J. Geophys. Res., 111, D08303,
 21 doi:10.1029/2005JD006527, 2006.

22 Wang, Q.Y., Gao, R.S., Cao, J.J., Schwarz, J.P., Fahey, D.W., Shen, Z.X., Hu, T.F., Wang, P.,
 23 Xu, X.B., and Huang, R.J.: Observations of high level of ozone at Qinghai Lake basin in the
 24 northeastern Qinghai-Tibetan Plateau, western China, J. Atmos. Chem., 72, 19–26, 2015.

25 Wiegele, A., Glatthor, N., Höpfner, M., Grabowski, U., Kellmann, S., Linden, A., Stiller, G.,
 26 and von Clarmann, T.: Global distributions of C₂H₆, C₂H₂, HCN, and PAN retrieved from
 27 MIPAS reduced spectral resolution measurements, Atmos. Meas. Tech., 5, 723-734,
 28 10.5194/amt-5-723-2012, 2012.

29 Worden, J., Jones, D.B.A., Liu, J., Parrington, M., Bowman, K., Stajner, I., Beer, R., Jiang, J.,
 30 Thouret, V., Kulawik, S., Li, J.-L. F., Verma, S., and Worden, H.: Observed vertical

distribution of tropospheric ozone during the Asian summertime monsoon, *J. Geophys. Res.*, 114, D13304-D13320, 10.1029/2008jd010560, 2009.

Xiong, X., Houweling, S., Wei, J., Maddy, E., Sun, F., and Barnett, C.: Methane plume over south Asia during the monsoon season: satellite observation and model simulation, *Atmos. Chem. Phys.*, 9, 783-794, 2009.

Xu, W., Lin, W., Xu, X., Tang, J., Huang, J., Wu, H., and Zhang, X.: Long-term trends of surface ozone and its influencing factors at the Mt. Waliguan GAW station, China – Part 1: Overall trends and characteristics, *Atmos. Chem. Phys.*, 16, 6191–6205, 2016.

Xu, W., Xu, X., Lin, M., Lin, W., ~~Tang, J.~~, Tarasick, D., Tang, J., Ma, J., and Zheng, X.: Long-term trends of surface ozone and its influencing factors at the Mt. Waliguan GAW station, China, — - Part 2: The roles of anthropogenic emissions and climate variability~~Variation mechanism and links to some climate indices~~, *Atmos. Chem. Phys. Discuss.*, 18, 773-798, <https://doi.org/10.5194/acp-2017-483>, ~~2017~~2018.

Xue, L.K., Wang, T., Zhang, J.M., Zhang, X.C., Deliger, Poon, C.N., Ding, A.J., Zhou, X.H., Wu, W.S., Tang, J., Zhang, Q.Z., and Wang, W.X.: Source of surface ozone and reactive nitrogen speciation at Mount Waliguan in western China: New insights from the 2006 summer study, *J. Geophys. Res.*, 116, 10.1029/2010jd014735, 2011.

Yeh, T.-C., Lo, S.-W., and Chu, P.-C.: The wind structure and heat balance in the lower troposphere over Tibetan Plateau and its surroundings, *Acta Meteor. Sinica* (in Chinese), 28, 108-121, 1957.

Yin, X., Kang, S., de Foy, B., Cong, Z., Luo, J., Zhang, L., Ma, Y., Zhang, G., Rupakheti, D., and Zhang, Q.: Surface ozone at Nam Co (4730 m a.s.l.) in the inland Tibetan Plateau: variation, synthesis comparison and regional representativeness, *Atmos. Chem. Phys. Discuss.*, <https://doi.org/10.5194/acp-2017-175>, 2017.

Zanis, P., Ganser, A., Zellweger, C., Henne, S., Steinbacher, M., and Staehelin, J.: Seasonal variability of measured ozone production efficiencies in the lower free troposphere of Central Europe, *Atmos. Chem. Phys.*, 7, 223-236, 10.5194/acp-7-223-2007, 2007.

Zellweger, C., Ammann, M., Buchmann, B., Hofer, P., Lugauer, M., Rüttimann, R., Streit, N., Weingartner, E., and Baltensperger, U.: Summertime NO_y Speciation at the Jungfrauoch, 3580 m asl, Switzerland, *J. Geophys. Res.*, 105, 6655–6667, 2000.

[Zellweger, C., Klausen, J., Buchmann, B., and Scheel, H.-E.: System and Performance Audit of Surface Ozone, Carbon Monoxide, Methane and Nitrous Oxide at the GAW Global Station Mt. Waliguan and the Chinese Academy of Meteorological Sciences \(CAMS\) China, June 2009, WCC-Empa Report 09/2Rep., 61 pp, Empa, Dübendorf, Switzerland, available at: \[https://www.wmo.int/pages/prog/arep/gaw/documents/WLG_2009.pdf\]\(https://www.wmo.int/pages/prog/arep/gaw/documents/WLG_2009.pdf\) \(last access: 15 January 2018\), 2009.](#)

Zhang, H., Xu, X., Lin, W., and Wang, Y.: Wintertime peroxyacetyl nitrate (PAN) in the megacity Beijing: Role of photochemical and meteorological processes, *J. Environ. Sci.*, 26, 83–96, 10.1016/S1001-0742(13)60384-8, 2014.

[Zhang, J.M., Wang, T., Ding, A.J., Zhou, X.H., Xue, L.K., Poon, C.N., Wu, W.S., Gao, J., Zuo, H.C., Chen, J.M., Zhang, X.C., and Fan, S.J.: Continuous measurement of peroxyacetyl nitrate \(PAN\) in suburban and remote areas of western China, *Atmos. Environ.*, 43, 228-237, 2009a.](#)

Zhang, L., Jacob, D.J., Boersma, K.F., Jaffe, D.A., Olson, J.R., Bowman, K.W., Worden, J.R., Thompson, A.M., Avery, M.A., Cohen, R.C., Dibb, J.E., Flock, F.M., Fuelberg, H.E., Huey, L.G., McMillan, W.W., Singh, H.B., and Weinheimer, A.J.: Transpacific transport of ozone pollution and the effect of recent Asian emission increases on air quality in North America: an integrated analysis using satellite, aircraft, ozonesonde, and surface observations, *Atmos. Chem. Phys.*, 8, 6117–6136, doi:10.5194/acp-8-6117-2008, 2008.

Zhang, Q., Streets, D.G., Carmichael, G.R., He, K.B., Huo, H., Kannari, A., Klimont, Z., Park, I.S., Reddy, S., Fu, J.S., Chen, D., Duan, L., Lei, Y., Wang, L.T., Yao, Z.L., Asian emissions in 2006 for the NASA INTEX-B mission, *Atmos. Chem. Phys.* 9, 5131-5153, 2009**b**.

[Zhang, Q., Kang, S., and Zhang, G.: Changes of snow line altitude for glaciers on western Nyainqentanglha range observed by remote sensing, *Scientia Geographica Sinica*, 36, 1937-1944, 2016.](#)

Zhang, R., Wang, H., Qian, Y., Rasch, P. J., Easter, R. C., Ma, P.-L., Singh, B., Huang, J., and Fu, Q.: Quantifying sources, transport, deposition and radiative forcing of black carbon over the Himalayas and Tibetan Plateau, *Atmos. Chem. Phys.*, 15, 6205–6223, 2015.

- 1 Zhao, S., Ming, J., Sun, J., and Xiao, C.: Observation of carbonaceous aerosols during 2006–
2 2009 in Nyainqêntanglha Mountains and the implications for glaciers, Environ. Sci. Pollut.
3 Res., DOI 10.1007/s11356-013-1548-6, 2013.
- 4 Zheng, X. D., Shen, C. D., Wan, G. J., Liu, K. X., Tang, J., and Xu, X. B.: $^{10}\text{Be}/^7\text{Be}$ implies
5 the contribution of stratosphere-troposphere transport to the winter-spring surface O_3 variation
6 observed on the Tibetan Plateau, Chinese Sci. Bull., 56, 84–88, 2011.
- 7 Zhou, X., Lou, C., Li, W.L. and Shi, J.E. Ozone changes over China and low center over
8 Tibetan Plateau, Chin. Sci. Bull., 40, 1396–1398, 1995.
- 9 [Zhu, L., Fischer, E.V., Payne, V.H., Worden, J.R., and Jiang, Z.: TES observations of the](#)
10 [interannual variability of PAN over Northern Eurasia and the relationship to springtime fires,](#)
11 [Geophys. Res. Lett., 42, 7230-7237, doi:10.1002/2015GL065328, 2015.](#)
- 12 Zhu, T., Lin, W.L., Song, Y., Cai, X.H., Zou, H., Kang, L., Zhou, L.B., and Akimoto, H.:
13 Downward transport of ozone-rich air near Mt. Everest, Geophys. Res. Lett. 33 (23), L23809,
14 doi: 10.1029/2006GL027726, 2006.

Table 1 ~~Concentrations of~~ Measured and modeled PAN at different heights ~~above over~~ the TP. ~~Data from literature are acquired either through remote sensing method or global modeling, while data from this work are estimates based on analysis of ground measurements.~~

Average PAN concentration(ppb)	Period	Height ^a	Method	Reference
<u>0.35(0.11-0.76)^b</u>	<u>17-24 August</u> <u>2011</u>	<u>4.7 km</u>	<u>Ground</u> <u>measurements</u>	this work
<u>0.44(0.21-0.99)^b</u>	<u>15 May - 13 July</u> <u>2012</u>	<u>4.7 km</u>	<u>Ground</u> <u>measurements</u>	
around 0.5 <u>0.52(0.31-</u> <u>0.72)^b</u>	<u>25-22 May</u> <u>August 2011</u> <u>2011</u>	<u>4.7 km</u> <u>~350</u> <u>hPa</u>	<u>Ground</u> <u>measurements</u> <u>with impact</u> <u>from the UT</u>	
0.6-0.7 <u>0.40(0.24-</u> <u>0.50)^b</u>	<u>22-25 August</u> <u>May 2011</u> <u>2012</u>	<u>4.7 km</u> <u>~350</u> <u>hPa</u>	<u>Ground</u> <u>measurements</u> <u>with impact</u> <u>from the UT</u>	
<u>0.62(0.27-0.99)^b</u>	<u>1-6 June 2012</u>	<u>4.7 km</u>	<u>Ground</u> <u>measurements</u> <u>with impact</u> <u>from South</u> <u>Asia</u>	
<u>0.44(0.14)^c</u>	<u>22 July - 16</u> <u>August 2006</u>	<u>3.8 km</u>	<u>Ground</u> <u>measurements</u>	<u>Xue et al.(2011)</u>
<u>0.35-0.45^d</u>	March 2003	333 hPa	<u>MIPAS</u>	Moore and
<u>0.15-0.23^d</u>		234 hPa	<u>MIPAS</u>	Remedios (2010)
<u>0.35-0.5^d</u>	August 2003	278 hPa	<u>MIPAS</u>	
<u>0.15-0.23^d</u>		185 hPa	<u>MIPAS</u>	
<u>0.1-0.15^d</u>	October 2007	12 km	<u>MIPAS</u>	Wiegele et al.(2012)

0.1-0.2 ^d	21 October 2003	12 km	MIPAS	Glatthor et al.(2007)
0.1-0.2^d	9-13 August 1997	18 km	Space Shuttle experiment	Ungermann et al.(2016)
0.3-0.5^d	June-August 2008	2-6 km	CRISTA-2	Fischer et al.(2014)
0.2-0.4^d		6-10 km	GEOS-Chem modeling	
			GEOS-Chem simulation	
0.15-0.2^d	June-September 1995-2004	6-10 km	ECHAM5-HAMMOZ model simulation	Fadnavis et al. (2014)

^a [Either elevation above the sea level or air pressure layer.](#)

^b [Overall average with the range of hourly mean.](#)

^c [Overall average with standard deviation.](#)

^d [Reading based on the color scale given in the reference.](#)

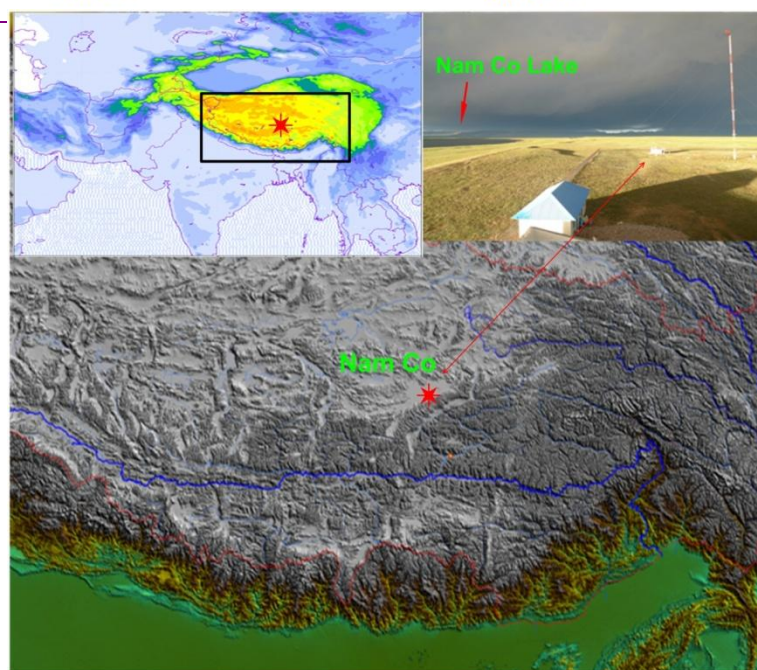
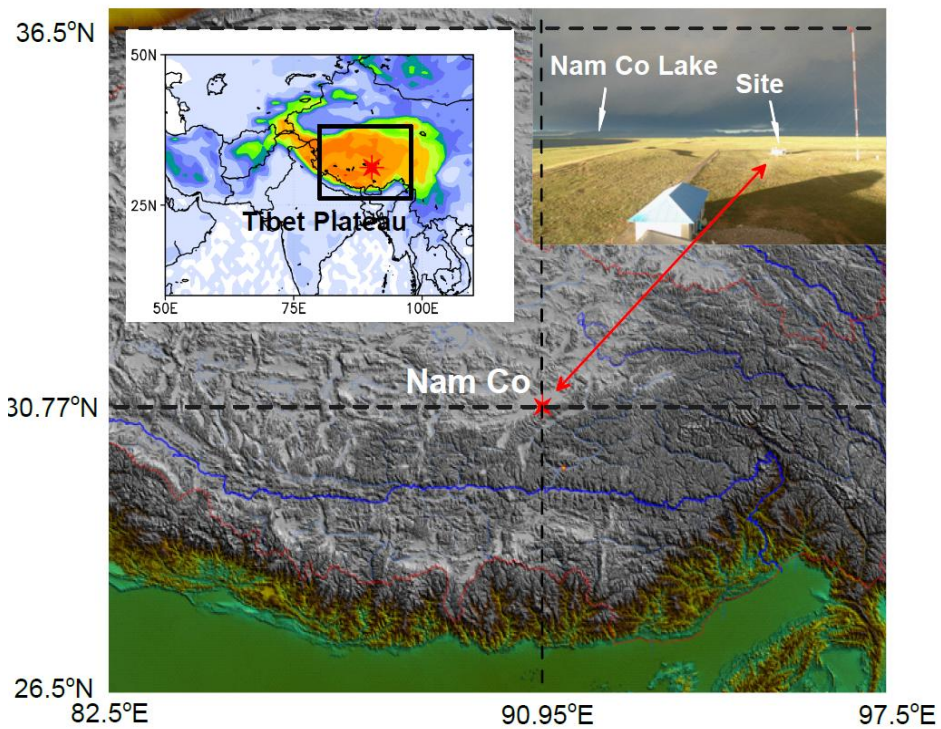
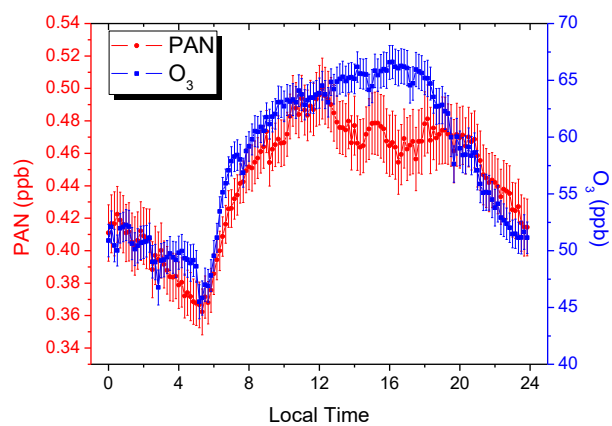


Fig.1 Map showing location of the observation site and local environment.



1
2 Fig.2 Diurnal patterns of PAN and O₃. All data are processed as 10 minutes resolution. The
3 vertical bars represent one standard error of the mean.
4

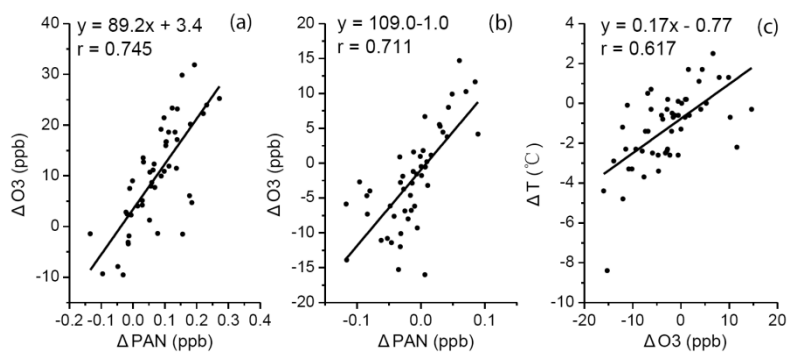
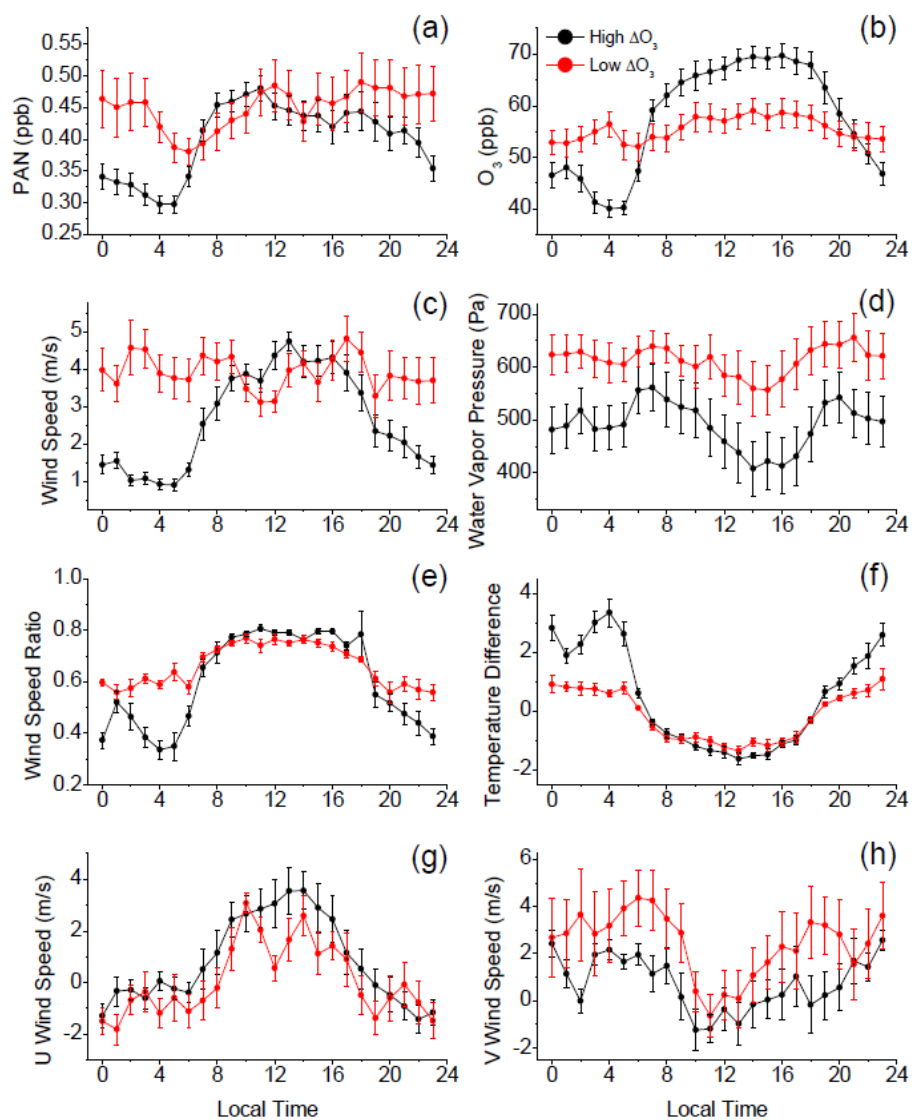


Fig.3 Scatter plots of ΔPAN (variation of the PAN concentration), ΔO_3 (variation of the O_3 concentration) and ΔT (variation of temperature) in specific time spans: (a) from 5:00 LT to 9:00 LT; (b, c) from 2:00 LT to 4:00 LT. All correlations shown in the figures are statistically significant at $\alpha=0.01$.



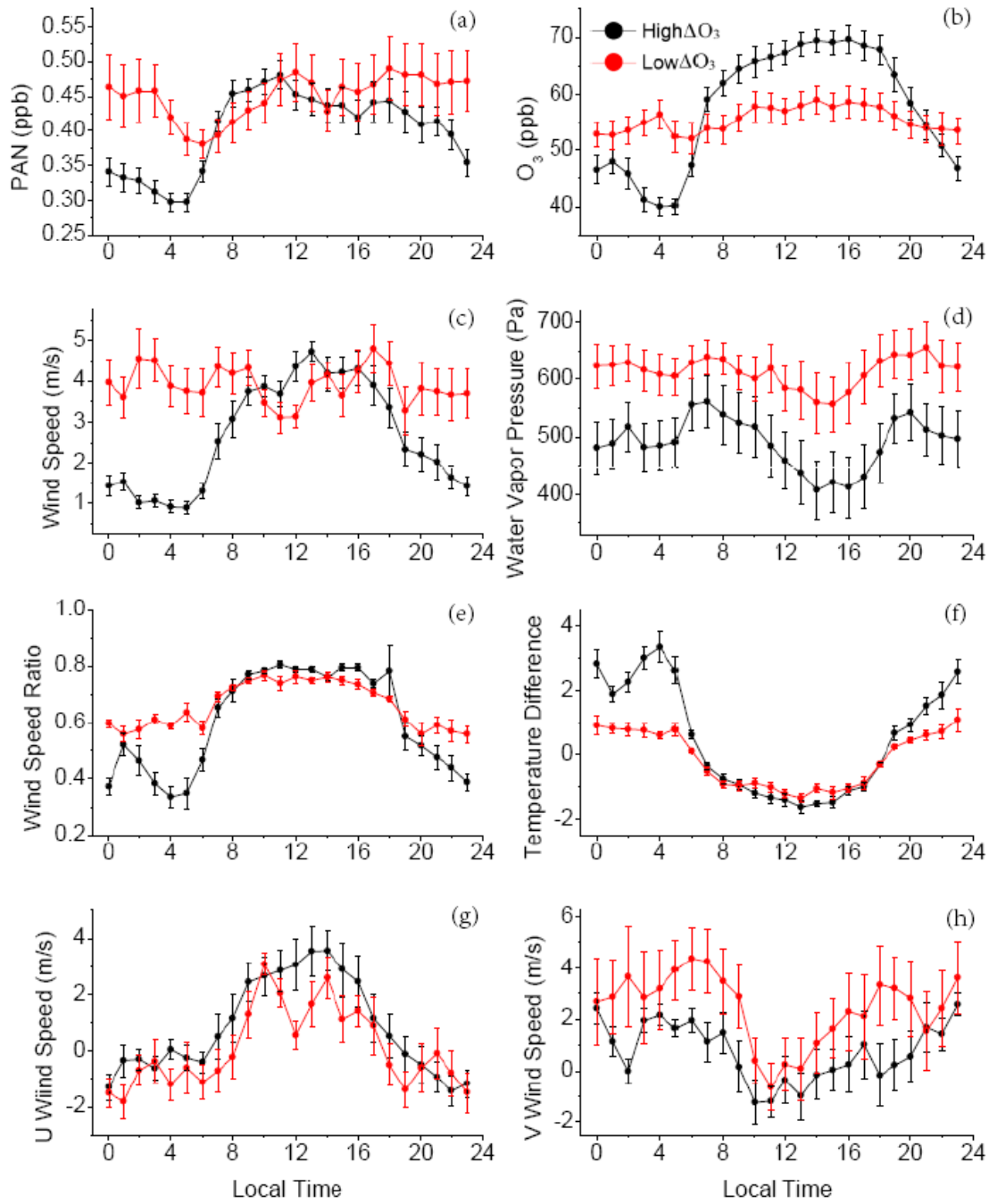


Fig. 4 Diurnal patterns of PAN (a), O₃ (b), Wind Speed (c), Water Vapor Pressure (d), Wind Speed Ratio (e, ratio of 10 meters height wind speed and 2 meters height wind speed), Temperature Difference (f, subtraction of 20 meters height temperature and 10 meters height temperature), U wind speed (g) and V wind speed (h). Black curves represent diurnal curves of 15 days with greatest ΔO_3 from 7:00 BJT-LT to 11:00 BJT-LT, and red curves represent diurnal curves of 15 days with smallest ΔO_3 correspondently. The vertical bars represent one standard error of the mean.

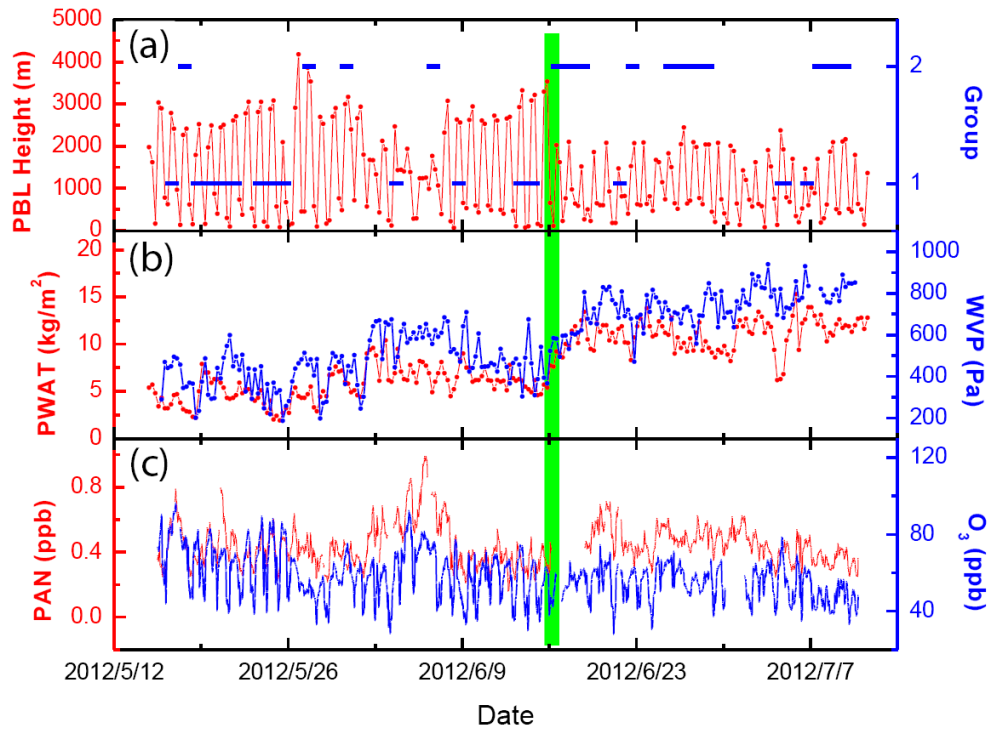
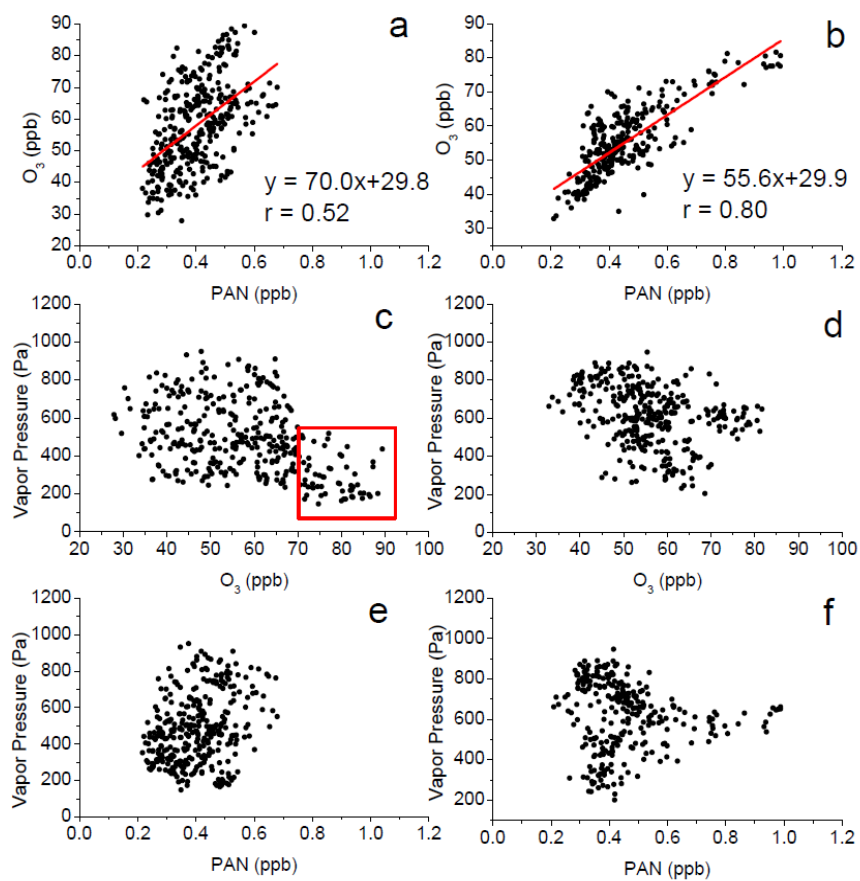
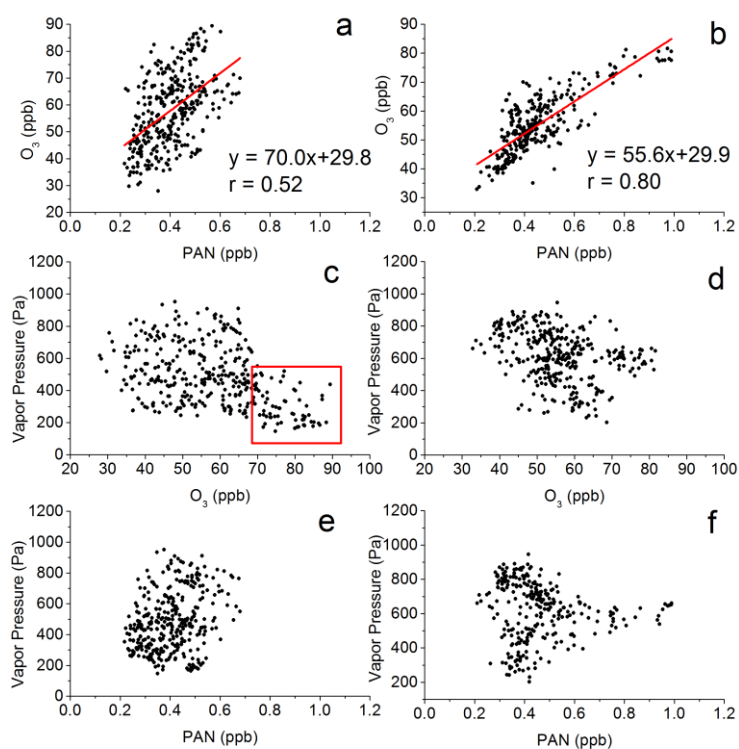


Fig. 5 Distributions of two groups of days (classified following Fig. 4) and time series the PBL height, PWAT (Precipitable Water of Entire Atmosphere), WVP (Water Vapor Pressure), PAN and O₃. Groups 1 and 2 represent two groups of days with different O₃ enhancement (ΔO_3) during 5:00-10:00 LT, with Group 1 including 15 days with the greatest ΔO_3 (denoted as High ΔO_3 in Fig. 4) and Group 2 including 15 days with the smallest ΔO_3 (denoted as Low ΔO_3 in Fig. 4). The PBL Height and PWAT were acquired from the FNL data with temporal resolution of 6 hours. WVP were calculated and processed as 6-hours resolution data from field observation. PAN and O₃ concentrations were processed as hourly data.



1



2

Fig. 6 Scatter plots of hourly O₃- versus PAN, Vapor Pressure- versus O₃, Vapor Pressure-
versus PAN of group 1 (a,c,e) and group 2 (b,d,f), following Fig. 4. The correlation shown in
Figs. 6(a) and 6(b) are significant at $\alpha=0.01$. The data points within the red rectangle in Fig.
6(c) represent O₃ levels higher than 70 ppb and WVP lower than 500 hPa.

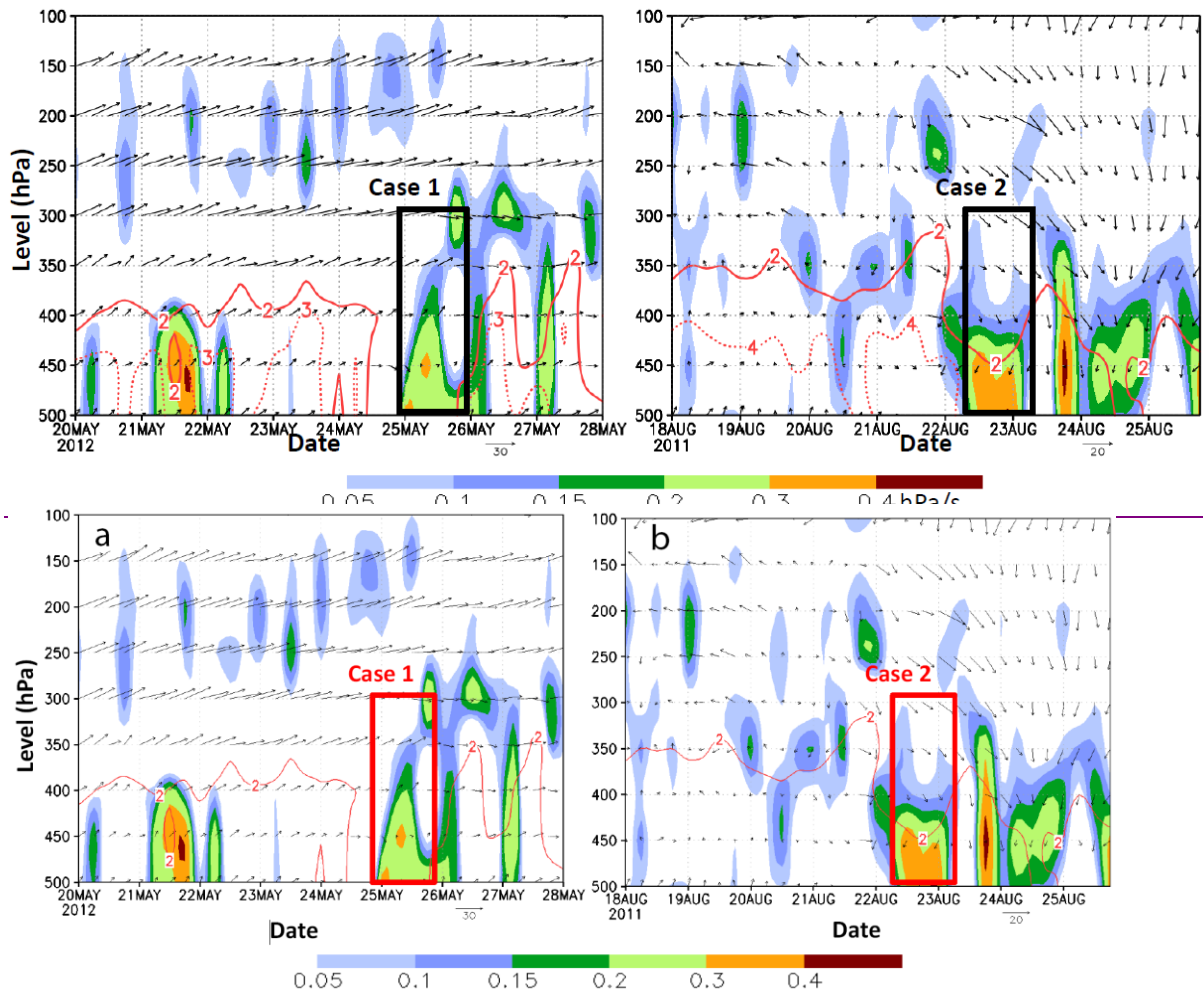


Fig. 7 Omega (shaded), specific humidity (red line) and horizontal wind field in dependence of time and height in two time frames. (a) From 20 to 28 May 2012; (b) From 15-18 to 25 August 2011. Case 1 and Case 2 correspond to two significant downdraft events.

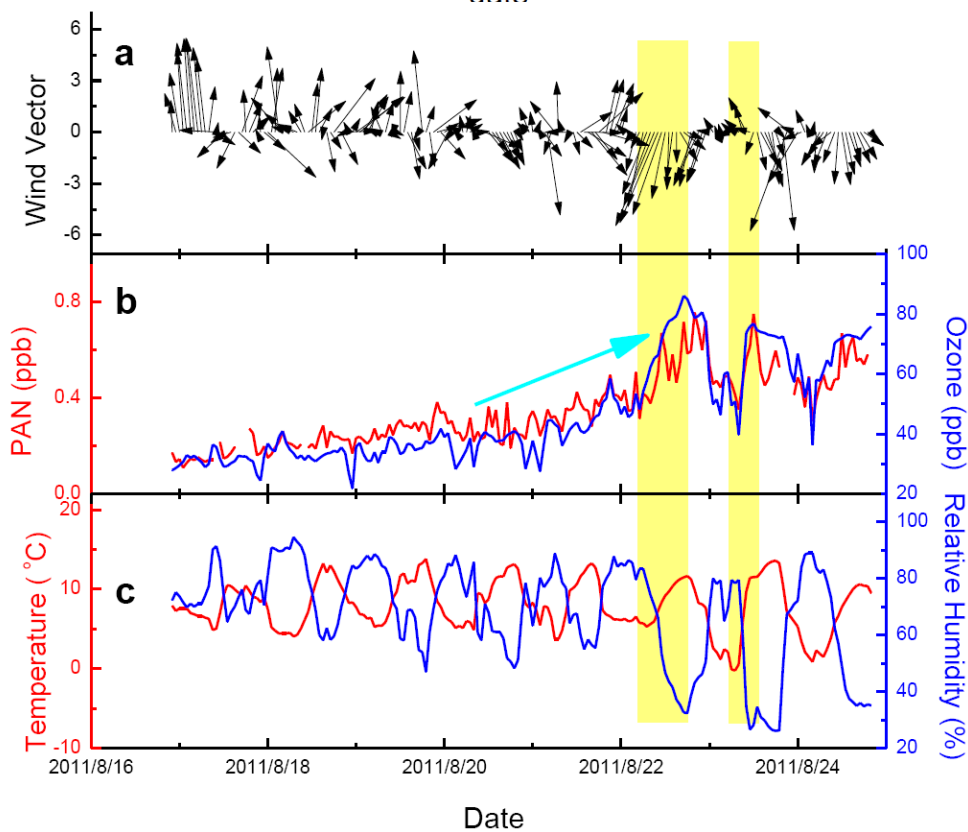
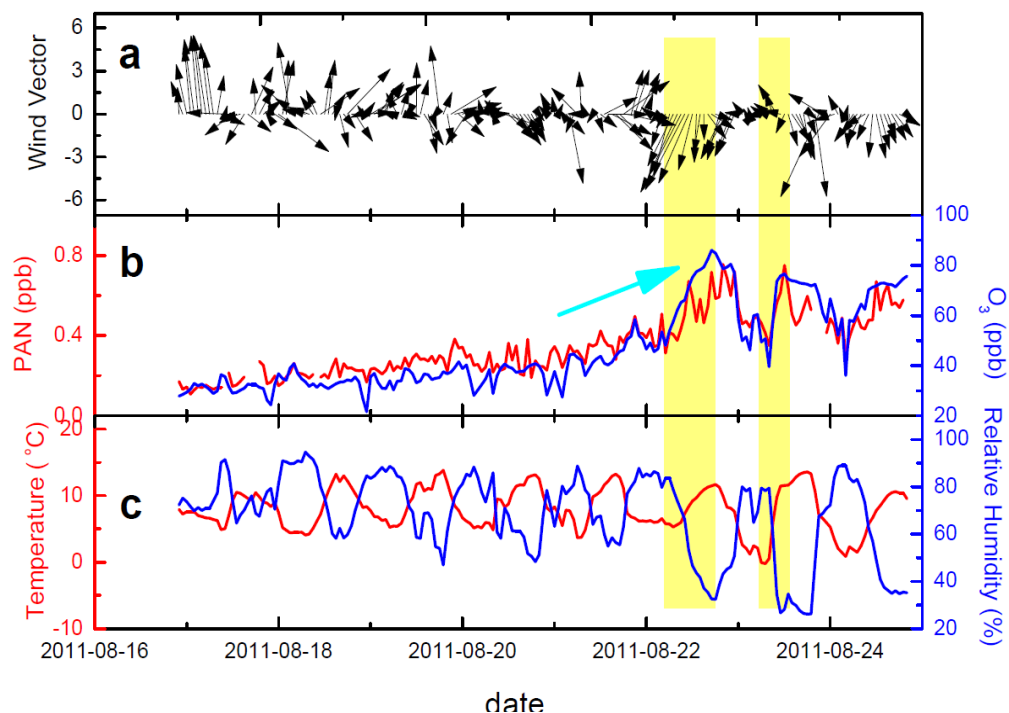
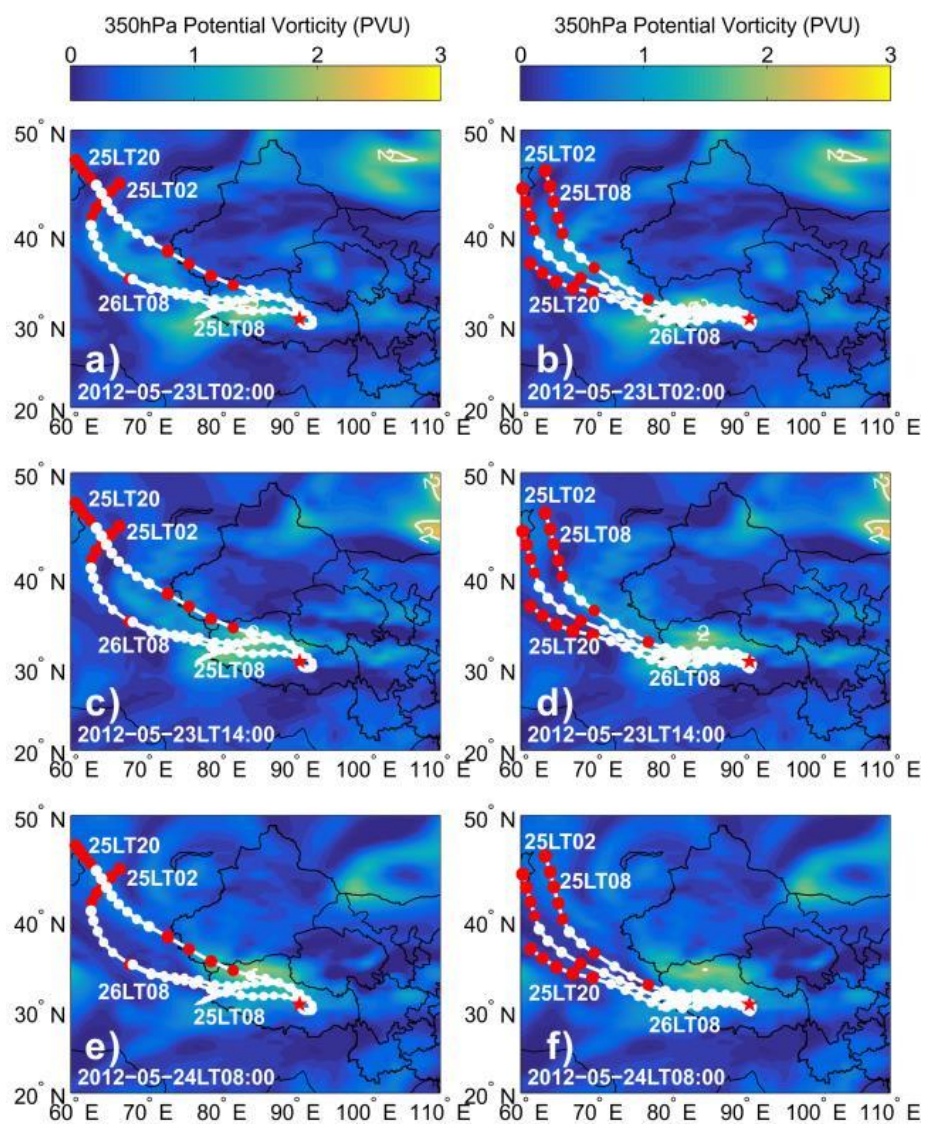


Fig. 8 Time series of (a) surface wind vectors, (b) PAN and O₃, and (c) temperature and relative humidity during 1617-254 August 2011. Yellow shadows represent the short periods controlled by downward motion. The blue arrow indicates the increasing trend of PAN and O₃.



1

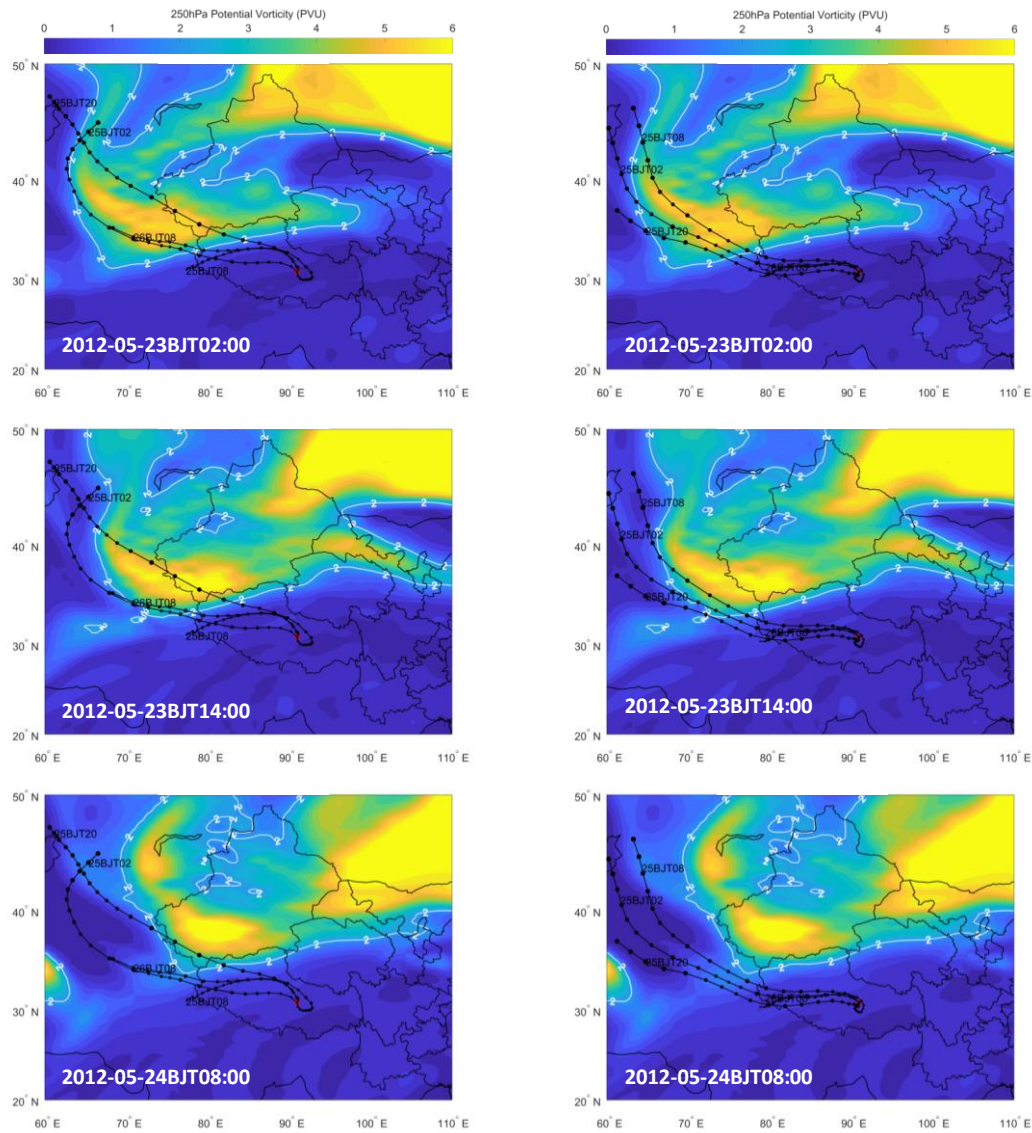
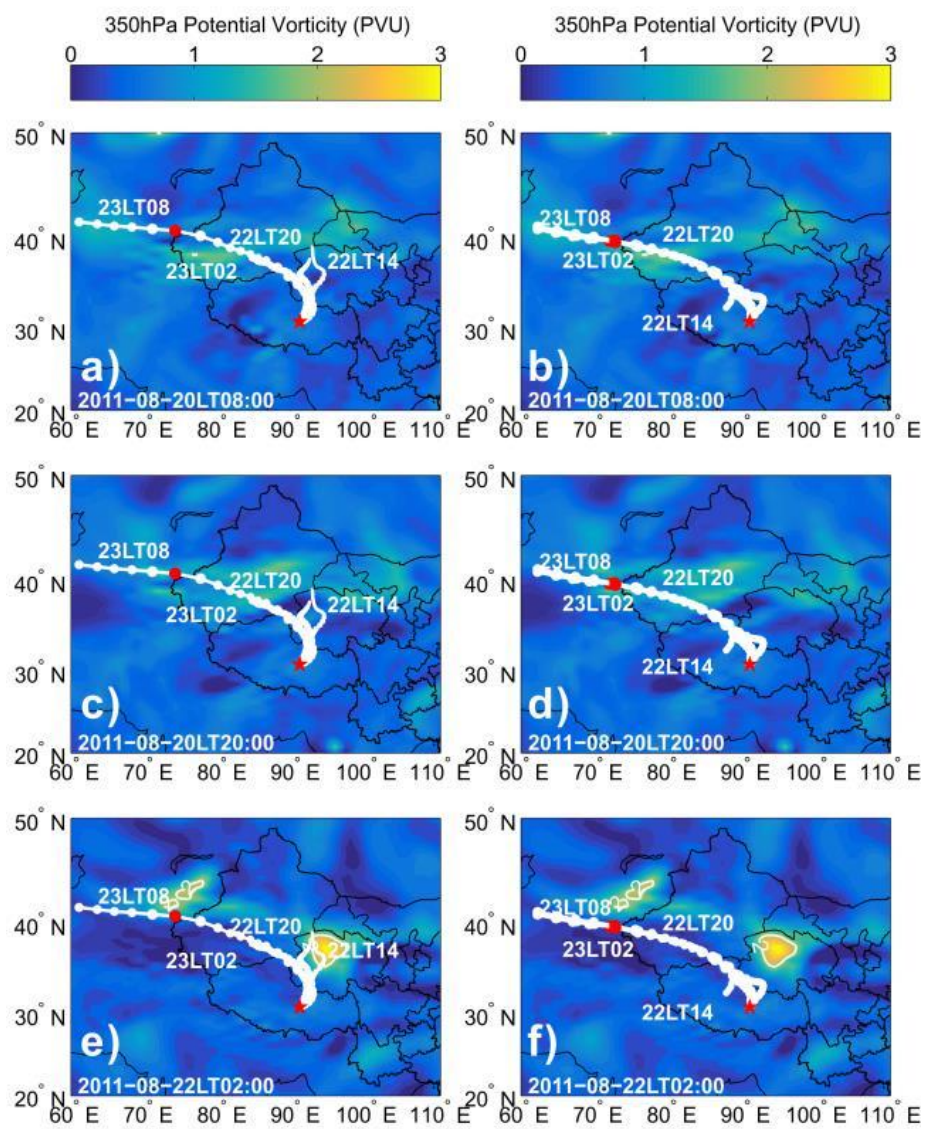


Fig. 9 Plots showing 250–350 hPa potential vorticity fields at three time-points during 23–24 May 2012 and back trajectories of air masses arriving at 500 m (left a,c,e) and 1500 m (right b,d,f) above the ground of the NMC site (red star) during 25–26 May 2012.



1

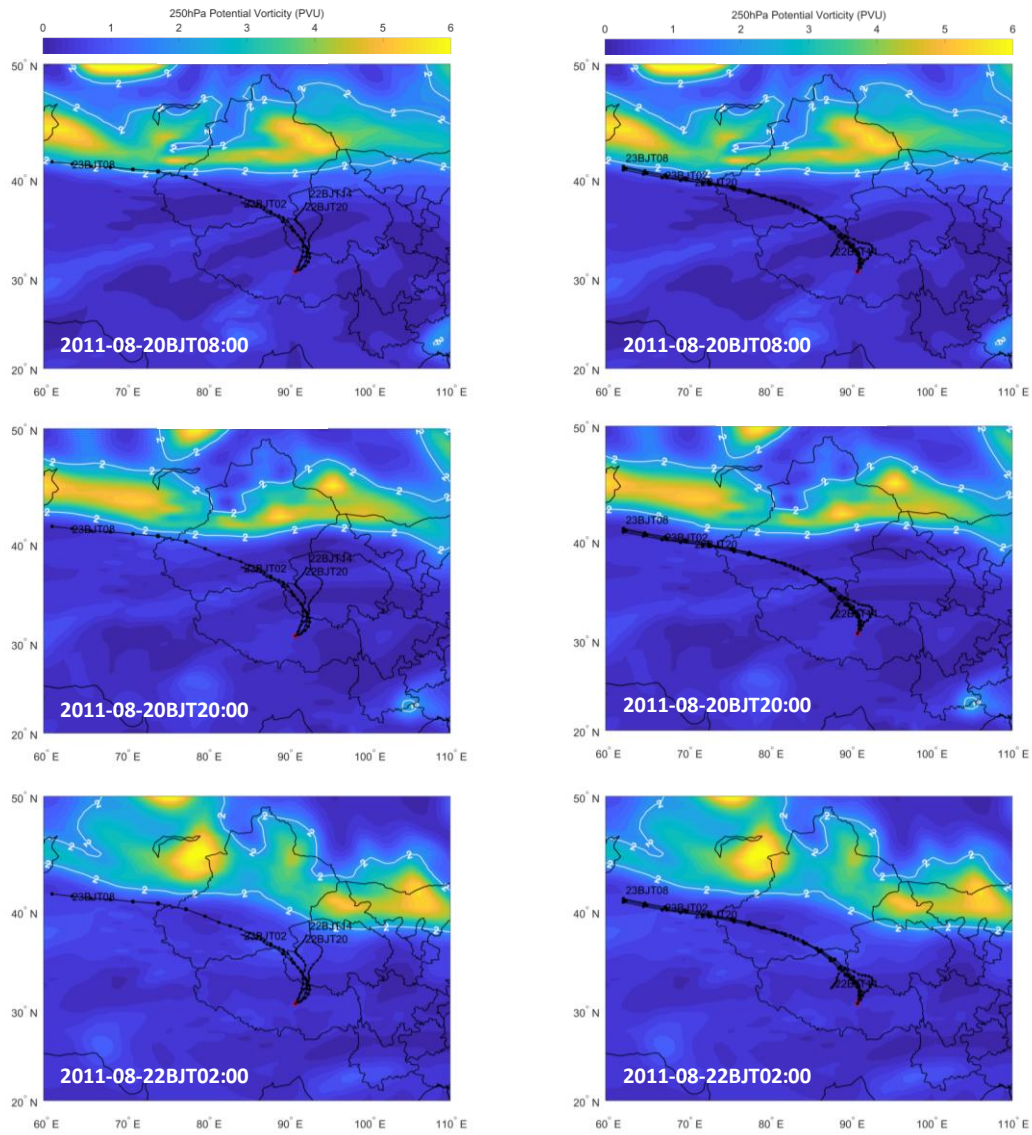


Fig. 10 Plots showing 250 hPa potential vorticity fields at three timepoints during 20–22 August 2011 and back trajectories of air masses arriving at 500 m (left) and 1500 m (right) above ground of the NMC site (red star) during Same as Fig. 9, but for 22–23 August 2011.

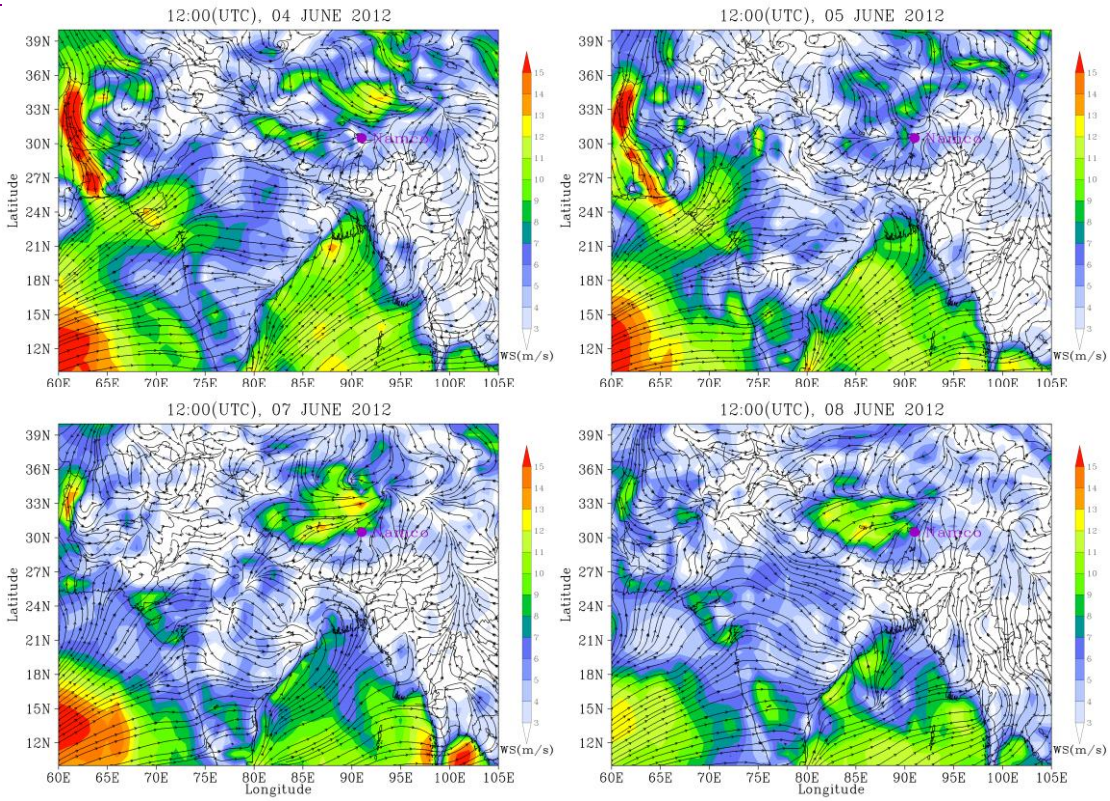
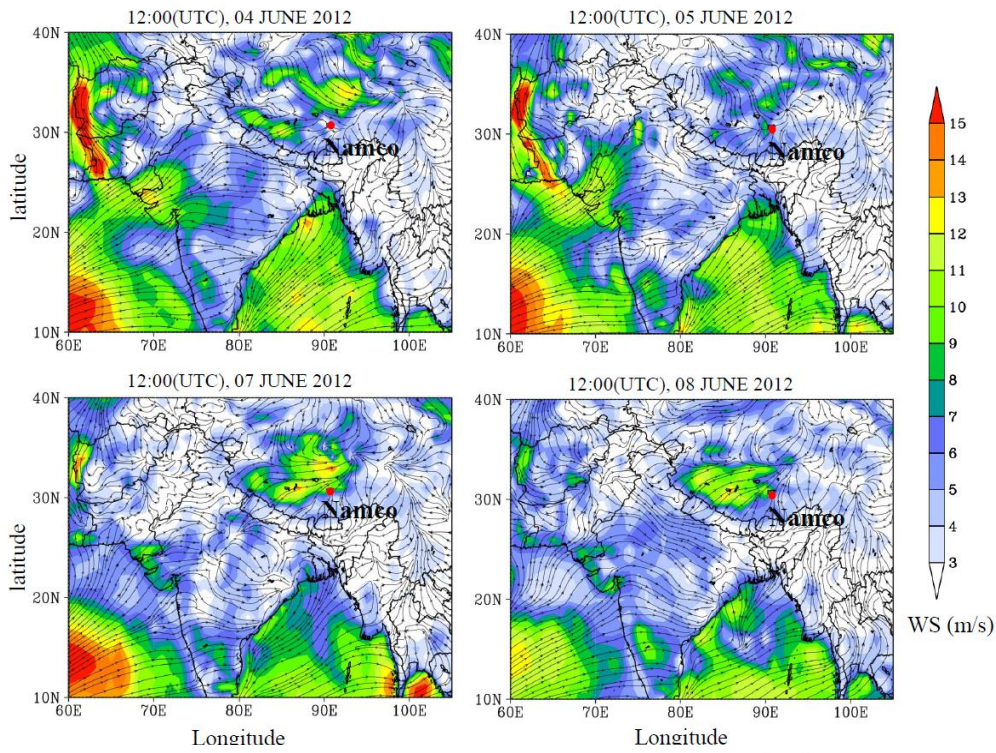


Fig. 11 Average fields of wind at sigma=0.995 for 12:00 (UTC) of 4, 5, 7 and 8 June 2012.

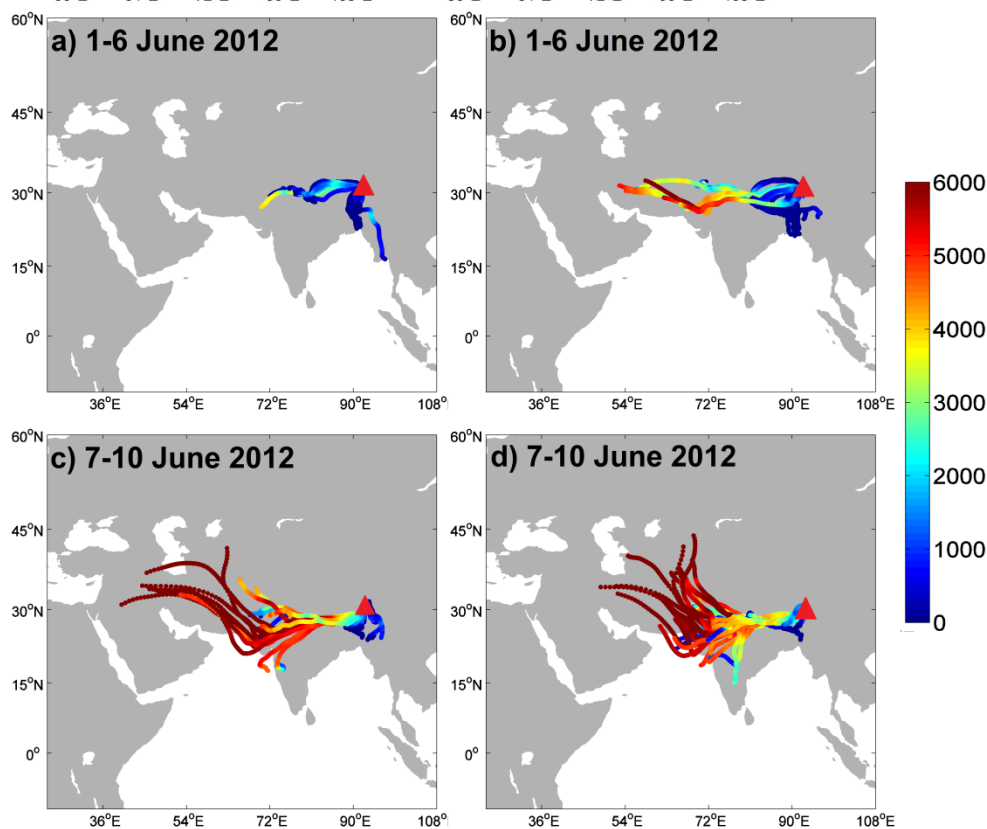
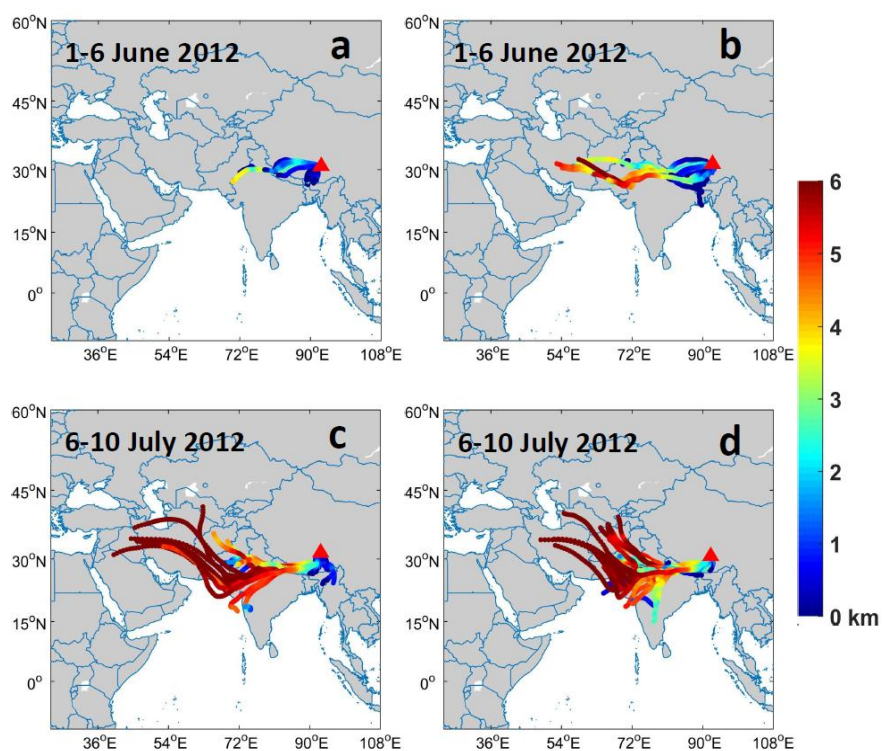


Fig. 12 Backward air trajectories arriving at NMC with endpoint heights of 500 meters (a,c) 1500 meters (b,d) for the periods 1-6 June 2012 (a,b) and 7-10 June 2012 (c,d). The color scale shows trajectory heights in km above ground level.

Supplementary Materials for

First simultaneous measurements of peroxyacetyl nitrate (PAN) and ozone at Nam Co in the central Tibetan Plateau: impacts from the PBL evolution and transport processes

Xiaobin Xu¹, Hualong Zhang^{1,*}, Weili Lin^{1,2,**}, Ying Wang¹, [Wanyun Xu¹](#), and Shihui Jia^{1,**}

¹ State Key Laboratory of Severe Weather & Key Laboratory for Atmospheric Chemistry of China Meteorological Administration, Chinese Academy of Meteorological Sciences, Beijing, China

² Meteorological Observation Center, China Meteorological Administration, Beijing, China

* now at : Guangdong Meteorological Observatory, Guangzhou, Guangdong, China

** [now at: College of Life and Environmental Sciences, Minzu University of China, Beijing, China](#)

*** [now at: School of Environment and Energy, South China University of Technology, Guangzhou, Guangdong, China](#)

Correspondence to: Xiaobin Xu (~~xuxb@camsema.cn~~xiaobin_xu@189.cn)

Indirect calibration of PAN measurements

To obtain acceptable results using the indirect calibration method, we need two assumptions. First, the ambient concentration of CCl₄ at the observation site should be nearly constant during the measurement period. Second, whatever the ECD sensitivity changes with varying environmental conditions, the changes in relative responses of the ECD to PAN and CCl₄ should be the same during the period of consideration. In polluted areas, the first assumption is inapplicable simply because there is large spatial and temporal variation of CCl₄ emission. Even at the regional background site often impacted by polluted air masses, the CCl₄ concentration could be highly varying (Yao et al., 2010). However, CCl₄ is believed to be well mixed to a large scale in clean area air due to ~~sparse~~[negligible](#) emission and long

lifetime (42 ± 12 years), thus its concentration at remote sites can be treated as constant in a short period (Simmonds et al., 1998). Based on this idea, Wang et al. (2000) suggested ~~the feasibility of~~ using CCl_4 as an internal ~~reference in calibrator~~ the preparation of gas standard gas mixtures. The second assumption is prerequired for any application of similar indirect calibration and normally applicable if the ECD sensitivity is stable with a GC run. On the basis of the two assumptions above, the ratio between the PAN and CCl_4 signals is used as the key quantity for correcting the PAN data. Therefore, the corrected PAN concentration is eventually determined by following expression:

$$C'_{\text{PAN}} = (C_{\text{PAN}} \times S'_{\text{PAN}} \times S_{\text{CCl}_4}) / (S_{\text{PAN}} \times S'_{\text{CCl}_4}), \quad (1)$$

where, C'_{PAN} and C_{PAN} are the concentrations of ambient and standard PAN, respectively; S'_{PAN} and S_{PAN} are the PAN signals of air sample and standard sample, respectively; and S'_{CCl_4} and S_{CCl_4} are the CCl_4 signals of the air sample and the surrogate CCl_4 signal of the calibration, respectively. Since the standard sample did not contain CCl_4 , the CCl_4 signal of the air sample prior to ~~the a~~ calibration was taken as the surrogate of ~~the~~ CCl_4 signal for the calibration run (S'_{CCl_4}). This may introduce additional uncertainty to the PAN data as the ECD sensitivity may change from run to run. However, the change of the ECD sensitivity should be minor between consecutive runs within relative short time. Therefore, equation (1) is acceptable in our indirect calibration.

References

- Simmonds, P. G., Cunnold, D. M., Weiss, R. F., Prinn, R. G., Fraser, P. J., McCulloch, A., Alyea, F. N., and O'Doherty, S.: Global trends and emission estimates of CCl_4 from in situ background observations from July 1978 to June 1996, *J. Geophys. Res.*, 103, 16017–16027, 10.1029/98JD01022, 1998.
- Wang, J.-L., Lin, W.-C., and Chen, T.-Y.: Using atmospheric CCl_4 as an internal reference in gas standard preparation, *Atmos. Environ.*, 34, 4393–4398, 2000.
- Yao, B., Zhou, L.X., Zhang, F., Xu, L., Zang, K.P., Zhang, X.C., Zhang, X.L., Zhou, H.G., Dong, F., and Zhou, L.Y.: In-situ measurement of atmospheric carbon tetrachloride (CCl_4) at the Shangdianzi Global Atmosphere Watch regional station, *Acta Scientiae Circumstantiae*, 30(12), 2377-2382, 2010.

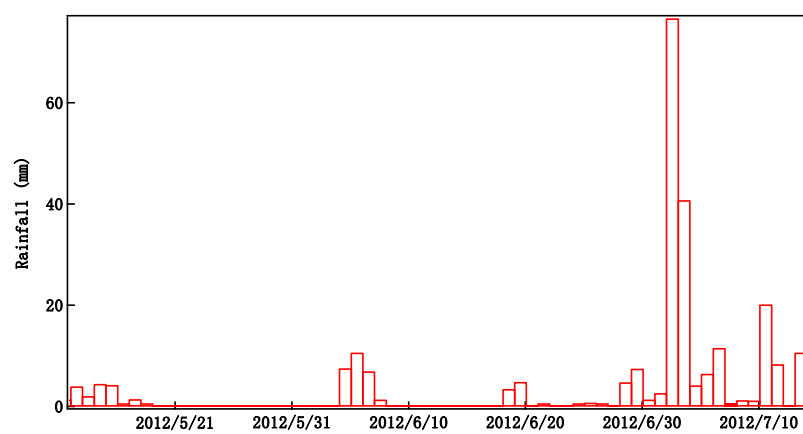
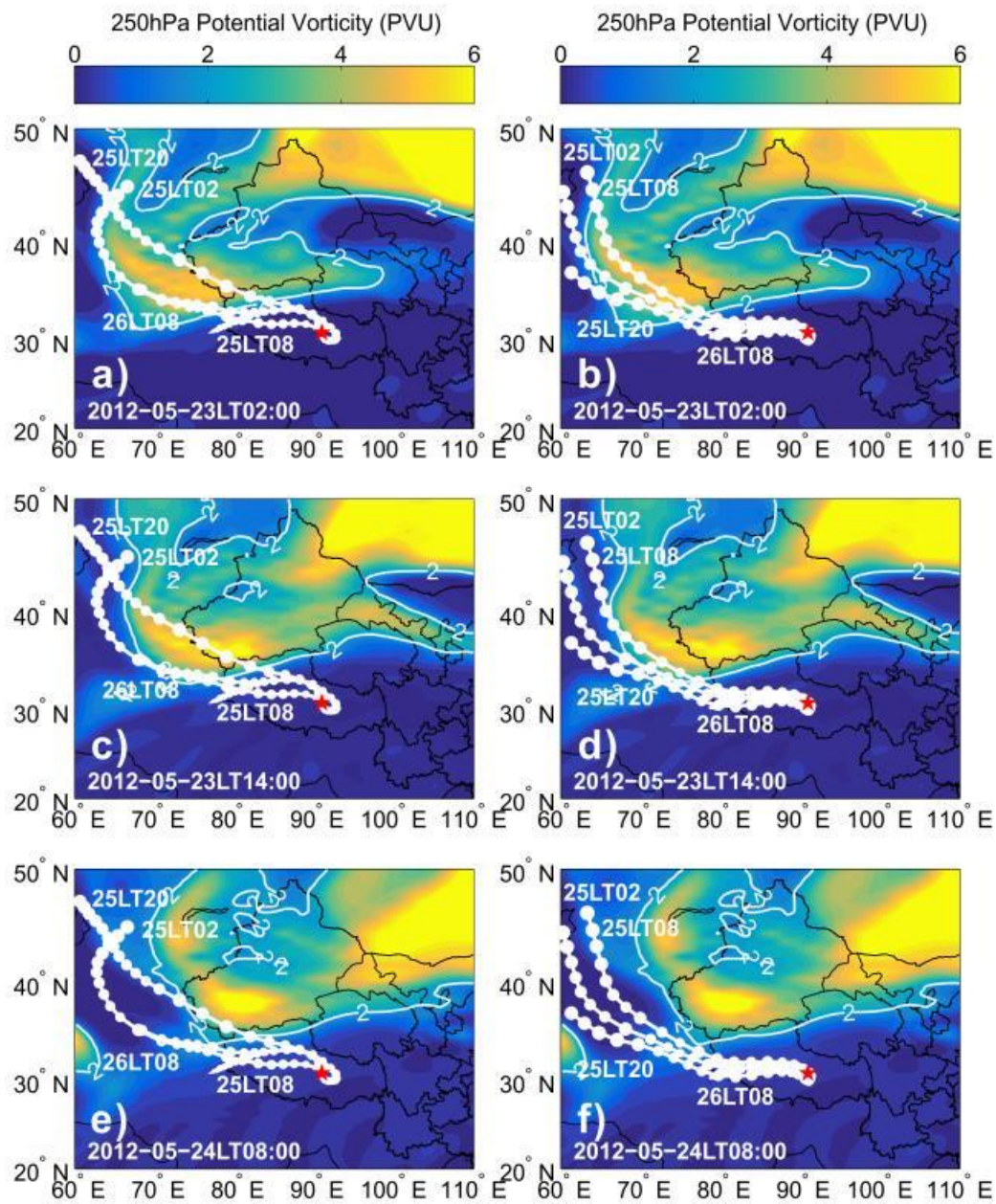


Figure S1 Daily rainfall during the observation period in 2012.



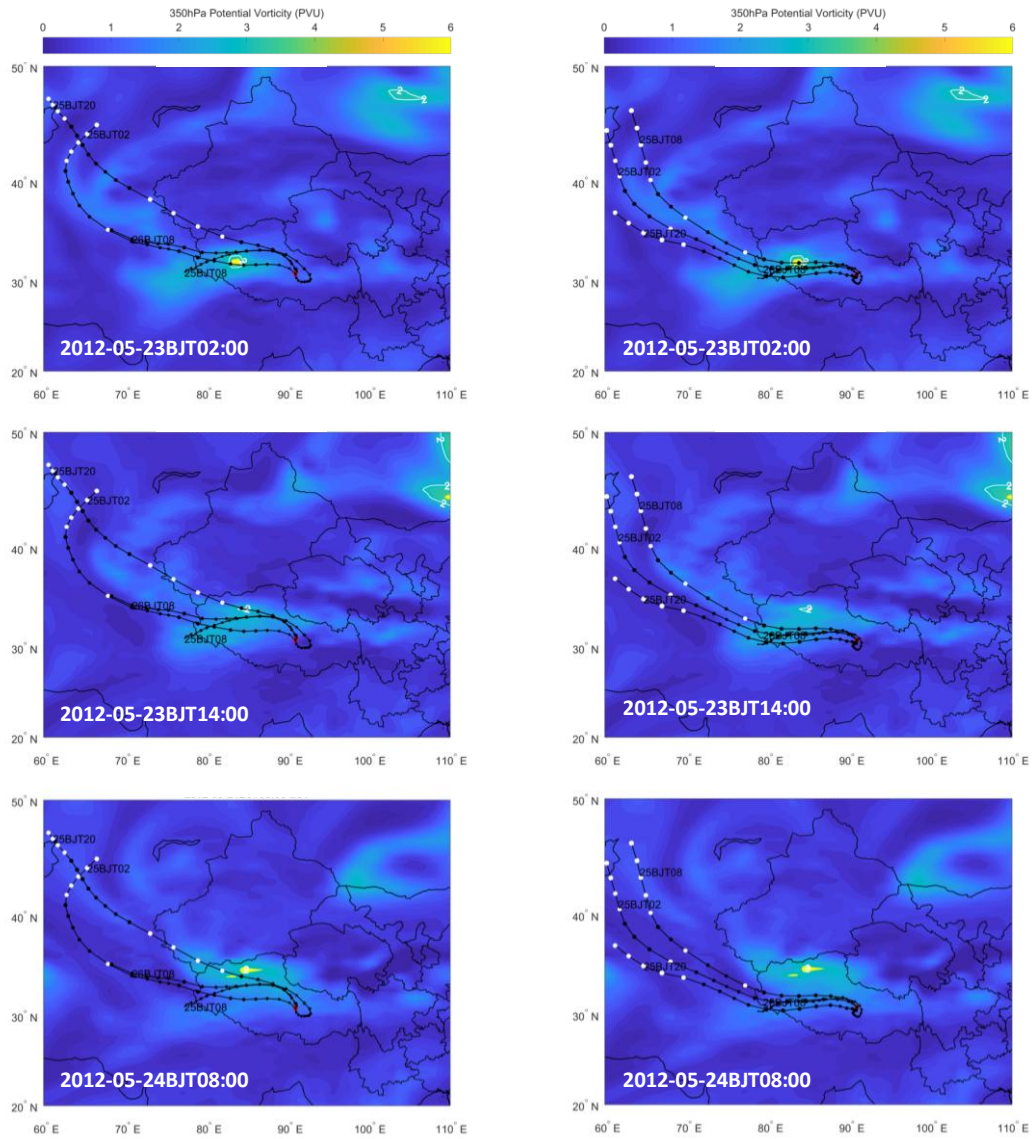
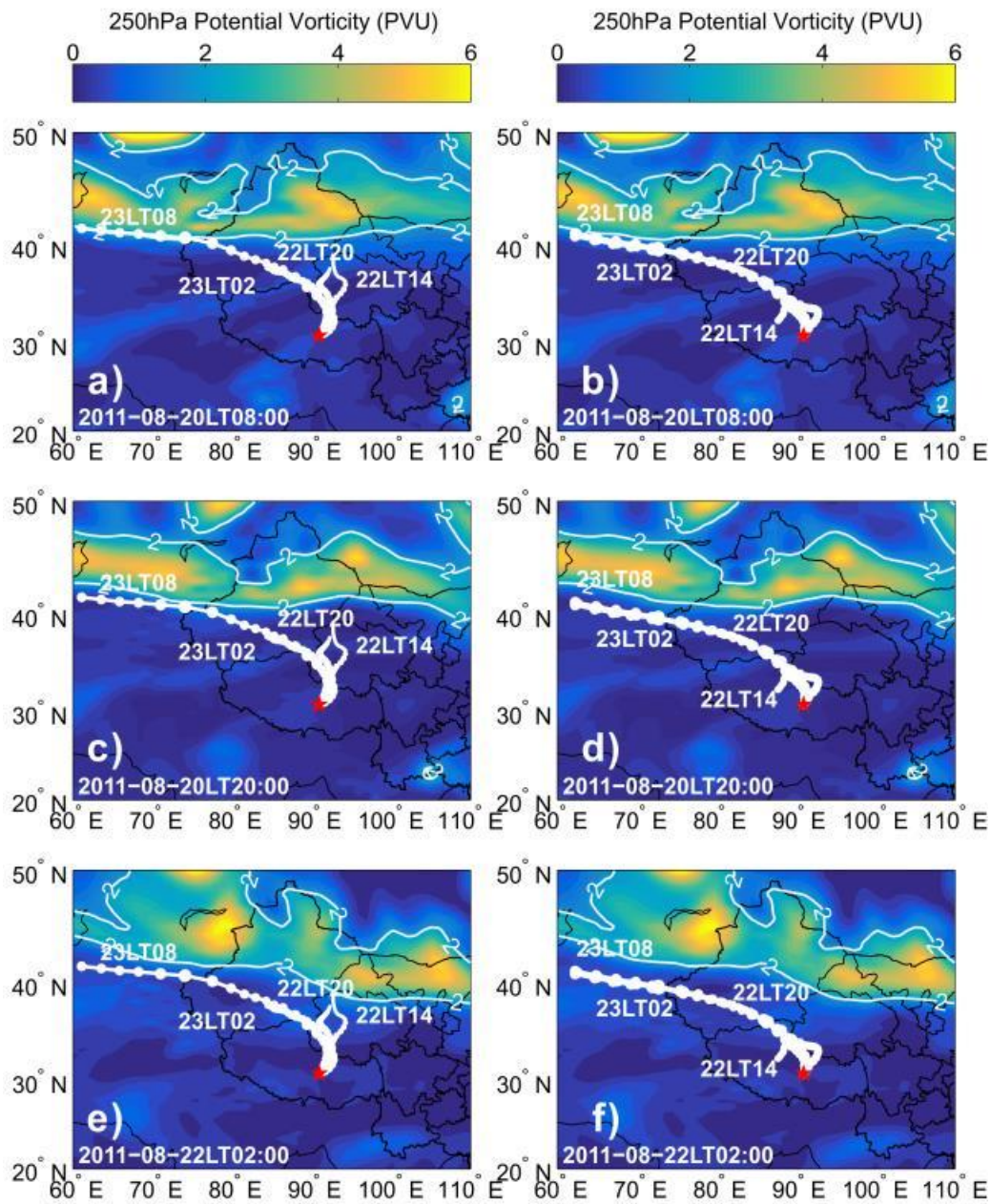


Figure S2 Plots showing 350–250 hPa potential vorticity fields at three timepoints during 23–24 May 2012 and back trajectories of air masses arriving at 500 m (left) and 1500 m (right) above ground of the NMC site (red star) during 25–26 May 2012. The white dots denote trajectory heights over the 350 hPa level.



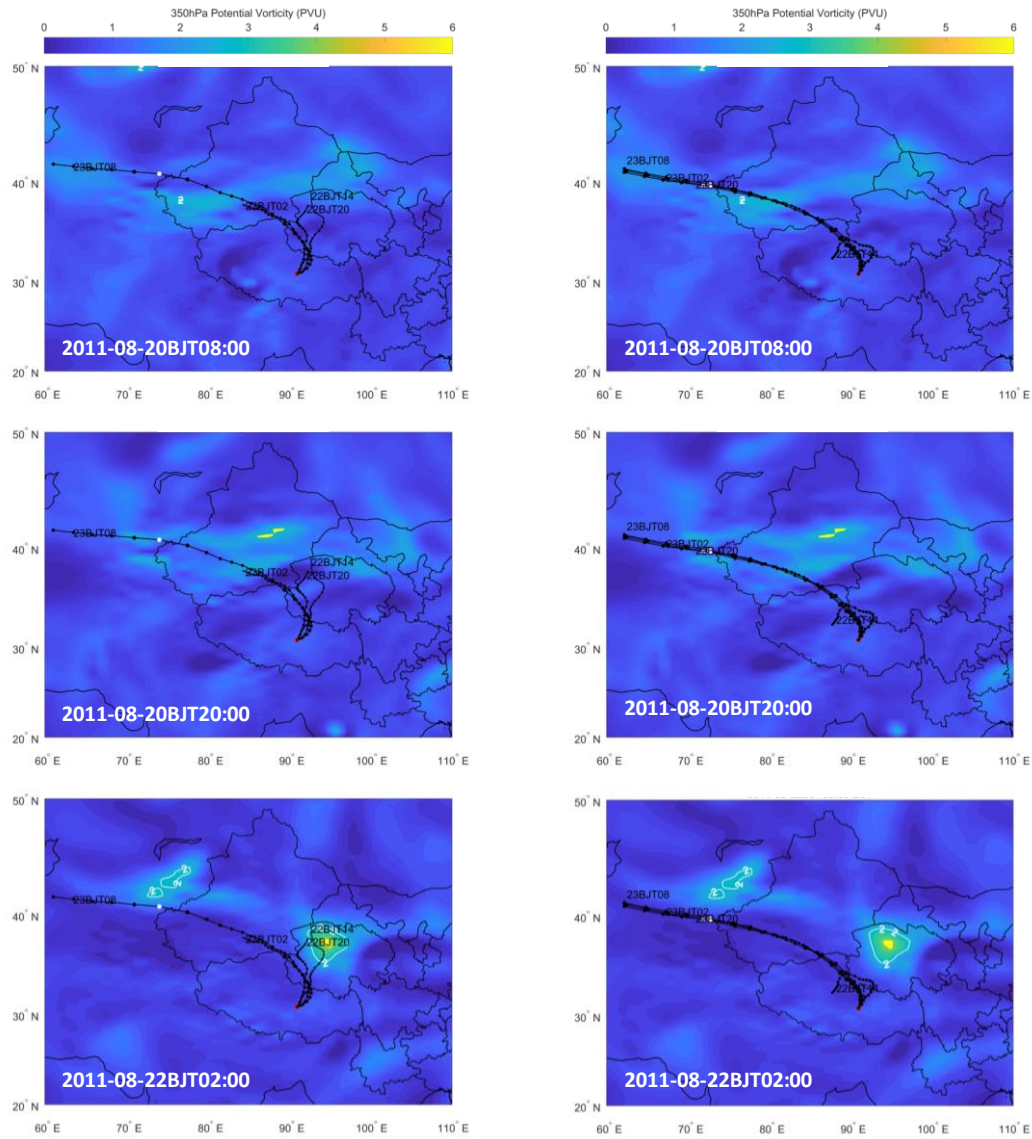
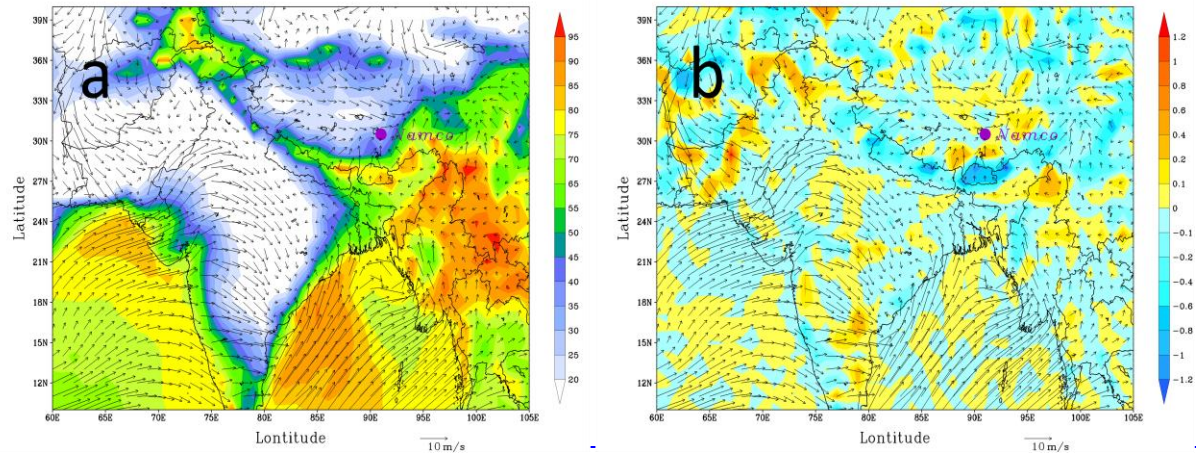


Figure S3 ~~Plots showing 350 hPa potential vorticity fields at three timepoints during 20–22 August 2011 and back trajectories of air masses arriving at 500 m (left) and 1500 m (right) above ground of the NMC site (red star)~~Same Figure S2, but for during 22–23 August 2011. ~~The white dots denote trajectory heights over the 350 hPa level.~~



30-31 MAY 2012

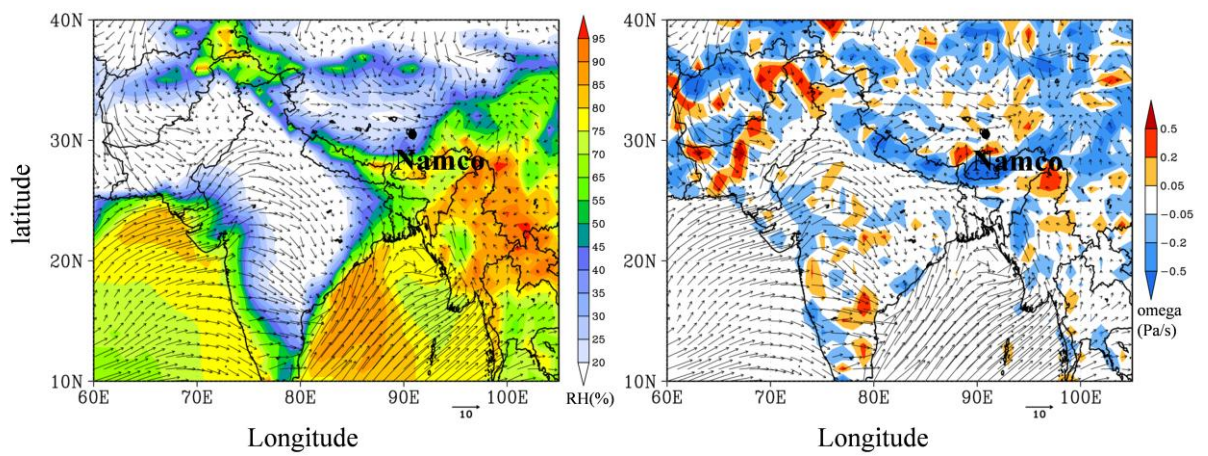
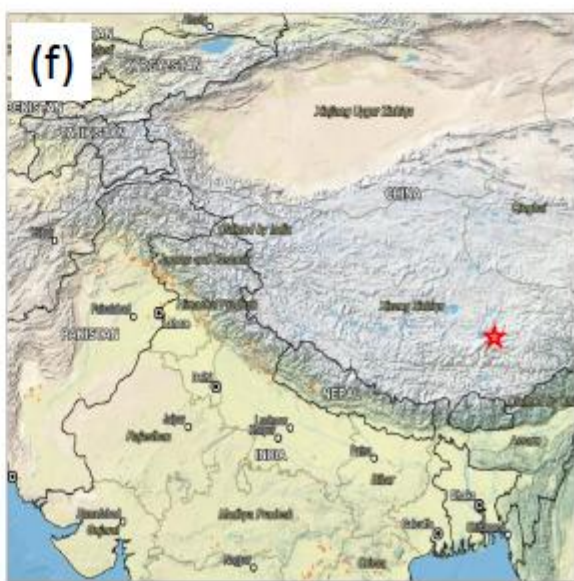
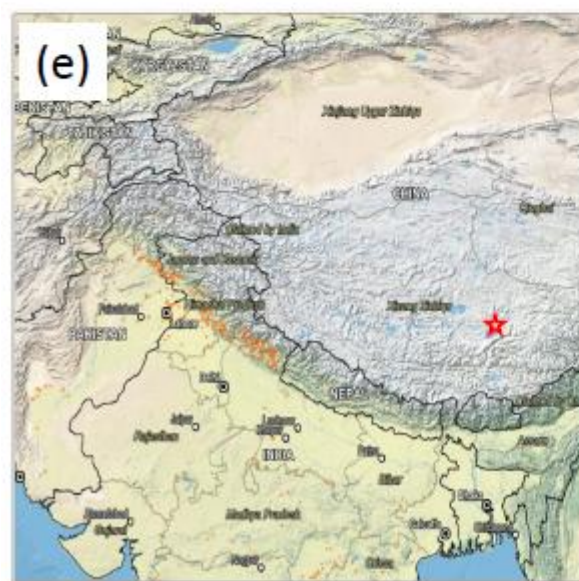
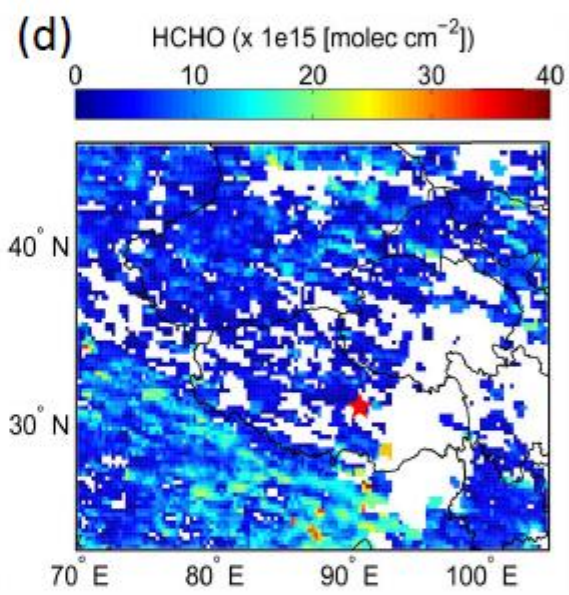
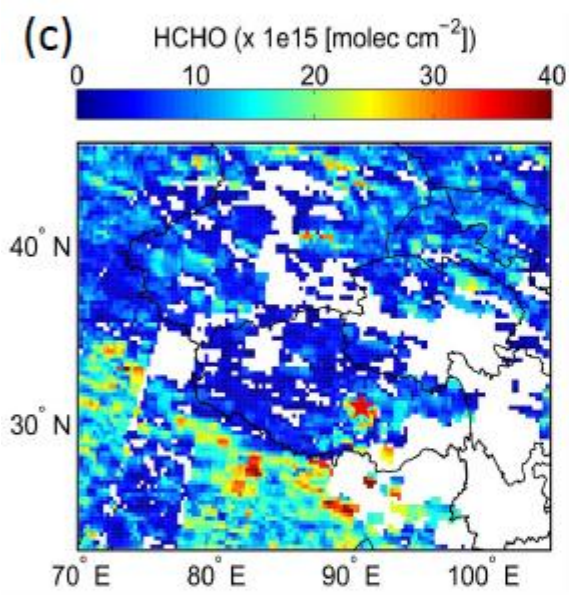
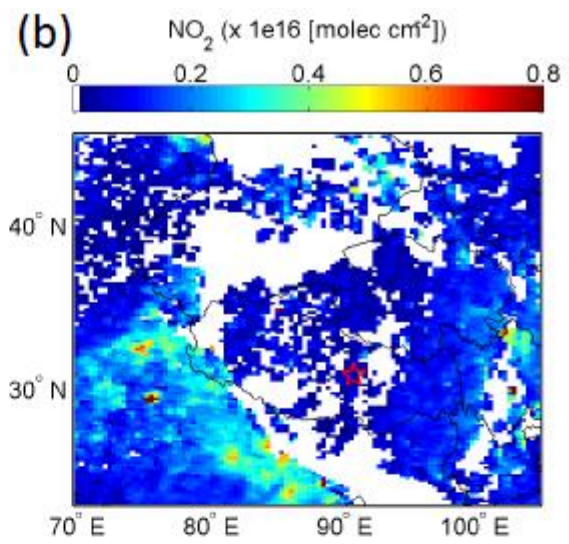
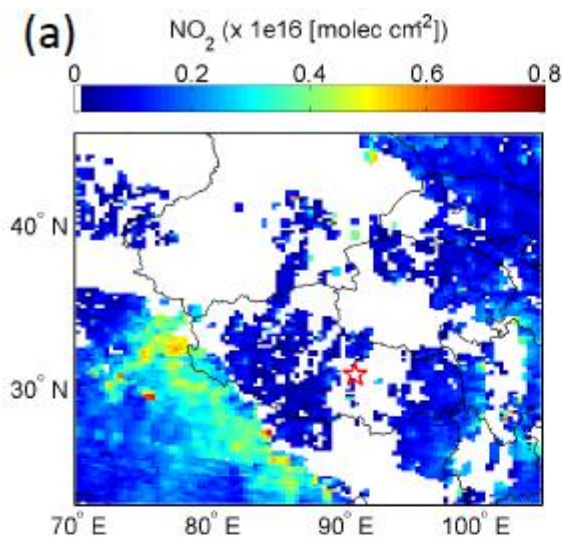


Figure S4 Average fields of wind, relative humidity (a) and omega (b) at sigma=0.995 for the periods 30-31 ~~June~~May 2012.



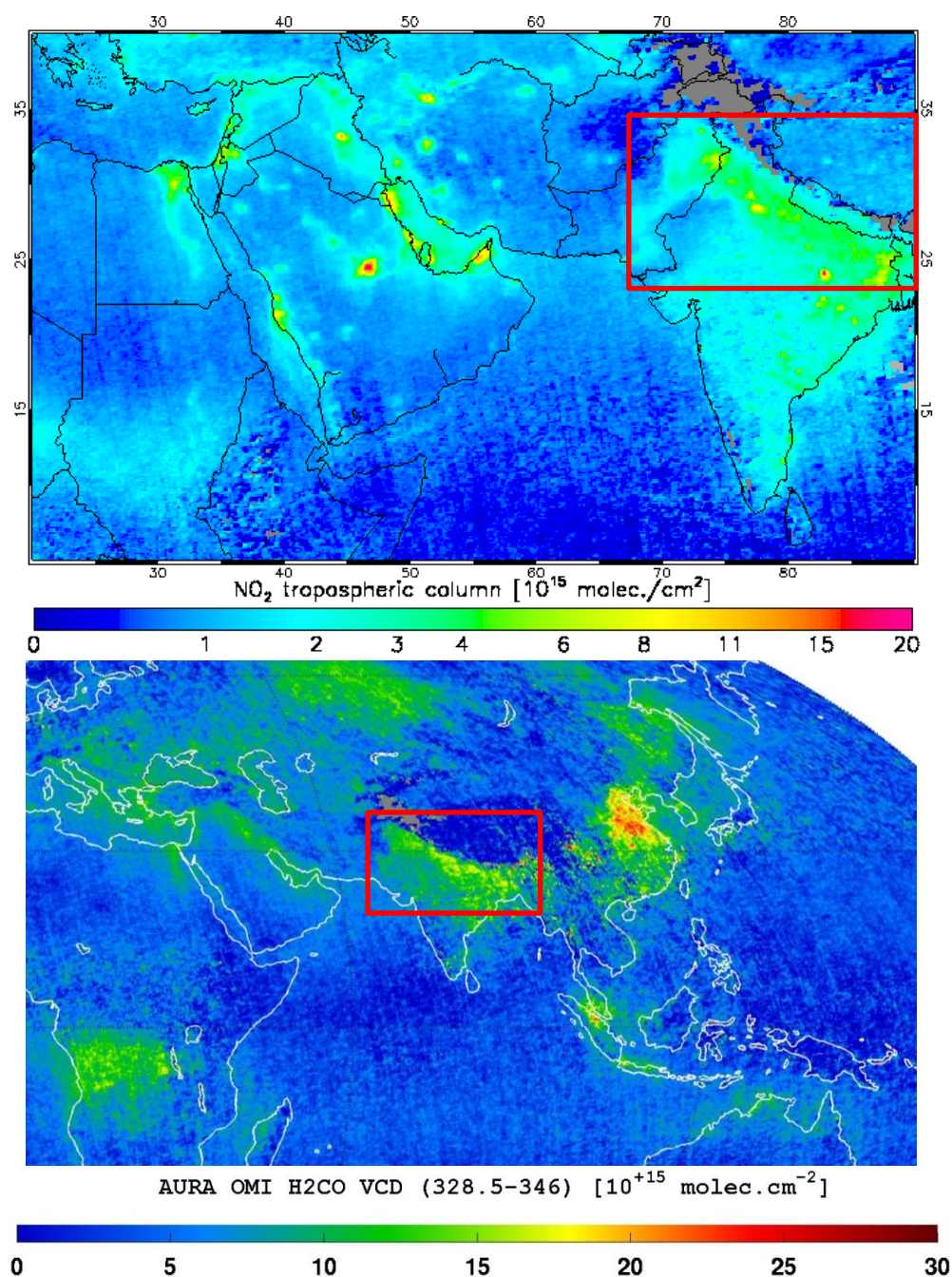


Figure S5 Average column densities of tropospheric NO₂ ([upper a,b](#)) and HCHO ([bottom c,d](#)), and maps with fire spots ([e,f](#)) for the periods [1-3 June 2012 \(a,c,e\)](#) and [4-6 June 2012 \(b,d,f\)](#); with Northern India marked by red rectangles. The Daily original tropospheric NO₂ data are from the OMI observations and made available by NASA (<https://daac.gsfc.nasa.gov/datasets>), and Daily tropospheric HCHO column maps are from GOME-2 observations and provided by the Tropospheric Emission Monitoring Internet Service (TEMIS) at The Royal

1 Netherlands Meteorological Institute (KNMI), The Netherlands
2 (<http://www.temis.nl/index.php>). Fire spots maps present the fire locations (orange dots)
3 observed by MODIS and are produced by NASA's Web Fire Mapper
4 (<https://firms.modaps.eosdis.nasa.gov/firemap/>).
5

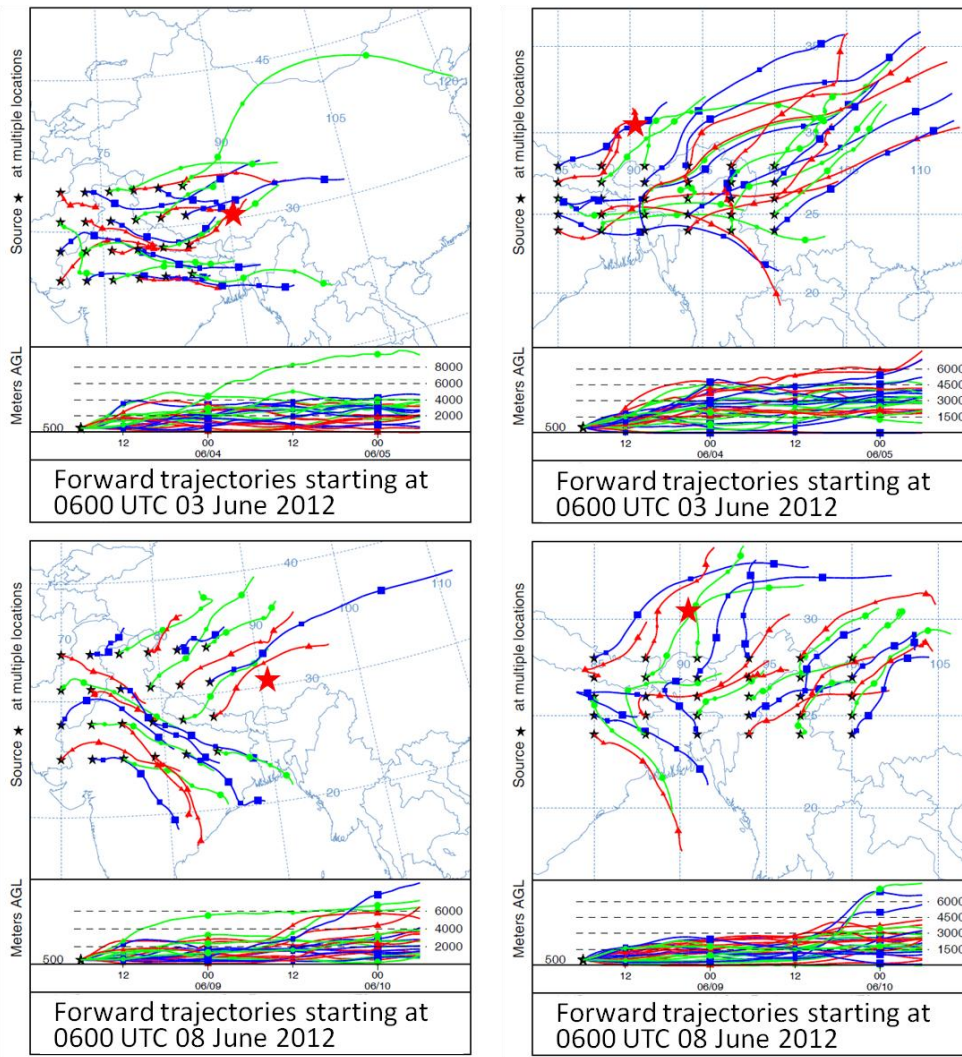


Figure S6 Matrices of 48-h air mass forward trajectories starting at 0600 UTC 3 June 2012 (upper panel) and 0600 UTC 8 June 2012 (bottom panel) from the domains west and south of the NMC site (red star). The online HYSPLIT model (https://ready.arl.noaa.gov/HYSPLIT_traj.php; Stein et al., 2015; Rolph et al., 2017) were used to produce the trajectory matrices. The starting height of the trajectories is 500 m above ground level.

Stein, A.F., Draxler, R.R., Rolph, G.D., Stunder, B.J.B., Cohen, M.D., and Ngan, F.: NOAA's HYSPLIT atmospheric transport and dispersion modeling system, *Bull. Amer. Meteor. Soc.*, 96, 2059-2077, 2015.

Rolph, G., Stein, A., and Stunder, B.: Real-time Environmental Applications and Display system: READY. *Environmental Modelling & Software*, 95, 210-228, 2017.